A.D. MDLXII

DEPARTMENT OF BIOMEDICAL SCIENCES

PhD COURSE IN LIFE SCIENCES ANDBIOTECHNOLOGIES

UNIVERSITY OF SASSARI

Coordinator: Prof. Leonardo Antonio Sechi

Cycle XXXII

Target identification of small molecules with antiproliferative properties

By

Lyu Weidong

Supervisors: Prof. Luigi Marco Bagella

Ph.D. School in Life Sciences and Biotechnologies

Department of Biomedical Sciences University of Sassari

Prof. David J. Kelvin

Division of Immunology, International Institute of Infection and Immunity

Shantou University Medical College

Academic Year: 2018-2019

Lyu Weidong
Target identification of small molecules with antiproliferative properties
PhD school in Life Science and Biotechnologies
University of Sassari

INDEX

ABSTRACT

Cancer constitutes a serious threat to human health and life. Due to the increase of aging of the population, environmental degradation, unhealthy living habits and other factors, the incidence of cancer is on the rise throughout the world.

1,3,4-oxadiazole derivatives are widely used in the research of antineoplastic drugs. On the basis of previous work, 16 new 1,3,4-oxadiazole compounds with different structural types were designed and synthesized on the basis of 2j, in order to obtain new efficacious anticancer with low toxicity and side effects.

In the present research, the CCK-8 method was utilized to screen 16 newly synthesized anti-tumor small molecules, for antiproliferative activity using three separate cell lines Hela, McF7, and PC-3. The results showed that 7FB, 16FB, 8VDB, 22VDB, and 23VDB had a significant inhibitory effect on tumor cell lines. These compounds were tested in order to evaluate their effects on cell cycle progression. The results indicated that all the small molecules tested caused cell cycle arrest at G2/M phase in a time-dependent manner in Hela and PC-3 cells.

In order to further study 2j and its derivatives possible targets and identify molecular mechanisms, the differentially expressed genes were determined after 2j, 16FB and 8VDB treatment. RNA-seq was performed and data were analyzed using functional (GO term) and pathway (KEGG) enrichment of the differentially expressed genes (DEGs). The hub genes of anti-tumor small molecules were determined by the analysis of protein-protein interaction networks. This CMap information provided insight into the model action of anti-tumor small molecule drugs.

Using $|\log2FC| > 2$, and $p < 0.05$ as the screening criteria for differentially expressed

genes we compared 2j, 16FB, and 8VDB treatment at different time points and used functional (GO term) and pathway (KEGG) analysis to show that the enrichment results for the three small molecules were similar. Although the hub genes of the top 15 sorted genes were different, the function and signal pathways involved were the same for all three small molecules when the total differentially expressed genes were analyzed together. 2j and its derivatives 16FB, 8VDB affect biological processes such as regulation of mitotic cell cycle phase transition, microtubule-based process, DNA damage checkpoint, and positive regulation of cell death. Specifically, FoxO signaling pathway, apoptosis, p53 signaling pathway, cellular senescence and other signaling pathways that inhibit the proliferation of cells and eventually led to cell death of tumor cell lines.

In conclusion, experimental results showed that 2j and its derivatives mainly caused tumor cell death through G2/M phase arrest. The DEGs identified by RNA-seq and the gene network hubs furthered the understanding of the molecular mechanism of action of 2j and its derivatives. The results showed that 2j and its derivatives were tubulin inhibitors, mainly affected tumor cells through the cell cycle, FoxO signaling pathway, and apoptotic and p53 signaling pathways. Based on STRING analysis of function gene networks, hub genes were identified and the small molecular targets obtained by CMap comparison, the possible targets of 2j, 16FB and 8VDB could be TUBA1A, TUBA4A, and TUBB. Molecular docking results indicated that 2j interacted at the colchicine-binding site on tubulin.

1 . Background

1.1 Cancer

In 2017, cancer was the second leading cause of death worldwide. Although cardiovascular disease is still the primary cause of death among middle-aged people worldwide, cancer kills more than twice as many people in wealthier countries, and is likely to become the leading cause of death in the coming decades as death rates from heart-related diseases continue to decline (Dagenais, Leong et al. 2019, Yusuf, Joseph et al. 2019). The 2018, global cancer statistics show that lung, breast and colon cancer account for one-third of global cancer incidence and death rate. In terms of global cancer morbidity and mortality, men are at higher risk than women, and among men, lung cancer is the most commonly diagnosed cancer. Due to poor prognosis, the death toll is 1.8 million, accounting for 18.4% of all cancer deaths, the incidence is followed by prostate and colorectal cancer while the mortality rate is followed by liver and gastric cancer. Breast cancer is the leading cause of death in women, the incidence is followed by colorectal, lung and cervical cancer (Bray, Ferlay et al. 2018).

In 2018, the number of new cancer patients in the world has exceeded 18.1 million, which is a significant increase compared to 12.7 million people in 2008. Over the same period, the number of deaths among cancer patients has also increased, in specific from 7.6 million to 9.6 million (Bray, Ferlay et al. 2018). The rapid growth of global cancer morbidity and mortality may be linked to rapid population growth, population ageing, and socioeconomic development. In fast-growing economies, the pathogenesis of cancer is also changing. Cancer can result from a variety of known risk factors, such as living environment, lifestyle and genetic factors, of which environmental factors are the most important and preventable. The major cancer risk factors currently known include smoking, being overweight, pathogenic infections,

UV radiation, lack of physical activity, and lifestyle changes due to economic progress (Jha 2009, Bray, Jemal et al. 2012, Bray and Soerjomataram 2015).

1.2 Oxadiazole derivatives with antitumor activity

Although the research on cancer has made remarkable progress in recent years, the treatment of cancer is still a worldwide problem due to the shortcomings of existing anti-tumor drugs (Guengerich 2011). The main problems correlated to these current treatments are strong side effects, poor selectivity and drug resistance. Therefore, the focus of the current research and development is shifting to targeted drugs that are specifically able to aim the abnormal molecular signaling in tumor cells. To overcame the disadvantages of traditional cytotoxic drugs, target-specific anti-tumor drugs which discriminate between normal cells and tumor cells are under development (Baudino 2015, Dieterich and Detmar 2016, Gandalovicova, Rosel et al. 2017). With the emergence of high-throughput screening and combinatorial chemistry, the development of novel anticancer drugs increased dramatically. However, chemotherapeutic drugs often lead to systemic toxicity, drug resistance, adverse reactions, all leading to failure of tumor chemotherapy. Therefore, the development of new anticancer drugs with strong efficacy, superior tolerability and high safety is urgent (Gerber 2008, Vera-Badillo, Al-Mubarak et al. 2013, Rodriguez-Enriquez, Gallardo-Perez et al. 2014, Perez-Herrero and Fernandez-Medarde 2015).

Oxadiazole is a five-membered heterocycle that can be used as a general lead compound in the design of a variety of drugs (Vaidya, Jain et al. 2016). Oxadiazole is classified into four isomers according to the position of nitrogen in the five-membered heterocyclic ring. Among them, 1,3,4-oxadiazole is the most widely used (Khalilullah, Ahsan et al. 2012). Compared with other isomerized oxadiazole, 1,3,4-derivatives show higher water solubility, lower lipophilicity and metabolic stability(Figure 1).The

properties of 1,3,4-oxadiazoles enable them to bind effectively to growth factors, enzymes, kinases and receptors in biological systems. This class of compounds has properties: anticancer (Glomb, Szymankiewicz et al. 2018), antibacterial (Janardhanan, Chang et al. 2016), anti-tuberculosis (De, Khambete et al. 2019), anti-inflammatory (Chawla, Naaz et al. 2018), and antiviral activity (Benmansour, Eydoux et al. 2016). 1,3,4-oxadiazole derivatives have a wide range of functions and therefore are good candidates for future anticancer drugs (Bajaj, Asati et al. 2015).

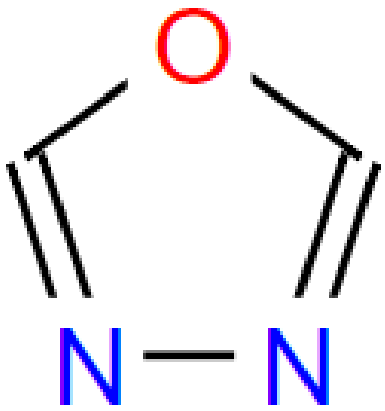

Figure 1. 1,3,4-oxadiazole

1.2.1 Inhibition of tumor angiogenesis

Since Folkman put forward the concept of tumor neovascularization, the research on inhibitors of tumor neovascularization has made great progress (Weidner and Folkman 1996, Folkman 2006). The growth, invasion and metastasis of tumor depend on the formation of neovascularization. Anti-tumor neovascularization therapy is an important tool for tumor therapy. Vascular endothelial growth factor (VEGF) is an important angiogenic factor, which is closely related to the occurrence and

development of tumors and plays an important role in the occurrence and development of tumors. VEGF and VEGFR are the most common anti-angiogenic research targets, which can promote tumor angiogenesis, tumor cell proliferation, tumor cell invasion and metastasis. Therefore, VEGF and its receptor VEGFR have become important targets for anti-tumor angiogenesis. VEGF and its receptor VEGFR are targeted to inhibit angiogenesis in tumor tissues by blocking the VFGF/VEGFR signaling pathway, thereby blocking the nutrient source and migration pathway of tumor, so as to achieve the purpose of tumor therapy (Weidner and Folkman 1996, Kieran, Kalluri et al. 2012, Young and Reed 2012, Miller 2016).

Akhilesh Kumar et al. synthesized a new series of 1,3,4 oxadiazoles, in the synthesized derivatives, 1a and 1b had significant anti-proliferation and anti-angiogenic effects. The mechanism may be mediated by downregulation of VEGF and inhibition of translocation of HIF-1α in tumor cells (Kumar, D'Souza et al. 2009).

Alexander S. Kiselyov and collaborators synthesized a series of novel ((pyridine-4-yl)ethyl) pyridine derivatives that are active against kinase VEGFR-1 and-2 by changing the aromatic amino substituents on 1,3,4-oxadiazole ring. Based on previous experiments, it was found that these compounds were similar to the reported clinical and candidates drugs PTK787 (Vatalanib TM) (Kiselyov, Semenova et al. 2006).

1.2.2 Targeting tyrosine kinase

The protein kinase family, protein tyrosine kinases (PTKs) can be divided into two categories: receptor tyrosine kinase (RTK) and non-receptor tyrosine kinase (NRTK) (Mano 1999). PTKs play an important role in cell signal transduction, and their function is closely related to tumors by transferring the phosphate group from ATP to

the tyrosine residue of a downstream protein and making it phosphorylated. Since the function of tyrosine kinase is closely related to tumors, several anti-tumor drugs targeting PTKs have emerged in the past few years and they are characterized by high selectivity and low toxicity (Boutayeb, Zakkouri et al. 2012, Jiao, Bi et al. 2018). Currently, several receptor and non-receptor tyrosine kinases have been targeted for anti-tumor drug screening, including epidermal growth factor receptor (EGFR) (Lee, Shiao et al. 2014, Singh, Attri et al. 2016), fibroblast growth factor receptor (FGFR) (Porta, Borea et al. 2017), and platelet-derived growth factor receptor (PDGFR) (Papadopoulos and Lennartsson 2018).

KaiLiu et al. used AutoDock Tools to screen 2-mercaptan-5-aryloxy diazole derivatives. The results showed that these 2-mercaptan-5-aryloxy diazole derivatives had strong EGFR inhibitory activity. Therefore, according to the previous results, a series of 2-(benzyl sulfide) -5-aroxydiazole derivatives were designed and synthesized, and the inhibitory activity of EGFR was evaluated. It was found that among the synthesized compounds, 3e had strong inhibitory activity on tumor growth inhibition, based on this 3e might be a promising lead compound against tumor growth (Liu, Lu et al. 2012).

1.2.3 Targeting histone deacetylases

Epigenetic regulation affects gene expression without changing the DNA sequence, and its abnormal regulation is involved in the occurrence and development of tumors, inflammation and metabolic diseases. Among them, histone acetylation plays an important role in the epigenetic regulation of cancer, and the imbalance of histone and non-histone acetylation is crucial in the tumor progression (Ropero and Esteller 2007). Therefore, histone acetylation is considered an important novel target for tumor therapy (Schizas, Mastoraki et al. 2018). Histone deacetylase inhibitor (histo &

edeacetylase inhibitor, HDACi) is able to induce tumor cell differentiation, inhibit tumor cell cycle, induce DNA damage and tumor cell death by regulating the process of acetylation and deacetylation in nucleus. Collectively, it has become a new hot spot in the field of antitumor target therapy. According to the different structure of HDACi, it can be divided into four categories: hydroxamic acids, benzamides, fatty acids and cyclic peptides. HDACi has significant effects on apoptosis, autophagy and programmed death pathway of tumor cells (de Ruijter, van Gennip et al. 2003, Falkenberg and Johnstone 2014, Lakshmaiah, Jacob et al. 2014).

Sergio Valente and collaborators synthesized hydroxylamines and 2-aminolines containing 1,3,4-oxadiazole (Valente, Trisciuoglio et al. 2014). Among them, 2t, 2x and 3i are characterized by selectivity and by the ability to inhibit HDAC1. In U937 leukemia cells, 2t had the strongest ability to induce apoptosis. When combined with doxorubicin in acute myeloid leukemia (AML), cell lines and U937 cells, 3i showed the same efficacy as ms-275, which is considered one of the most potent HDACi in cell differentiation.

1.2.4 Targeting key signaling pathways in cancer development

Malignant tumor occurs when cells undergo genetic changes that enable them to proliferate infinitely. The proliferation of cells is regulated by signaling pathways, and unlimited proliferation of tumor cells is often due to problems in signaling pathways. Several key signaling pathways associated with cancer development include: NF-κb signaling pathway, Raf/MEK/MAPK signaling pathway, p53 signaling pathway, Wnt signaling pathway, PI3K/Akt/mTOR signaling pathway, JAK-STAT signaling pathway, and more (Chalhoub and Baker 2009, He and Karin 2011, Gentzler, Altman et al. 2012, Calon, Tauriello et al. 2014, Hu and Hu 2018). Changes in key regulatory factors in these signaling pathways will lead to carcinogenesis of cells, promote tumor

cell proliferation and mediate tumor cell invasion and migration. Therefore, these crucial signaling pathways associated with tumorigenesis have become important targets for anti-tumor research.

Chakrabhavi Dhananjaya Mohan et al. synthesized a series of 1,3,4-oxadiazole compounds with 2-(3-chlorobenzo [b] thiophen-2-yl)-5-(3methoxyphenyl)-1,3,4 oxadiazole (CMO) as lead compounds. The effects of CMO on cell cycle, apoptosis and phosphorylation of NF-κB signaling pathway proteins in hepatocellular carcinoma cells were investigated. It was noted that CMO could induce apoptosis and inhibit cell proliferation in a time- and dose-dependent manner. In addition, CMO was able to inhibit transcriptional activity and DNA binding ability of NF-κB. The results suggest that CMO is an inhibitor of the NF-κB signaling pathway (Mohan, Anilkumar et al. 2018).

1.2.5 Targeting Immune checkpoint inhibitor

B7 is an indispensable family of costimulatory molecules for activation of T cells. Programmed death ligand-1 (PD-L1) is one member of this family. PD-L1 is widely expressed in activated T cells and B cells, thymic endothelial cells, dendritic cells, macrophages and cancer cells, and can be induced by cytokines. Programmed death receptor-1 (PD-1) is the receptor of PD-L1, which is widely expressed on thymocytes, activated mature T cells, B cells and myeloid cells. The binding of PD-L1 to the receptor PD-1 on the surface of activated T cells can inhibit the response of T cells by inducing apoptosis and blocking cell cycle. Up-regulated expression of PD-L1 was found in several cancers including leukemia, multiple myeloma, myelodysplastic syndrome and other hematological tumors, as well as in bladder cancer, gastric cancer, renal cell carcinoma, lung cancer, liver cancer, melanoma and other solid tumors. The prognosis of patients with high expression of PD-L1 is poor(Tamura, Ohira et al.

2015). The high expression of PD-1 could also be detected on the surface of tumor-specific T lymphocytes. Definitely, the higher the expression of PD-1, the more obvious the inhibition of T cell function. Inhibition of PD-1 and CTLA-4 can prevent T cells exhaustions and enhance anti-tumor immunity, which provides a new strategy for immunotherapy of human tumors (Buchbinder and Desai 2016, Li, Li et al. 2016, Alsaab, Sau et al. 2017). At present, various small molecule inhibitors of PD-1/PD-L1 are in different stages of preclinical development (Dhanak, Edwards et al. 2017). Sasikumar et al. designed and synthesized 1,3,4-oxadiazole derivatives which can be used as immunomodulators, as they are able to effectively inhibit PD-1 signal pathway (Sasikumar December 25, 2018.).

1.2.6 Telomerase inhibitor

Telomeres are composed of telomere DNA and telomere binding protein (TBP) in normal somatic cells, gradually shorten with cell divisions and eventually lead cells to apoptosis. Telomeres have the function of maintaining chromosome stability and genome integrity and are involved in the localization of chromosomes in the nucleus and the regulation of gene expression. It is a special reverse transcriptase, which can use its own RNA as a template to reverse the repeat unit of telomere to the end of human chromosome, preventing telomere from shortening with cell division. It is inactivated in most somatic cells, so in normal cells, proliferation and apoptosis is a normal or controlled process (Zvereva, Shcherbakova et al. 2010, Podlevsky and Chen 2012). Tumor cells can proliferate infinitely and immortalization has an important relationship with telomerase activity. By prolonging the G-protruding portion of the telomere, the infinite proliferation of cells ensues and the maintenance of the telomere length is preserved. Telomerase activation in tumor cells prevents the telomere of tumor cells from shortening through cell divisions. It blocks the normal replication-decay mechanism of cells. Telomerase reactivation was observed in at

least 90% of human advanced tumors, while there was almost no telomerase activity in normal cells or tissues (Jafri, Ansari et al. 2016). Consequently, the inhibition of telomerase activity can induce telomere shortening and eventually lead to cell senescence and apoptosis. The inhibition of telomerase activity is of great significance for the prevention and treatment of tumor and has gradually become a target for the treatment of malignant tumor (Harley 2008, Mocellin, Pooley et al. 2013, Ruden and Puri 2013).

Current literature investigation suggests that 1,3,4-oxadiazole is a promising anticancer drug lead compound. Its mode of action appears to be through inhibition of telomerase activity. Marco Tutone et al. synthesized a series of 1,3,4-oxadiazole derivatives, which have significant broad-spectrum anticancer activity in different cell lines. In addition, quantitative structure-activity relationship analysis showed that these derivatives have telomerase inhibitory activity (Tutone, Pecoraro et al. 2018). Shalini Bajaj et al. found that 1,3,4-oxadiazole derivatives are characterized by good anti-telomerase activity, and their mechanism is related to the inhibition of different kinases, enzymes and growth factors (Bajaj, Roy et al. 2018).

1.2.7 Targeting cell cycle-related proteins and DNA damage system

Cell cycle regulation is closely related to physiological and pathological processes. One of the most basic biological characteristics of malignant tumor is malignant transformation and uncontrolled proliferation of tumor cells caused by discordant cell cycle regulation. Cell division and proliferation is driven and controlled by cyclins and their dependent kinase (CDK) (Malumbres 2014). Overexpression or abnormal activity of Cyclin, CDK, loss of CDK inhibitor, (CKI) expression and abnormal detection points are important factors in the pathogenesis of cancer (Sanchez-Martinez, Lallena et al. 2019). Therefore, the recovery of tumor cell cycle

regulation has become a potential target of anti-tumor drugs. In tumor cells, the enhancement of CDK activity will lead to uncontrolled cell, genomic instability, and chromosome instability (Vermeulen, Van Bockstaele et al. 2003, Asghar, Witkiewicz et al. 2015). Therefore, CDKs have always been regarded as a good target for the treatment of tumors and other proliferative disorders. CDK inhibitors are able to block the cell cycle and control cell proliferation (Malumbres and Barbacid 2009, Vijayaraghavan, Moulder et al. 2018).

JieRen et al. found that 4 β-(1,3,4-oxadiazole 2 amino5 methyl)-4-deoxypodophyllotoxin (OAMDP) was characterized by cytotoxic and anti-tumor activity. After treatment with OAMDP, S phase arrest or G2/M phase arrest was induced through regulation of cell cycle regulatory proteins, and autophagy could be induced, leading to cell cycle arrest and apoptosis (Ren, Liu et al. 2018).

Microtubules are important components for the cytoskeleton, they are dimers composed by two different type of tubulin subunits, which form a long tubular unit structure. Under normal physiological conditions, microtubule structure is in a dynamic equilibrium state of "depolymerization-polymerization" (Conde and Caceres 2009). Microtubules play an important regulatory role in physiological activities, such as maintaining cell morphology, participating in cell signal transduction, intracellular material transport, organelle transport and cell division (Kavallaris 2010). The most important characteristic of tumor cells is the uncontrolled and unlimited proliferation, and this process depends on the activity of intracellular tubulin. Destroying the dynamic balance of tubulin is an important way to inhibit the growth of tumor cells. Therefore, tubulin has become an important target for the research and development of anticancer drugs (Jordan and Wilson 2004, Dumontet and Jordan 2010, Zhao, Mu et al. 2016, Tangutur, Kumar et al. 2017, Kaul, Risinger et al. 2019). Currently, the known tubulin inhibitors can be divided into two categories: one is tubulin aggregates

that promote tubulin polymerization and the representative drugs are paclitaxel compounds, the other category is tubulin depolymerization agents, which inhibit tubulin polymerization. The representative drugs are vinblastine and colchicine.

A series of new 1,3,4-oxadiazole compounds were recently synthesized and their cytotoxicity was evaluated in an *in vitro* tumor model (Nieddu, Pinna et al. 2016). Four new compounds 2d, 2j, 2k and 2n showed growth inhibition in XTT test. The most active compound 2j showed high antitumor activity, IC 50 in the range of 0.05 -1.7 μM for different tumor cell lines (Figure 2). Cell cycle assays showed that compound 2j could induce G2/M arrest of cell cycle and had strong apoptotic activity as well. Immunofluorescence analysis showed that compound 2j is effectively able to inhibit the microtubule formation in cancer cell lines and lead to abnormal spindle formation, but it had no effect on normal human fibroblasts NB1, MRC-5 and IBR3. For these reasons, compound 2j is identified as a possible candidate for chemotherapy (Nieddu, Pinna et al. 2016).

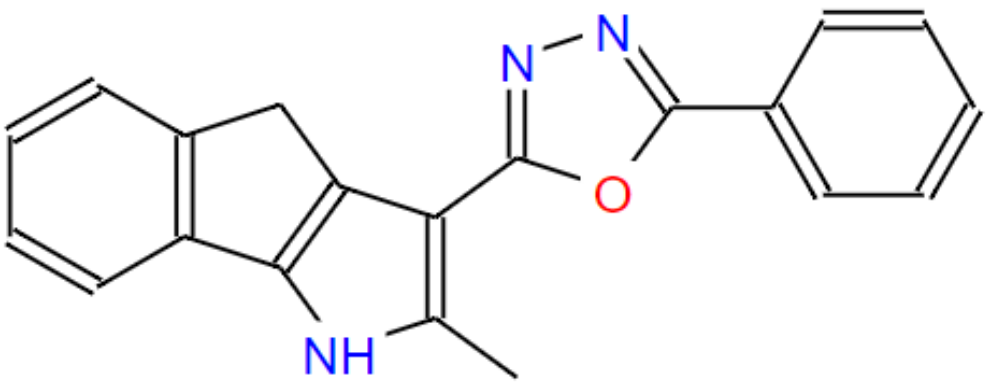

Figure 2. Novel Unsymmetrical 1,3,4-oxadiazoles 2j (Nieddu, Pinna et al. 2016).

1.3 Target Verification of small Molecular compounds

As a result of the continuous acceleration of drug discovery process, the uninterrupted

progress of synthesis technology and high through put screening technology, a large number of active small molecule compounds can be synthesized, however, their targets and mechanisms have not yet been elucidated. This has resulted in a lag in the research and development of new drugs. Drug targets are biological macromolecules in the body that can be acted on by drugs, such as certain proteins and nucleic acids. The discovery process of drug targets is mostly attributed to screening proteins that interact with drugs. This provides important clues to analyze the related signal transduction pathway and possible modes of action. Targeted drug molecules are not only conducive to further exploration of mechanisms in related basic research fields, but also helpful to clinical observation of drug metabolism.

Currently, target identification of small molecule compounds is mainly divided into two main strategic methods: direct method and indirect method. The direct method is identified by the covalent or non-covalent binding between small molecule compounds and proteins, followed by affinity purification or visualization. It mainly includes affinity chromatography and chemical probe technology (McFedries, Schwaid et al. 2013). Indirect methods and strategies mainly include a variety of analytical methods. The two types of target identification methods have their own advantages and disadvantages, and can complement each other in practical operations (Jung and Kwon 2015, Chang, Kim et al. 2016).

With the development of genomics, transcriptome, proteomics, metabolomics and bioinformatics integration with multifactorial data, bioinformatics can play a key role in the discovery and identification of drug targets (Essebier, Lamprecht et al. 2017). The advantage of bioinformatics in the discovery and identification of drug targets is that it can integrate data from different databases and it is able to screen and analyze the functions of drug targets from an overall perspective, so as to evaluate the medicinal properties of drug targets and the potential side effects of drugs (Olsen,

Campos et al. 2014, Haanstra and Bakker 2015, Koeberle 2016). The main purpose of this study is to use transcriptomics to identify and verify the target of small molecule drugs and gain insight into the mechanism of action. Transcriptomic studies on gene function and gene structure at the overall level can reveal the precise molecular mechanisms of biological and disease processes. Transcriptome sequencing (RNA-seq) is a technical method used in transcriptome research where next generation sequencing techniques of randomly generated RNA species are performed. Because of its high sensitivity, high efficiency and high throughput RNA-seq technology has gradually replaced gene chip technology to study gene expression at the transcription level, and has been widely used in biology, medical research, clinical research and drug development. In this technique, the transcript is first reverse transcribed into a cDNA library, and then the DNA in the cDNA library is broken into small fragments and sequenced using a next generation sequencers. The resulting sequences are aligned or assembled from the beginning to form a complete transcriptional expression profile (Hrdlickova, Toloue et al. 2017).

An important challenge in drug discovery is to establish links between diseases, basic and clinical, and drugs. In 2006, Lamb et al constructed a correlation map (connectivity map, CMap) dataset based on the whole genome expression profile data of 1309 drugs acting on five human cancer cell lines, compared with pharmacology, toxicology and chromatographic techniques (Lamb 2007). This technology has the advantages of being comprehensive, high-throughput and accurate. Through the comparative analysis of gene expression profile imprinting under different physiological, pathological and drug effects, the relationship between gene-disease-drug was established and was successfully used in drug repurposing and drug discovery (Qu and Rajpal 2012). However, CMap only measures the gene expression profiles of more than 1,300 drugs in five cell lines, which limits its potential application. Library of Integrated Network-based Cellular Signatures

(LINCS) is based on CMap, the data scale is greatly increased in order to measure the changes in the transcriptome caused by different stimuli on greater numbers of cell lines to obtain greater numbers of expression profile data for association network analysis. Data of LINCS cell expression profile can be directly used to predict anticancer drugs by using the expression profile of small molecule compounds of interest; it can also be combined with the expression profile data of gene silencing and overexpression to identify the potential targets of anticancer drugs and identify the potential targets of small molecule compounds (Liu, Su et al. 2015). After years of development, CMap has been used as a bridge between elementary and system biology, clinical and drug discovery, especially in the field of anticancer drug discovery, such as drug precursor discovery, drug repositioning, and model of drug action (Musa, Ghoraie et al. 2018).

2 . Objectives

1,3,4-oxadiazole as a common heterocycle structure, is characterized by a wide range of biological activities, and an extensive range of applications in the research of antineoplastic drugs. In the initial stage of the project, different structural types of 1,3,4-oxadiazole compounds were designed and synthesized and it was discovered that they had a strong inhibitory activity against a variety of tumor cell lines. 2j, the most active drug showed high antitumor activity in different tumor cells, IC50 in the range of 0.05-1.7 μM (Nieddu, Pinna et al. 2016). Based on the previous work, this thesis aimed to utilize various new synthesized structural types of 1,3,4-oxadiazole compounds on the basis of 2j, in order to obtain a new type of anticancer drugs with good activity, high drug formation and low toxicity and side effects.

Cell cycle detection showed that compound 2j could induce G2/M cell cycle arrest

and had a strong apoptotic response, but the target and functional activities of 2j is unknown. In this thesis, it was hypothesized that 2j and 2j developed derivatives work by altering the cell cycle. Furthermore, it was proposed that cell cycle analysis and analysis of gene transcription profiling of cells treated with 2j and 2j derivatives could provide important insight regarding the target and mechanism of action.

Hela, PC-3, and McF-7 cells were selected as the main research cell lines of this project. Based on the previous work, the goal of this research is the utilization of 16 recently designed and synthesized new 1,3,4-oxadiazole compounds. Hela, PC-3, and McF-7 cells were treated with different doses of 2j and 2j derivatives at different times, respectively, to determine the time-effect and dose-effect relationships of their inhibition on tumor cells. The effects of 2j and 2j derivatives on the cell cycle of tumor cells were analyzed by flow cytometry. RNA-seq was used to analyze the influence of 2j and 2j derivatives on the transcriptome expression changes of Hela cells, to explore the mutual regulation relationship between differentially expressed genes, and to analyze the protein interaction network between differentially expressed genes. The obtained differentially expression genes were classified into positive and negative regulatory gene groups and compared with the gene expression maps of drugs or compounds in the CMap database. The highly correlated drug molecules were determined by the degree of correlation gene expression maps of drug molecules, and the possible targets and mechanisms of action of 2j and 2j derivatives. The relationship between small molecule drugs and target was further verified by molecular docking technology (Figure 3). The expectation is that the target of these compounds can be predicted by the method of bioinformatics, and the target and molecular mechanism of these compounds can be studied, so as to lay a foundation for further active research.

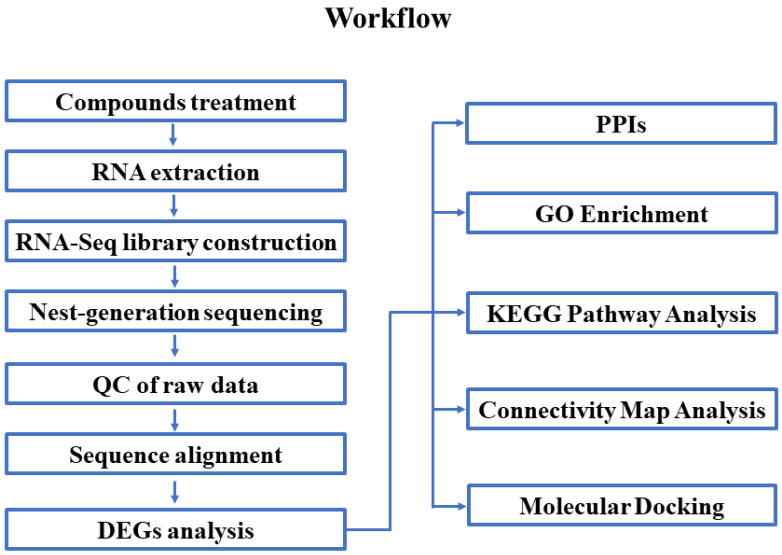

Figure 3. RNA-Seq analysis workflow

3 . Materials and methods

3.1 Cell culture and medium

Human cervical cancer cell line Hela, human prostate cancer cell line PC-3, and human breast cancer cell line MCF7 were obtained from the China Center for Type Culture Collection (CCTCC), and respectively maintained in F-12K, RPMI-1640, and DMEM medium (GIBCO) supplemented with 1% penicillin/streptomycin (Thermo) and 10% FBS (GIBCO). Cells were incubated at 37° and 5%CO_2.

3.2 Detection of the effect of compounds on the proliferation of tumor cells by CCK-8 assay

Hela, PC-3, and MCF7 cells in logarithmic growth phase were digested by trypsin, and a small amount of cell suspension was counted by adding the appropriate amount

of complete culture medium to resuspend the cells. According to the counting results, the cell density was adjusted to 2×10^4/mL, and then a 100 μL diluted cell suspension was added to each well of the 96 well plates. The 96 well cell culture plate was cultured in the incubator at 37° for 12 hours. After the tumor cells adhered to the well, the medium was replaced with fresh medium containing different concentrations of compounds. Dimethyl sulfoxide (DMSO), the vehicle to solubilize the molecules, was used as negative control group. After adding CCK-8 solution to each well, the cell culture plates were incubated at 37° for 2-4 hours. The absorbance value at 450nm was determined. The inhibition rate of cell proliferation was calculated according to the absorbance values of the experimental group, blank control group and negative control group. IC50 values were calculated by IC50 Calculator.

3.3 Cell cycle detection

Hela and PC-3 cells were digested by trypsin, and seeded in 6-well plates (2×10^5 cells/well). Twelve hours later, different compounds with a final concentration of 1 μM were added. After compound treatment, cells were collected and centrifuged at 1000rpm for 5 minutes, the supernatant was carefully sucked out and washed with PBS. After the cells were fixed with 75% ethanol, they were centrifuged at 1000rpm for 5 minutes, the supernatant was carefully removed and washed twice with PBS. 0.4ml propidium iodide staining solution (4ABiotech) was added to each cell sample and incubated at 37° for 30 minutes. Data was collected by flow cytometry and analyzed by modfit software.

3.4 mRNA Extraction, mRNA-seq Library Preparation, and Sequencing

Hela cells were digested with trypsin and seeded in 6-well plates (2×10^5 cells/well).

After 12 hours, 1 μM of the compounds and the blank control fresh medium were added (Table 1). The cells were treated at different times and were centrifuged at 1000 rpm for 5 minutes, the supernatant was carefully aspirated, and the cells were washed twice with PBS. After compounds treatment, collected cells were centrifuged at 1000 rpm for 5 minutes and the supernatant was carefully sucked out and washed twice with PBS. Total RNA was extracted with the RNeasy MINI Kit (Qiagen). The quality of total RNA was evaluated using an Agilent 2100 Bioanalyzer. The rRNA in total RNA was removed by RNaseH digestion and Ribosomal-depleted RNA was purified using VAHTSTM RNA Clean Beads. cDNA was synthesized by reverse transcription using random primers, dUTP was incorporated for labeling when synthesizing the second strand of cDNA. 150-200 bp fragment were obtained by magnetic bead purification, prepared libraries PE150 were prepared and were sequenced on the Hiseq500.

Table 1. Compound treatment

	Compound	Concentration	Treatment
1	**2j**	**1 μM**	**Hela (6 h,12 h,18 h)**
2	**16FB**	**1 μM**	**Hela (6 h,18 h)**
3	**8VDB**	**1 μM**	**Hela (6 h, 18 h)**

3.5 Quality Control, sequence alignment and differentially expressed Gene Analysis

Firstly, the raw reads obtained were quality controlled with fastqc. Trimmomatic was utilized to filter the adapter. Successfully, low-quality base and unmeasured base in the original data were used to obtain the final clean data. The hg38 reference genome

(grch38.p12.genome) and gene annotation GTF (GRCh38,version 30,Ensembl 96) were downloaded in genome database. After that, the reference genome and gene annotation files were obtained and used for digital gene expression analysis. STAR alignment and expression level analysis of clean reads obtained by RSEM were performed to obtain gene expression results of each sample. The expression value of a gene is measured in FPKM (fragments per kilo bases per million reads), and FPKM is the number of readings per million reading segments from a gene per 1000 base length. The expression level of the gene was measured by fragments per kilobases per million reads (FPKM). DEseq was used to analyze the different expression of the samples in the control group and the experimental group. The parameter values log2 fold-change and *p* value were set as the significant difference reference indexes. Differential gene screening criteria: $|\log FC| \geq 2$ and p value < 0.05.

3.6 Characterizing differentially expression genes by GO Enrichment , KEGG Pathway Analysis

In order to elucidate the biological process and molecular mechanism of DEGs, pathway enrichment and functional analysis of DEGs were conducted. Gene Ontology database (GO) enrichment and Kyoto Encyclopedia of Genes and Genomes (KEGG) pathway analysis were performed for functional and pathway enrichment. GO is an internationally standardized classification system of gene functions. According to the obtained DEGs, GO function items with significant enrichment can be mined from three levels: biological process, cellular component and molecular function. GO functional classification annotation of DEGs is given by GO functional analysis. On the other hand, GO function significance enrichment analysis of DEGs was given. The main biological functions of DEGs can be determined by GO significant enrichment analysis (Alam-Faruque, Dimmer et al. 2010).

The KEGG database facilitates the study of genes and expression information as a whole network, in fact it integrates data on genome, chemical molecules and biochemical systems, including metabolic pathways, drugs, diseases, gene sequences and genomes. The pathway significance enrichment analysis was based on KEGG pathway and hypergeometric test to find out the pathway that was significantly enriched in the DEGs compared with the whole genome background (Kanehisa 2002, Hashimoto, Goto et al. 2006).

3.7 Identify hub genes and key modules

In order to identify hub Genes and key modules, gene network analysis was performed by using STRING, which contains a database of predicted and experimentally verified protein-protein interactions. The string database extracts protein-protein interactions from experimental data through literature content management, and can also use bioinformatics methods to predict results. The biological methods used include gene fusion, chromosome proximity, phylogenetic tree, gene co-expression of gene chip data. The system uses a scoring mechanism to score the results obtained by different methods by combining the results of differential expression analysis with the interactions between the databases and the differentially expressed genes to construct an interaction network.

3.8 Connectivity Map Analysis of Differentially Expressed Genes

CMap has been extensively utilized to study drug's repurposing, discovery of drug leads, action mode of drugs and more. The gene expression profiles obtained from Hela cells treated with compounds *in vitro* were divided into positive and negative

regulatory gene groups and compared with the gene expression profiles of drugs or compounds in CMap database. According to the correlation degree of drug molecules, the highly related drug molecules were determined and the possible targets and mechanisms of drug molecules were summarized.

3.9 Verification of hub genes

Hela cells were treated with 1 μM of small molecular compounds and total RNA was extracted with Trizol reagent. The purified RNA was used as a template to synthesize cDNA by using Oligo (dT) as primer. The experimental procedure was carried out in accordance with the instructions of the reverse transcription kit. The DEGs were detected by Realtime-PCR (Table 2).

Table 2. Primers for hub genes validated by RT- PCR

Genes	Accession No	Primer	Sequence(5'-3')
IGFBP3	NM_001013398	IGFBP3-F	CGCTACAAAGTTGACTACGAGTC
		IGFBP3-R	GTCTTCCATTTCTCTACGGCAGG
KIFC3	NM_005550	KIFC3 -F	AGGTGGAGATGAAGGCTGTGCA
		KIFC3 -R	GAGCCCATTGTAGTCGTTGGTG
CDKN1C	NM_000076	CDKN1C -F	AGATCAGCGCCTGAGAAGTCGT
		CDKN1C -R	TCGGGGCTCTTTGGGCTCTAAA
TUBA1A	NM_006009	TUBA1A-F	CGGGCAGTGTTTGTAGACTTGG
		TUBA1A-	CTCCTTGCCAATGGTGTAGTGC

		R	
TUBA4A	NM_006000	TUBA4A-F	GGCAAGGAGATCATTGACCCAG
		TUBA4A-R	CATCAGGAGTGAGGTGAAGCCA
CDK6	NM_001259	CDK6-F	GGATAAAGTTCCAGAGCCTGGAG
		CDK6-R	GCGATGCACTACTCGGTGTGAA
TUBB	NM_178014	TUBB-F	CTGGACCGCATCTCTGTGTACT
		TUBB-R	GCCAAAAGGACCTGAGCGAACA
TUBB4B	NM_006088	TUBB4B-F	TTGGGAGGTGATCAGCGATGAG
		TUBB4B-R	CTCCAGATCCACGAGCACGGC

3.10 Molecular Docking

The crystal structure of tubulin was downloaded from RCSB PDB (extraction code: 5H7O) (Arnst, Wang et al. 2018), the original ligands and water molecules were removed from the crystal structure, they were hydrogenate, the point charge was calculated, and finally, ChemDraw software was used to map the molecular structure of compound 2j and perform energy optimization. The docking model of compound 2j and tubulin was simulated by AutoDuck4.2. Default parameters and Lamarck genetic algorithm were used for docking. The docking results were analyzed by PyMOL.

4. Results

4.1 Drug screening

4.1.1 CCK-8 screening of antineoplastic compounds

CCK-8 kit is a rapid and high sensitivity kit based on WST-8, widely used for the detection of cell activity and cytotoxicity to determine the number of living cells in cell proliferation or to perform toxicity experiments. In this study, 16 potential anti-tumor small molecules were screened by the CCK8 method. Hela, McF7 and PC-3 cell lines were chosen based on the origins or each cell lines and the use in previous drug studies. The candidate drugs were used at 2 μM for 48 hours. The results showed that 7FB, 16FB, 8VDB, 22VDB and 23VDB had significant inhibitory effects on Hela, McF7 and PC-3 (Figure 4). The IC50 on Hela cells was found to be 0.324 μM, 0.145 μM, 0.009 μM, 0.005 μM, and 0.083 μM, for each compound respectively. The IC50 on PC-3 cells was found to be 0.38 μM, 0.176 μM, 0.072 μM, 0.067 μM, 0.548 μM for each compound, and the IC50 of McF-7 cells was found to be 0.555 μM, 0.468 μM, 0.176 μM, 0.091 μM and 0.216 μM, respectively (Table 3). Subsequent experiments selected Hela, which is more sensitive to drug treatment, as the target cell line, in order to discover the mechanism of action of these anti-tumor drug candidates.

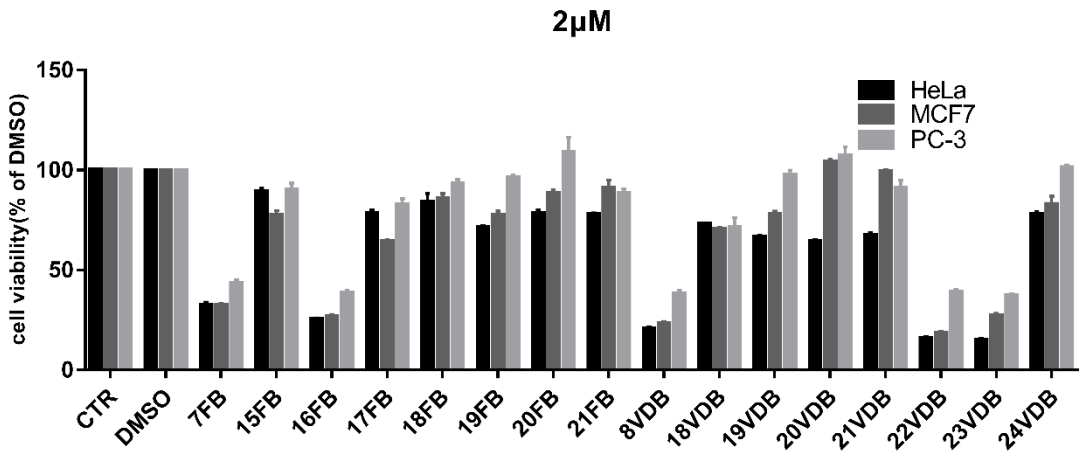

Figure 4. Inhibition of tumor cell proliferation *in vitro* as determined by CCK-8 assay (48 hours). The results showed that 7FB, 16FB, 8VDB, 22VDB and 23VDB had significant inhibitory effect on Hela, McF7and PC-3.

Table3. Detection of the inhibitory effect of candidate small antineoplastic molecules on the proliferation of Hela, McF7 and PC-3

	Hela IC_{50} (μM)	PC-3 IC_{50} (μM)	McF7 IC_{50} (μM)
7FB	**0.324**	**0.380**	**0.555**
16FB	**0.145**	**0.176**	**0.468**
8VDB	**0.009**	**0.072**	**0.176**
22VDB	**0.005**	**0.067**	**0.091**
23VDB	**0.083**	**0.548**	**0.216**

4.1.2 Cell cycle

The cell cycle refers to the process by the end of the previous division to the end of the next division, which is usually composed of G0/G1 phase, S phase, and G2/M phase. Cell-cycle aberrations are a hallmark of cancer, consequently, a crucial goal of

anti-cancer drugs, is to inhibit the proliferation of tumor cells by blocking cell cycle progression. In this study, DNA content cell cycle analysis by flow cytometry was evaluated in Hela cells and PC-3 cells after treatment with 2j, 7FB, 16FB, 8VDB, 22VDB and 23VDB respectively.

From the results (Figure 5), in Hela cells compared to the DMSO control, the G2/M phase increased by 75.65% when they were treated with 2j for 18 hours; the G2/M phase increased by 41.98% when treated with 7FB for 18 hours; the G2/M phase increased by 74.46% when treated with 16FB for 18 hours; the G2/M phase increased by 74.05% when treated with 8VDB for 18 hours; the G2/M phase increased by 70.94% when treated with 22VDB for 18 hours; the G2/M phase increased by 74.87% when treated with 23VDB for 18 hours. From the results B (Figure 6), in PC-3 cells compared to the DMSO control, the G2/M phase increased by 78.13% when treated with 2j for 18 hours; the G2/M phase increased by 46% when treated with 7FB for 12 hours; the G2/M phase increased by 77.9% when treated with 16FB for 12 hours; the G2/M phase increased by 77.47% when treated with 8VDB for 12 hours; the G2/M phase increased by 78.82% when treated with 22VDB for 12 hours; the G2/M phase increased by 74.64% when treated with 23VDB for 12 hours. In summary, 2j and its derivatives 7FB, 16FB, 8VDB, 22VDB, 23VDB are able to induce G2/M arrest of Hela and PC-3 cells in a time-dependent manner.

A

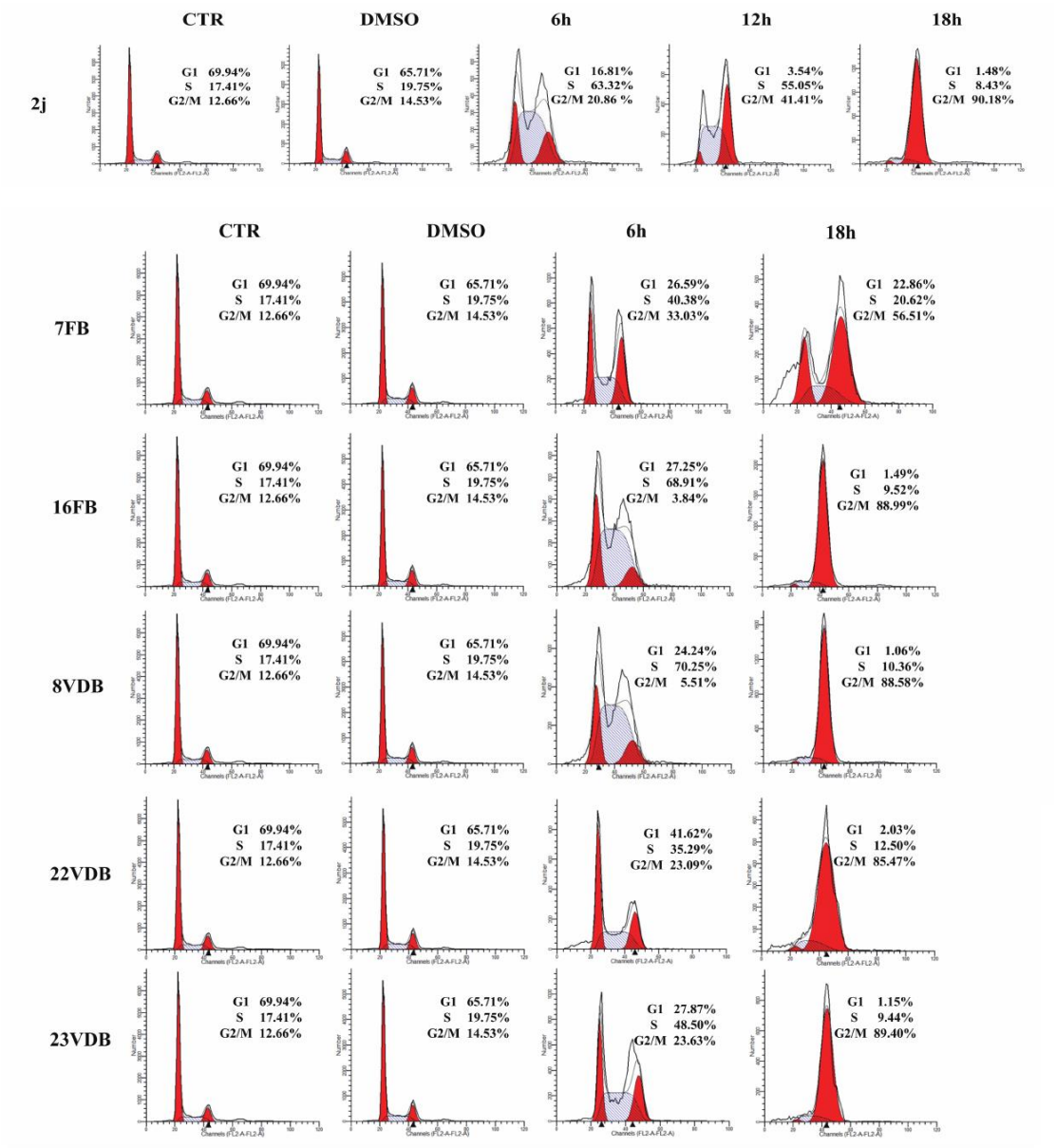

Figure 5. Cell cycle analysis of Hela treated with control, DMSO and compound treatment (2j, 7FB, 16FB, 8VDB, 22VDB, and 23VDB) for different lengths of time (hours).

B

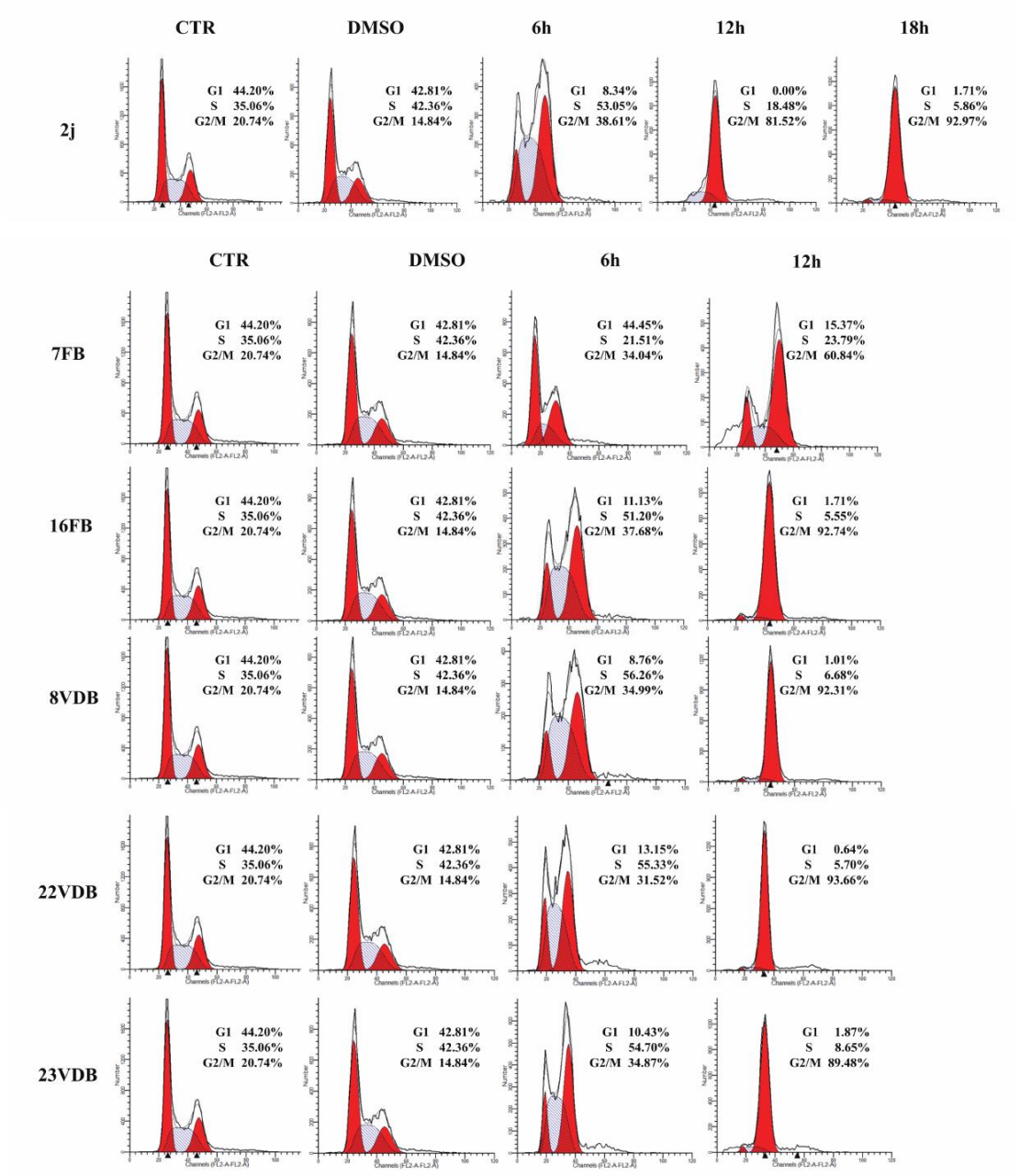

Figure 6. Cell cycle analysis of PC-3 treated with control, DMSO and compound treatment (2j, 7FB, 16FB, 8VDB, 22VDB, and 23VDB)for different lengths of time (hours).

4.2 Compounds treatment, RNA extraction and sequencing

After compounds treatment, total RNA was extracted with the RNeasy MINI Kit (Qiagen) and eluted in RNAase free water, 1% agarose gel electrophoresis was used to detect the total RNA extracted. The results show that 28S and 18S rRNA bands can be clearly seen (Figure 7). Agilent 2100 results showed that the extracted RNA RIN (RNA integrity number) values were greater than 9.5 (Figure 8), OD260/280nm between 1.8-2.1, the indicators met the RNA-seq database requirements. Sequencing was completed by Novogene Company.

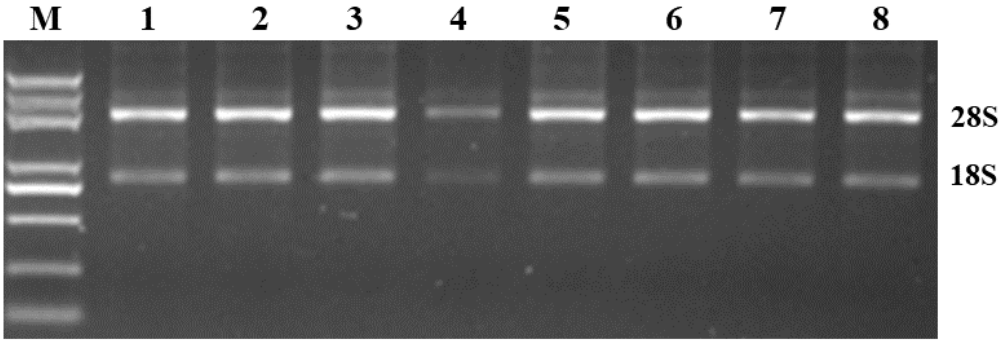

Figure 7. Total RNA detection by agarose gel electrophoresis.

1.DMSO; 2:2j 6 hours; 3:2j 12 hours; 4:2j 18 hours; 5:16FB 6 hours; 6:16FB 18 hours; 7:8VDB 6 hours; 8:8VDB 18 hours

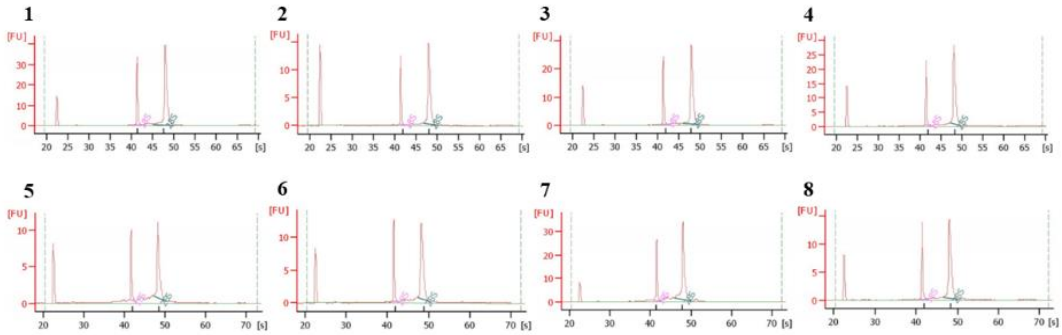

Figure 8. Agilent 2100 detects total RNA integrity

1.DMSO; 2:2j 6 hours; 3:2j 12 hours; 4:2j 18 hours; 5:16FB 6 hours; 6:16FB 18 hours; 7:8VDB 6 hours; 8:8VDB 18 hours

4.3 Processing and Mapping of RNA-Seq Data

After the completion of sequencing, the quality of the obtained original data was firstly assessed, and unqualified sequencing reads in the original sequencing data were removed with Trimmomatic to improve the accuracy and efficiency of subsequent analysis. The STAR alignment and expression analysis were performed after the clean reads were obtained. Based on the sequence alignment, the differential expression analysis was performed on the control sample and the experimental group sample by using DEseq2. The parameter values log2 fold-change and *p* value were used as the reference indicators for significant differences, set |log2FC|>2, and the *p* value was less than 0.05 as statistically significant differentially expressed gene.

According to the screening criteria of differential genes, compared with DMSO control, 36 genes were up-regulated and 89 genes were down-regulated after treatment with 1 μM 2j for 6 hours. 97 genes were up-regulated and 285 genes were down-regulated after treatment with 1 μM 2j for 12 hours while 99 genes were up-regulated and 128 genes were down-regulated after treatment with 1 μM 2j for 18 hours (Figure 9, 10). A total of 35 genes were found in common at 6 hours, 12 hours and 18 hours by comparing the DEGs (Figure 11).

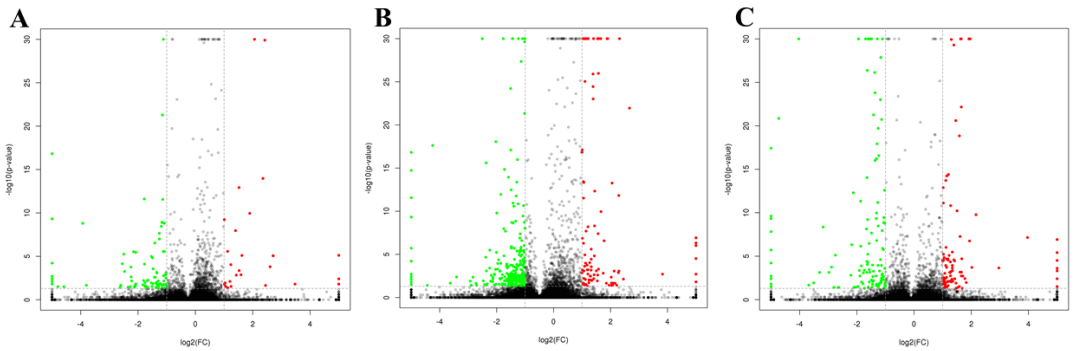

Figure 9. Volcanic map of differential genes, the differentially expressed genes set disturbed by 2j, the red dots (up-regulated) and green dots (down-regulated) represent significantly different genes, and genes with no significant differences are indicated by black dots; (|logFC| ≥ 2 and *p* value < 0.05).

A:DMSO VS 6 hours; B:DMSO VS 12 hours; C:DMSO VS 18 hours

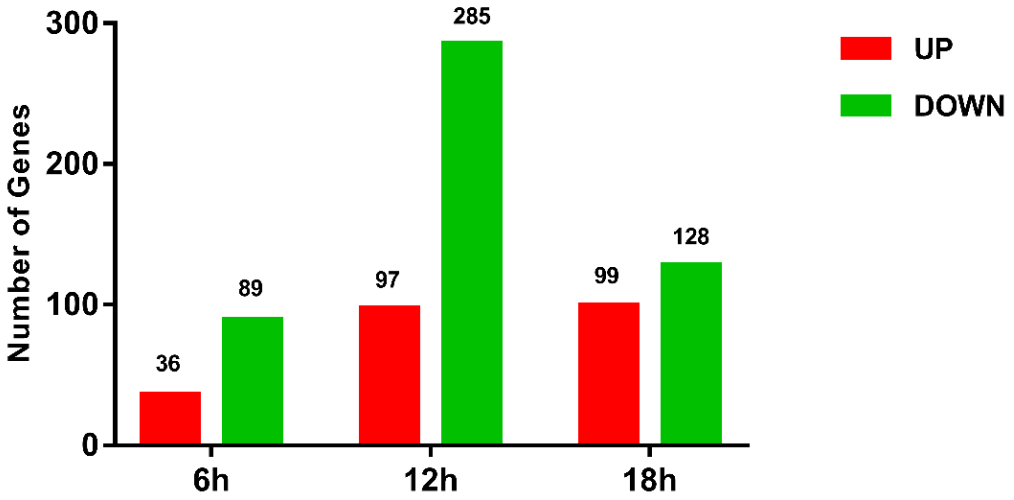

Figure 10. Histogram of differential genes, the differentially expressed genes set disturbed by 2j, (|logFC| ≥ 2 and*p* value < 0.05).

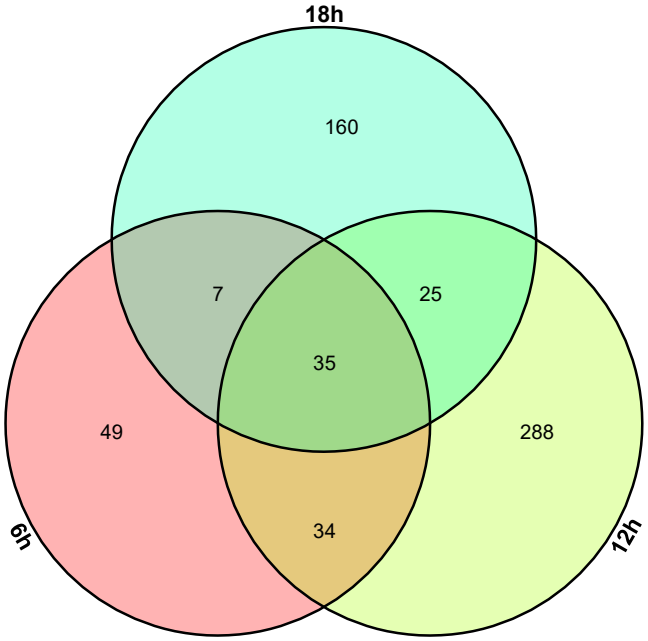

Figure 11.Venn diagrams illustrating the relationships between significantly DEGs in the three treatment times against the DMSO control.

According to the screening criteria of differential genes, compared to DMSO control, 107 genes were up-regulated and 175 genes were down-regulated after treatment with 1 μM 16FB for 6 hours; 167 genes were up-regulated and 164 genes were down-regulated after treatment with 1 μM 16FB for 18 hours (Figure 12, 13). A total of 117 genes were found at 6 hours and 18 hours by comparing the DEGs (Figure 14).

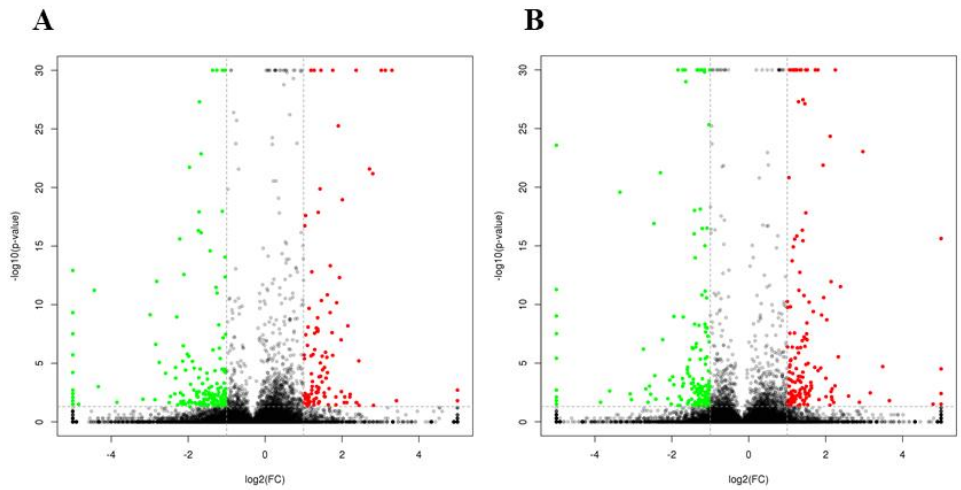

Figure 12. Volcanic map of differential genes, The differentially expressed genes set disturbed by 16FB, the red dots (up-regulated) and green dots(down-regulated) represent significantly different genes, and genes with no significant differences are indicated by black dots; (|logFC| ≥ 2 and *p* value < 0.05).

A:DMSO VS 6 hours; B:DMSO VS 18 hours

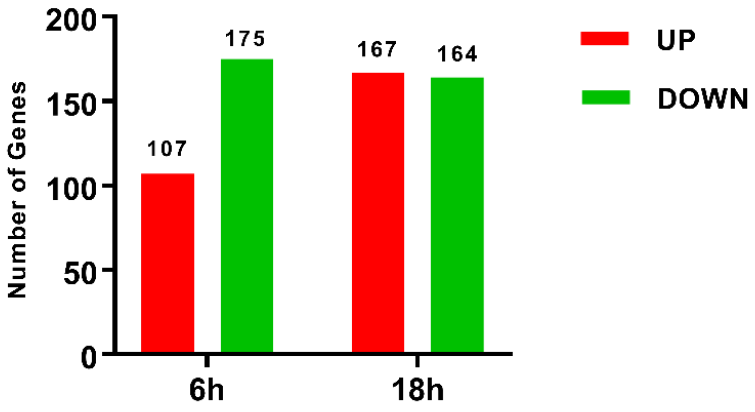

Figure 13. Histogram of differential genes, the differentially expressed genes set disturbed by 16FB, (|logFC| ≥ 2 and *P*value < 0.05).

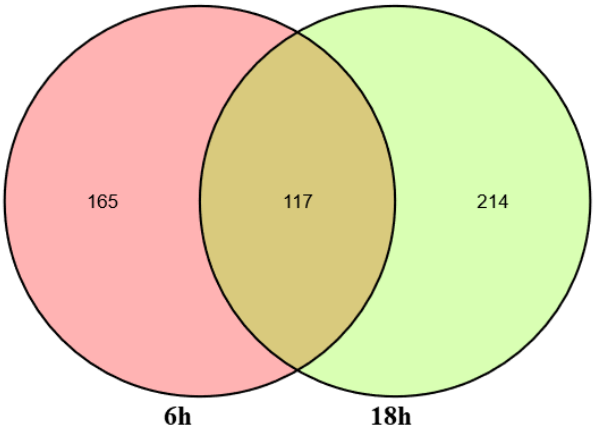

Figure 14. Venn diagrams illustrating the relationships between significantly DEGs in the three treatment times against the DMSO control.

According to the screening criteria of differential genes, compared to DMSO control, 122 genes were up-regulated and 82 genes were down-regulated after treatment with 1 μM 8VDB for 6 hours; 207 genes were up-regulated and 66 genes were down-regulated after treatment with 1 μM 8VDB for 18 hours (Figure 15, 16). A total of 96 genes were found at 6 hours and 18 hours by comparing the DEGs (Figure 17).

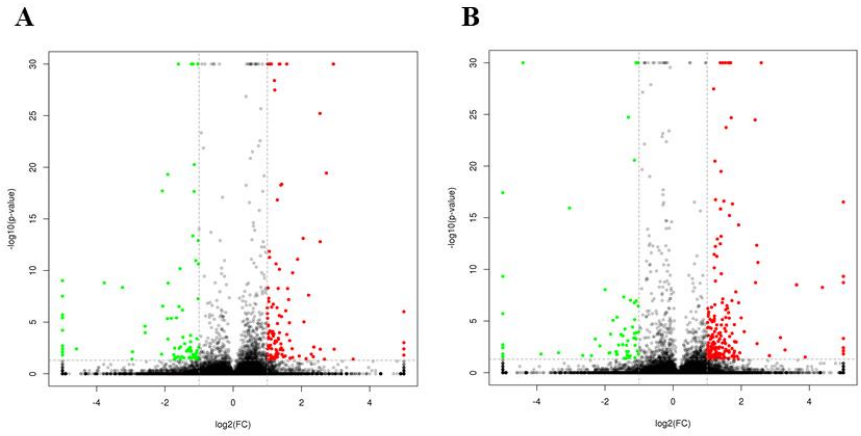

Figure 15. Volcanic map of differential genes, The differentially expressed genes set disturbed by 8VDB, the red dots (up-regulated) and green dots(down-regulated) represent significantly different genes, and genes with no significant differences are

indicated by black dots; (|logFC| ≥ 2 and *p* value < 0.05).

A:DMSO VS 6 hours; B:DMSO VS 18 hours

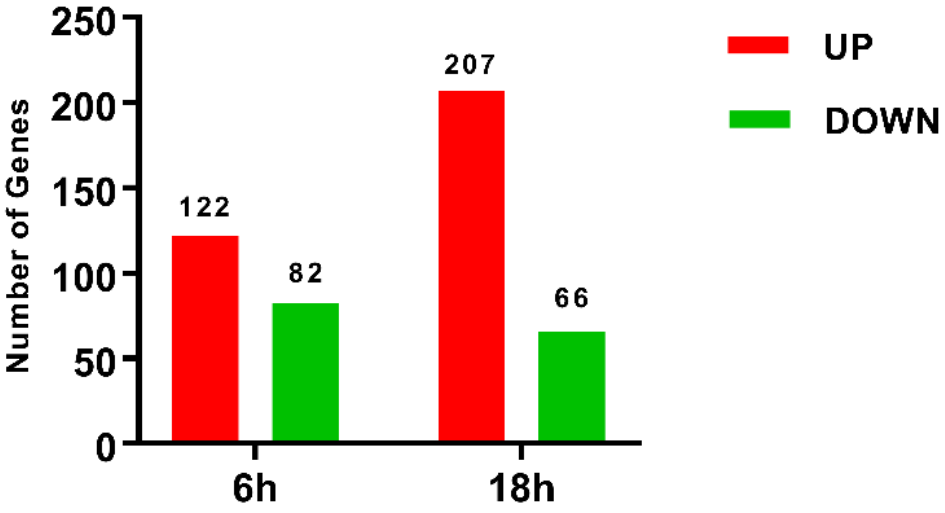

Figure 16. Histogram of differential genes, the differentially expressed genes set disturbed by 8VDB, (|logFC| ≥ 2 and *P*value < 0.05).

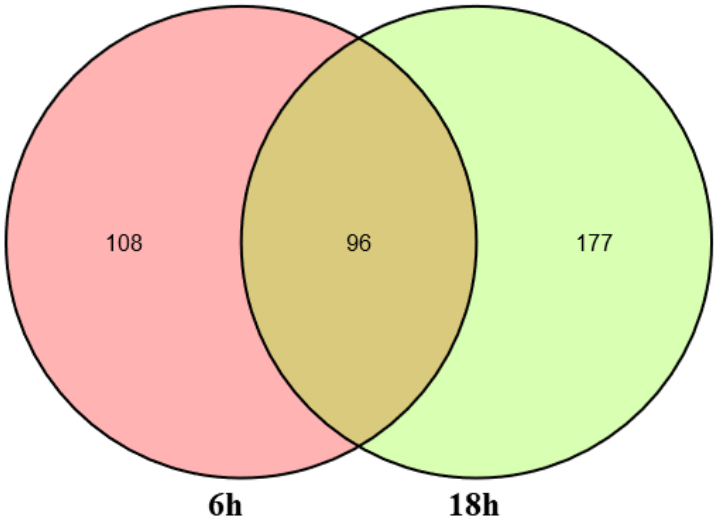

Figure 17. Venn diagrams illustrating the relationships between significantly DEGs in the three treatment times against the DMSO control.

4.4 GO analysis of differentially expressed genes

To understand the functions of different genes, GO analysis was carried out by online tools (OmicShare tools). GO was used to annotate the functions of differentially expressed genes in cells treated with 2j, 16FB, and 8VDB at different times. Biological process, cellular component and molecular function were determined to comprehensively analyze the functional information of DEGs. GO category results are presented in the following figures:

4.4.1 2j 6 hours

For biological processes, DEGs were mainly enriched in cellular progress, biological regulation and metabolic process. For cellular components, DEGs were mostly enriched in cell, organelle and extracellular matrix. For molecular function, DEGs were mainly enriched in binding, catalytic activity and regulators of molecular functions (Figure 18,19).

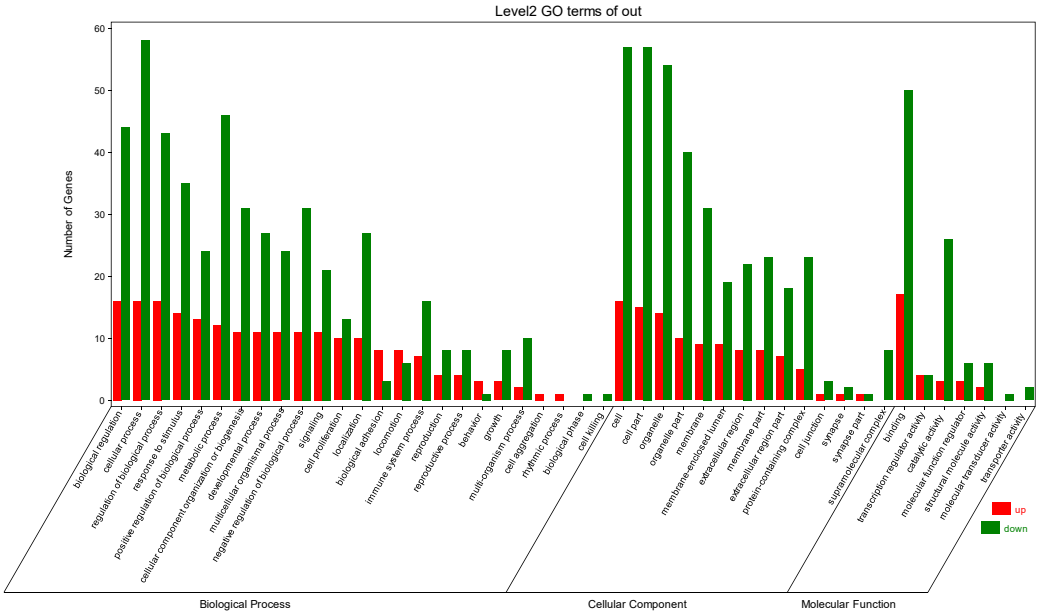

Figure 18. GO annotation of DEGs (2j 6 hours), red represents the up-regulation,

green represents the down-regulation

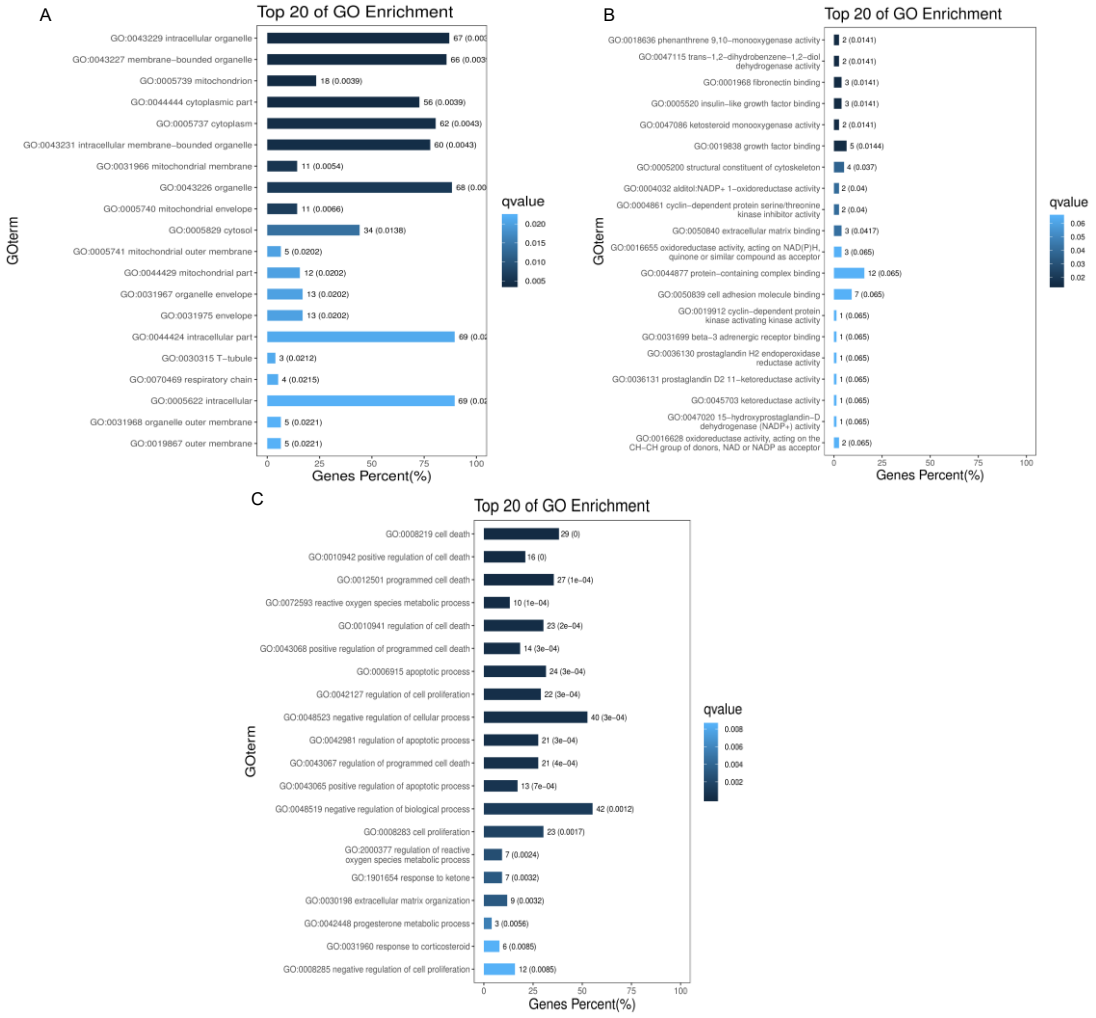

Figure 19. Top 20 GO annotation of DEGs (2j 6 hours)

A. cellular component; B. molecular function; C. biological process

4.4.2 2j 12 hours

For biological processes, DEGs were mainly enriched in cellular progress, biological regulation and metabolic process. For cellular components, DEGs were mostly

enriched in cell, organelle and membrane. For molecular functions, DEGs were mainly enriched in binding, catalytic activity and molecular function regulators (Figure 20, 21).

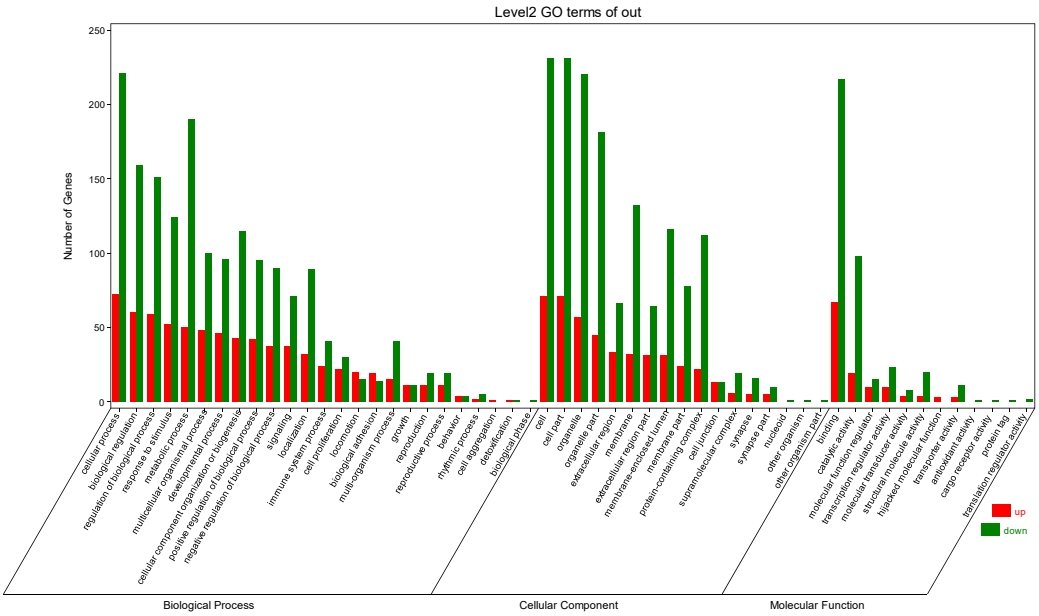

Figure 20. GO annotation of DEGs (2j 12 hours), red represents the up-regulation, green represents the down-regulation

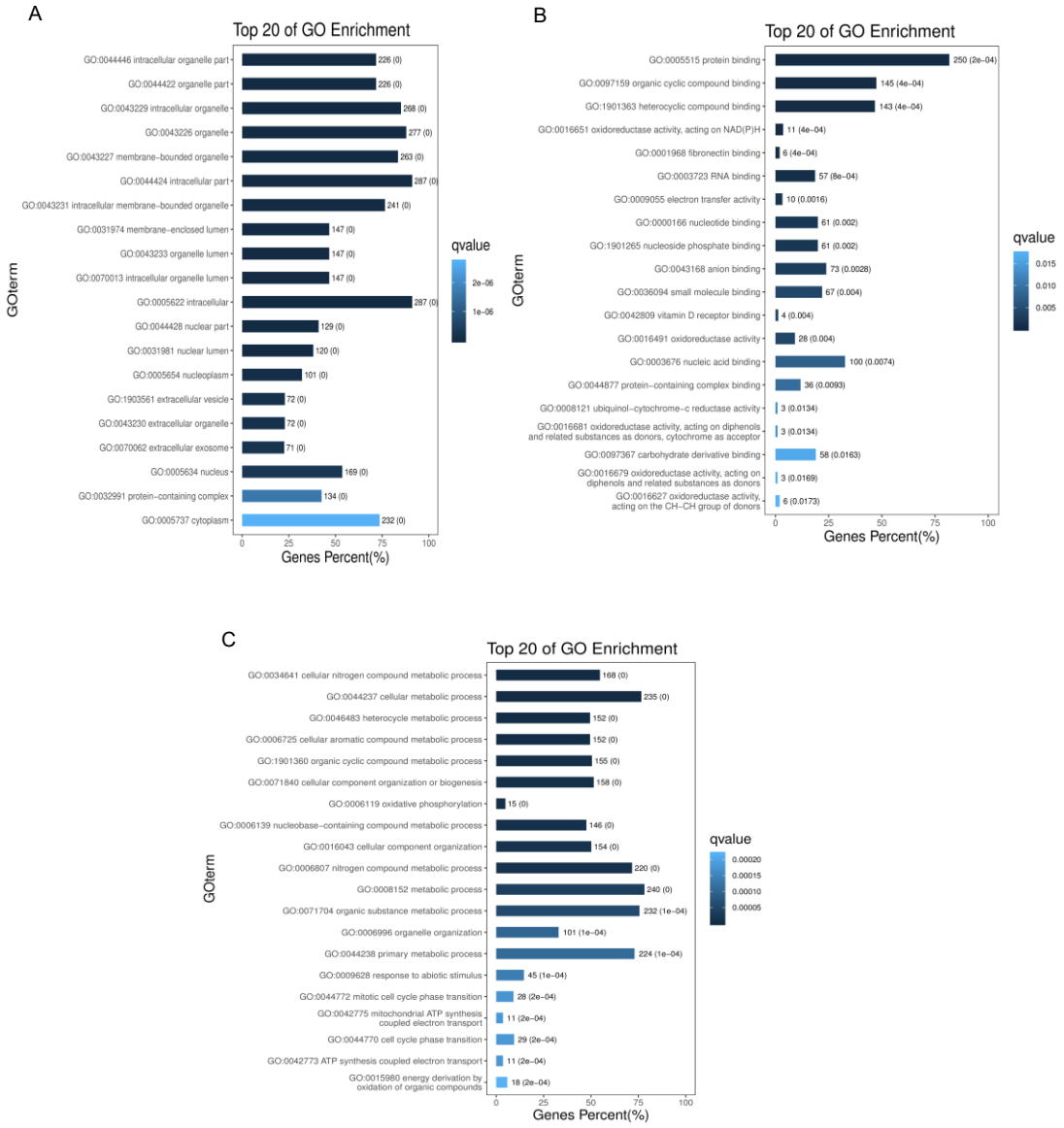

Figure 21. Top 20 GO annotation of DEGs (2j 12 hours)

A. cellular component; B. molecular function; C. biological process

4.4.3 2j 18 hours

For biological processes, DEGs were mainly enriched in cellular progress, biological regulation and metabolic process. For cellular components, DEGs were mostly enriched in cell, organelle and membrane-enclosed lumen. For molecular functions,

DEGs were mainly enriched in binding, catalytic activity and regulators of molecular functions (Figure 22,23).

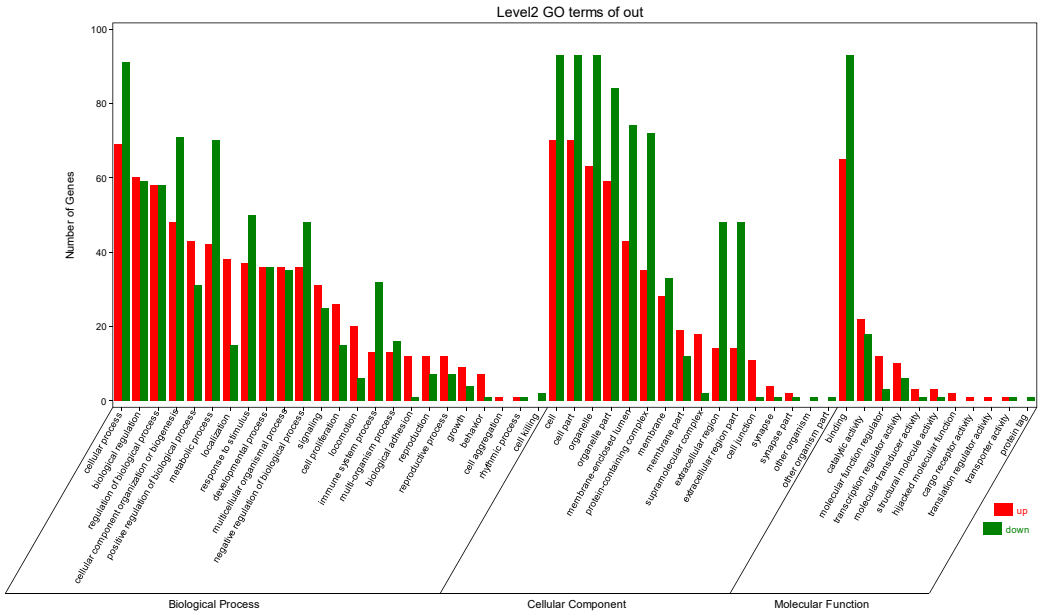

Figure 22. GO annotation of DEGs (2j 18 hours), the red represents the up-regulation, the green represents the down-regulation

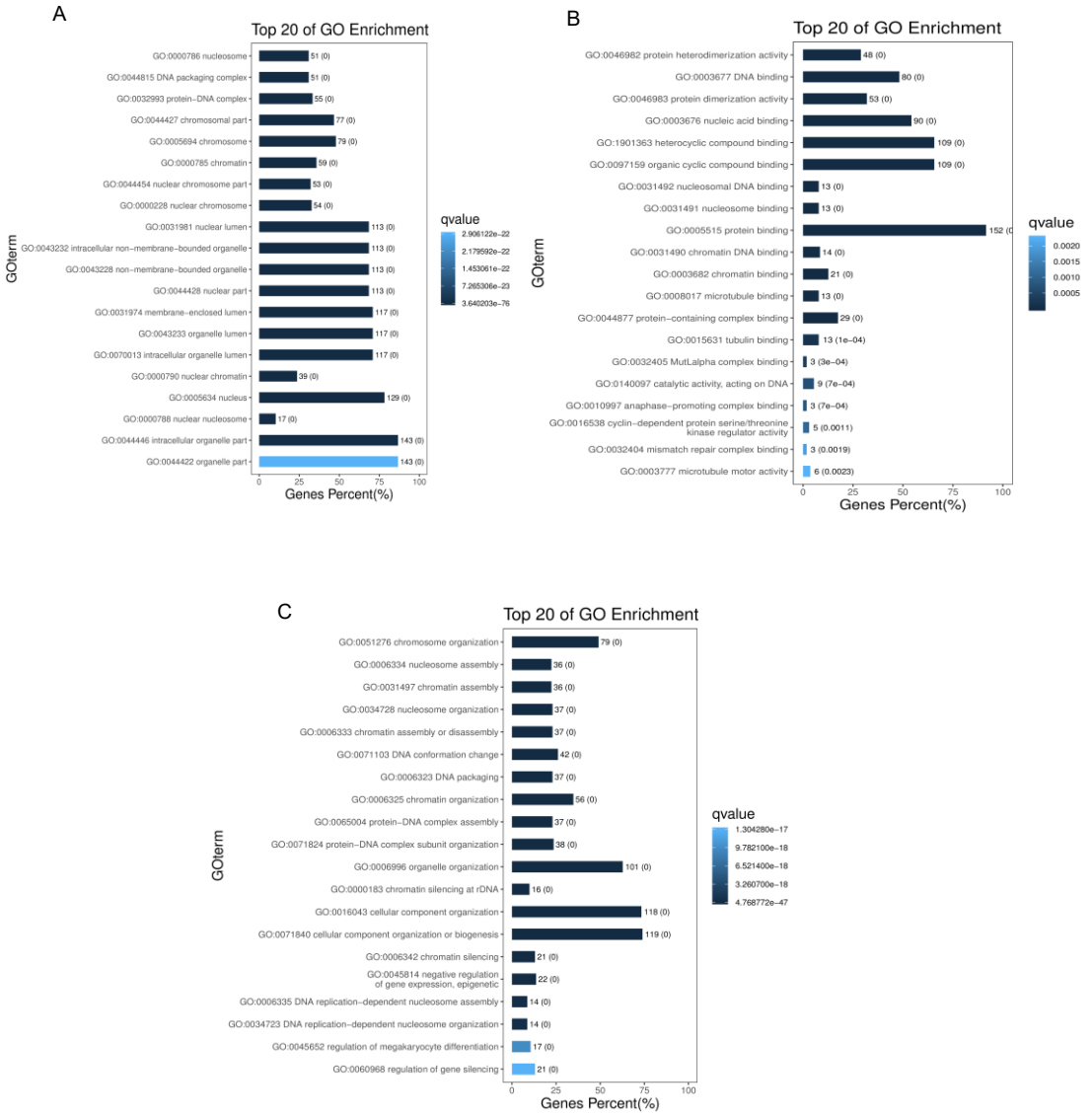

Figure 23. Top 20 GO annotation of DEGs (2j 18 hours)

A. cellular component; B. molecular function; C. biological process

Summary: compared to control, the gene ontology (GO) enrichment results showed that after being treated with 2j, for biological processes, DEGs were mainly enriched in cellular progress, biological regulation and metabolic process, while top GO was mainly enriched in chromosome organization, assembly or disassembly, and

chromatin silencing. For cellular components, DEGs were mostly enriched in cell, organelle and membrane-enclosed lumen, while top GO was mainly enriched in chromosome, nucleosome and DNA packaging complex. For molecular functions, DEGs were mainly enriched in binding, catalytic activity and regulators of molecular functions, while top GO was mainly enriched in DNA and protein binding.

4.4.4 16FB 6 hours

For biological processes, DEGs were mainly enriched in cellular progress, biological regulation and metabolic processes. For cellular components, DEGs were mostly enriched in cell, organelle and membrane. For molecular functions, DEGs were mainly enriched in binding, catalytic activity and regulators of molecular functions(Figure 24, 25).

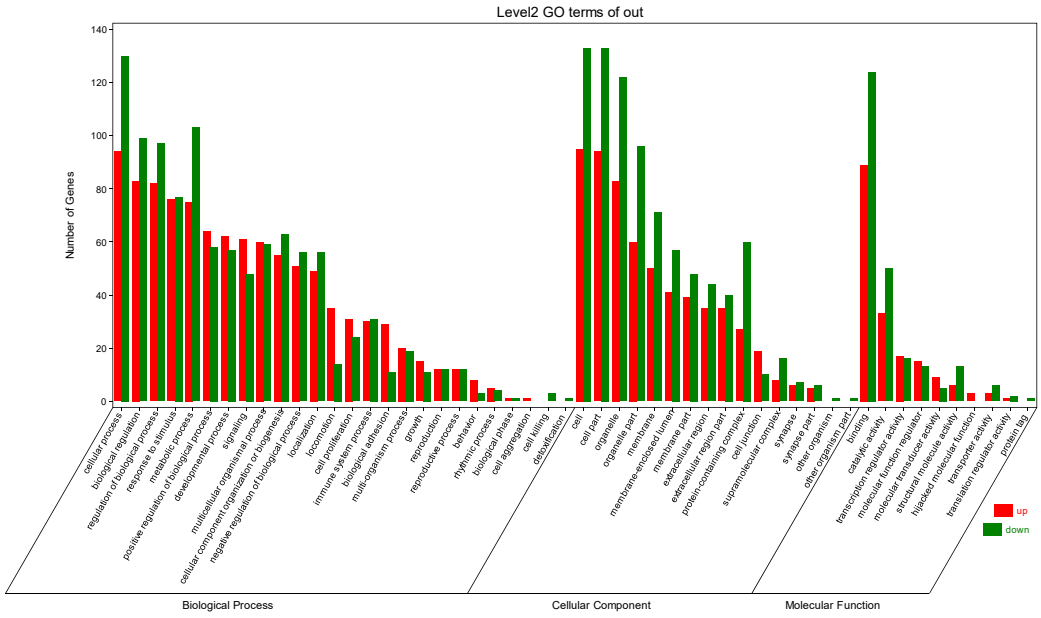

Figure 24. GO annotation of DEGs (16FB 6 hours), red represents the up-regulation, green represents the down-regulation

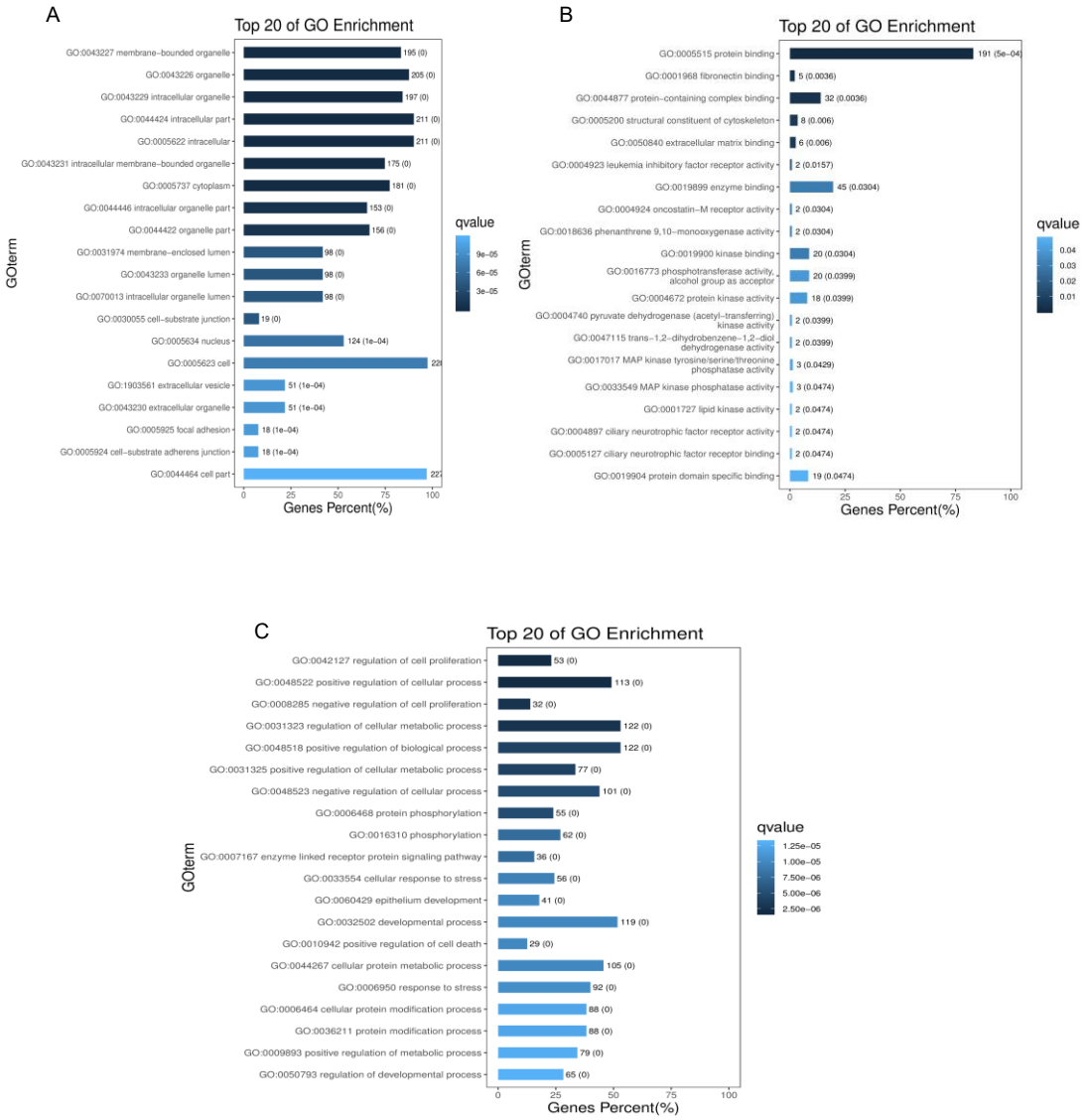

Figure 25. Top 20 GO annotation of DEGs (16FB 6 hours)

A. cellular component; B. molecular function; C. biological process

4.4.5 16FB 18 hours

For biological processes, DEGs were mainly enriched in cellular progresses, biological regulation and metabolic processes. For cellular component, DEGs were mostly enriched in cell, organelle and membrane-enclosed lumen. For molecular function, DEGs were mainly enriched in binding, catalytic activity and transcription function activity (Figure 26, 27).

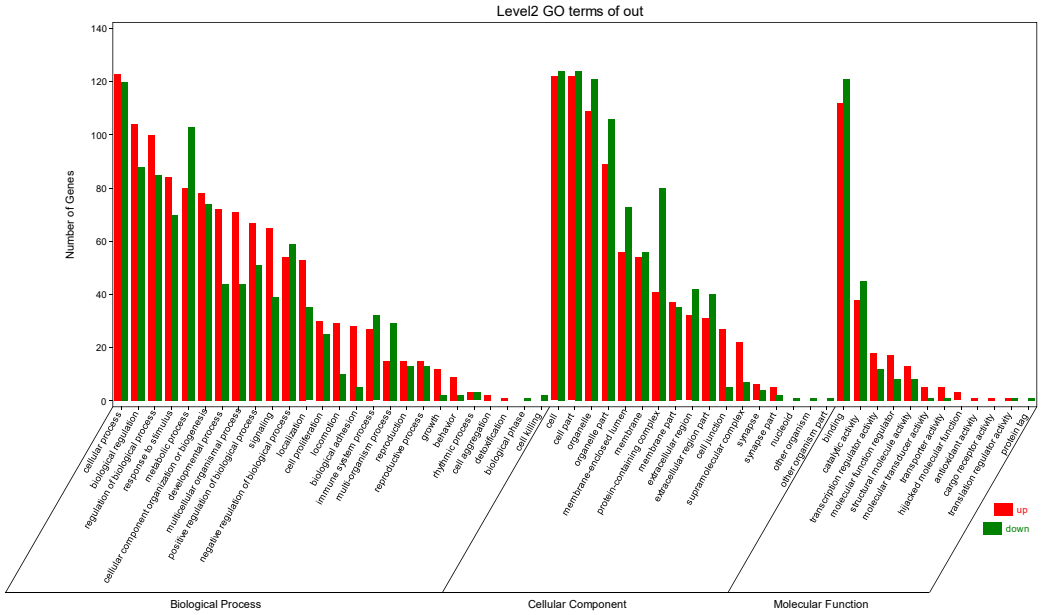

Figure 26. GO annotation of DEGs (16FB 18hours), red represents the up-regulation, green represents the down-regulation

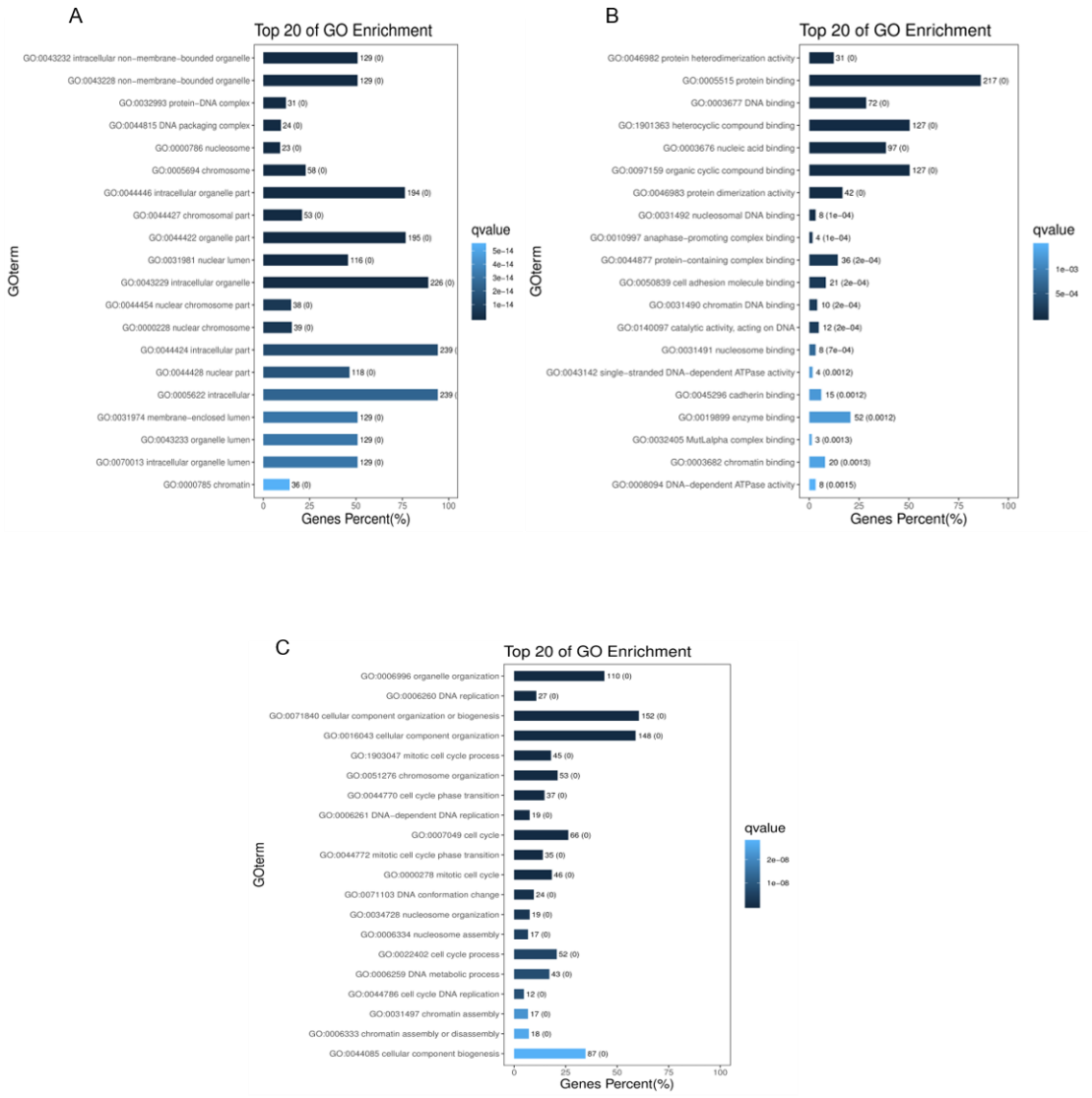

Figure 27. Top 20 GO annotation of DEGs (16FB 18 hours)

A. cellular component; B. molecular function; C. biological process

Summary: compared to control, the gene ontology (GO) enrichment results showed that after treatment with 16FB, for biological processes, DEGs were mainly enriched in cellular progresses, biological regulation and metabolic processes, however top GO was mainly enriched in chromosome organization, cell cycle, and cellular component organization. For cellular component, DEGs were mostly enriched in cell, organelle and membrane-enclosed lumen, while top GO was mainly enriched in intracellular

organelle, non-member-bounded organelle, and chromosome. For molecular function, DEGs were mainly enriched in binding, catalytic activity and transcription function activity, as top GO was mainly enriched in DNA binding, protein binding, and protein heterodimerization activity.

4.4.6 8VDB 6 hours

For biological processes, DEGs were mainly enriched in cellular progress, response to stimulus and metabolic processes. For cellular components, DEGs were mostly enriched in cell, organelle and membrane-enclosed lumen. For molecular functions, DEGs were mainly enriched in binding, catalytic and transcriptional activity (Figure 28, 29).

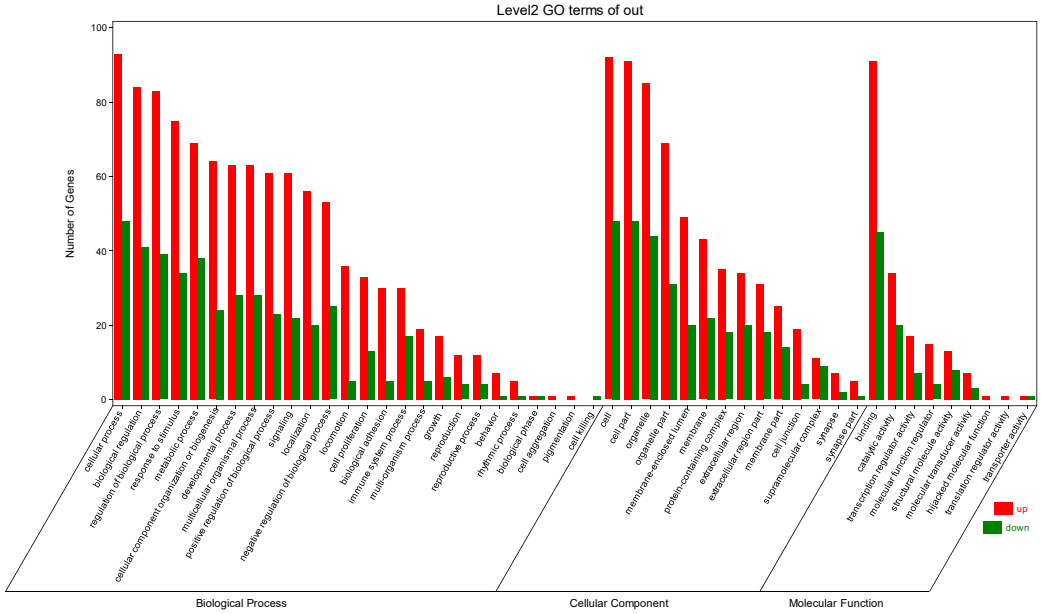

Figure 28. GO annotation of DEGs (8VDB 6 hours), red represents the up-regulation, green represents the down-regulation

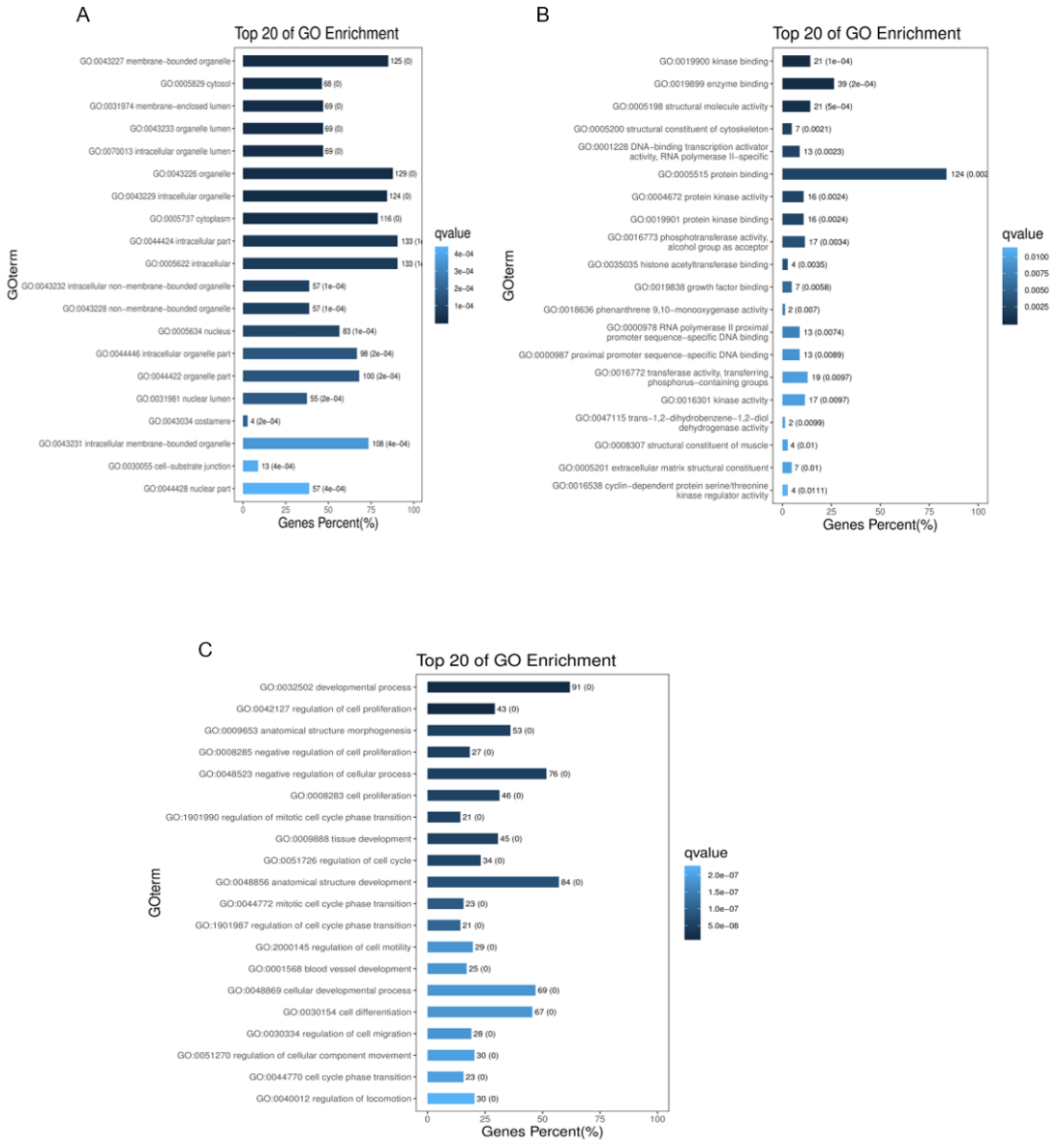

Figure 29. Top 20 GO annotation of DEGs (8VDB 6 hours)

A. cellular component; B. molecular function; C. biological process

4.4.7 8VDB 18 hours

For biological processes, DEGs were mainly enriched in cellular progress, biological

regulation and cellular component organization. For cellular components, DEGs were mostly enriched in cell, organelle and membrane-enclosed lumen. For molecular functions, DEGs were mainly enriched in binding, catalytic and transcription functional activity (Figure 30, 31).

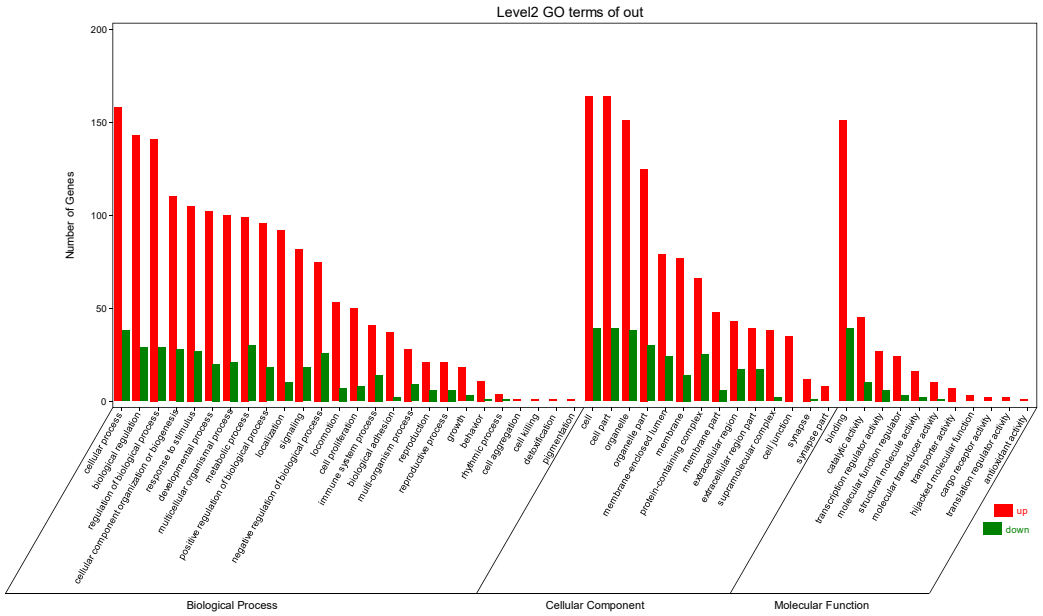

Figure 30. GO annotation of DEGs (8VDB 18 hours), red represents the up-regulation, green represents the down-regulation

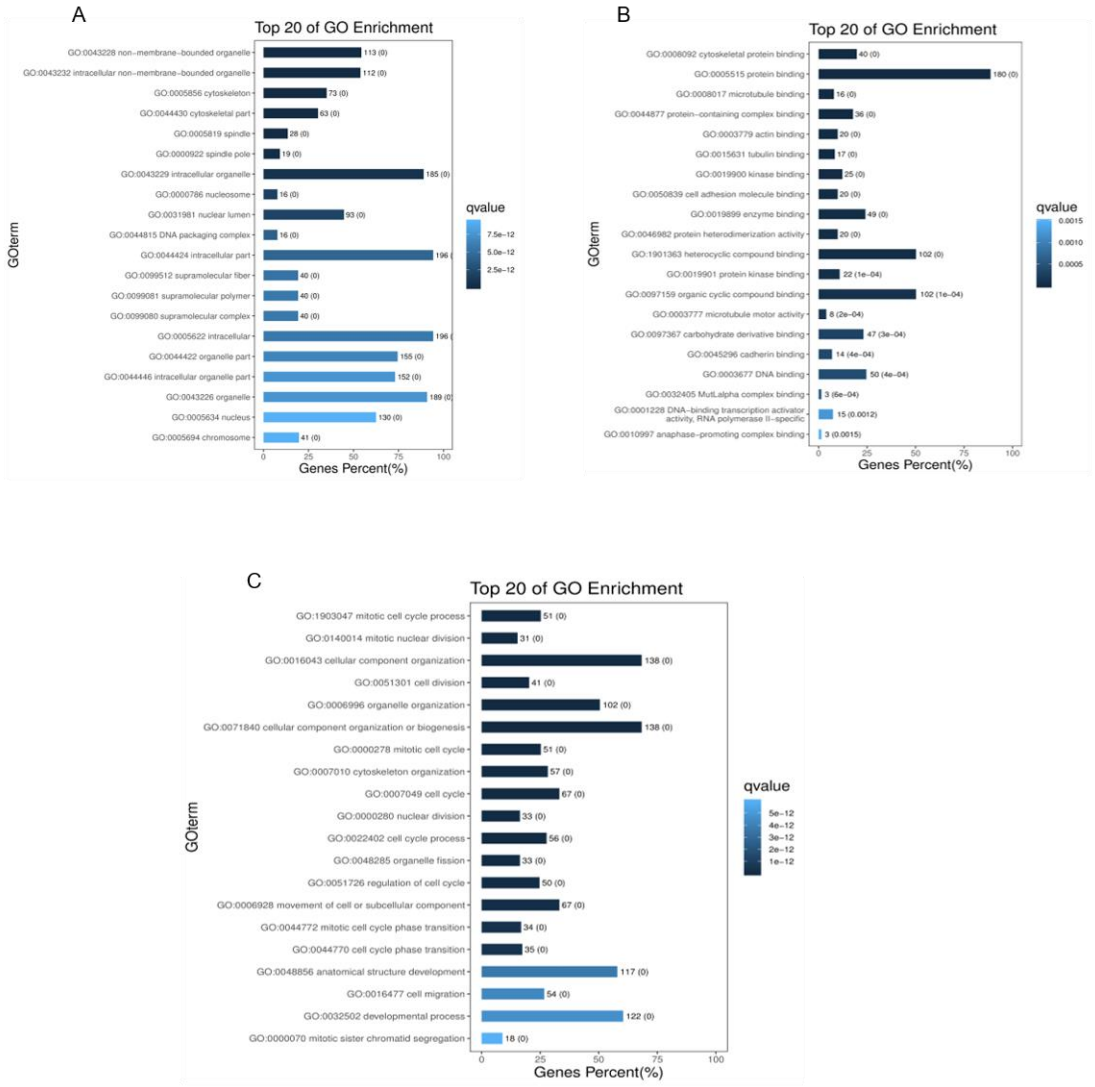

Figure 31. Top 20 GO annotation of DEGs (8VDB 18 hours)

A. cellular component; B. molecular function; C. biological process

Summary: compared to control, the gene ontology (GO) enrichment results showed that after being treated with 8VDB, for biological processes, DEGs were mainly enriched in cellular progress, biological regulation and cellular component organization, however top GO was mainly enriched in cell division, cell cycle, and cellular component organization. For cellular component, DEGs were mostly enriched in cell, organelle and membrane-enclosed lumen, while top GO was mainly enriched

in intracellular non-member-bounded organelle and cytoskeleton. For molecular function, DEGs were mainly enriched in binding, catalytic and transcription functional activity, however top GO was mainly enriched in DNA binding, protein and compound binding.

4.5 KEGG analysis of DEGs

For further characterization of the DEGs, KEGG pathway analysis was conducted using the online tools (OmicShare tools). Enrichment analysis of KEGG was not only used to find the pathway in which the differential genes were involved, but also to analyze the significance of each pathway. The *p* value represents the significance of the same conditions of the biological pathway, in specific the lower the *p* value, the more significant the role of the biological pathway. KEGG results are presented in the following sections:

4.5.1 2j 6 hours

After treatment with 1 μM 2j for 6 hours, compared to DMSO control, DEGs were mainly enriched in cancers, global and overview maps, signal transduction, and endocrine system (Figure 32). Top KEGG pathways were mainly enriched in MicroRNAs in cancer, p53 signaling pathway, ferroptosis, apelin signaling pathway, transcriptional misregulation in cancers, gap junction, oxidative phosphorylation, and tight junction (Figure 33).

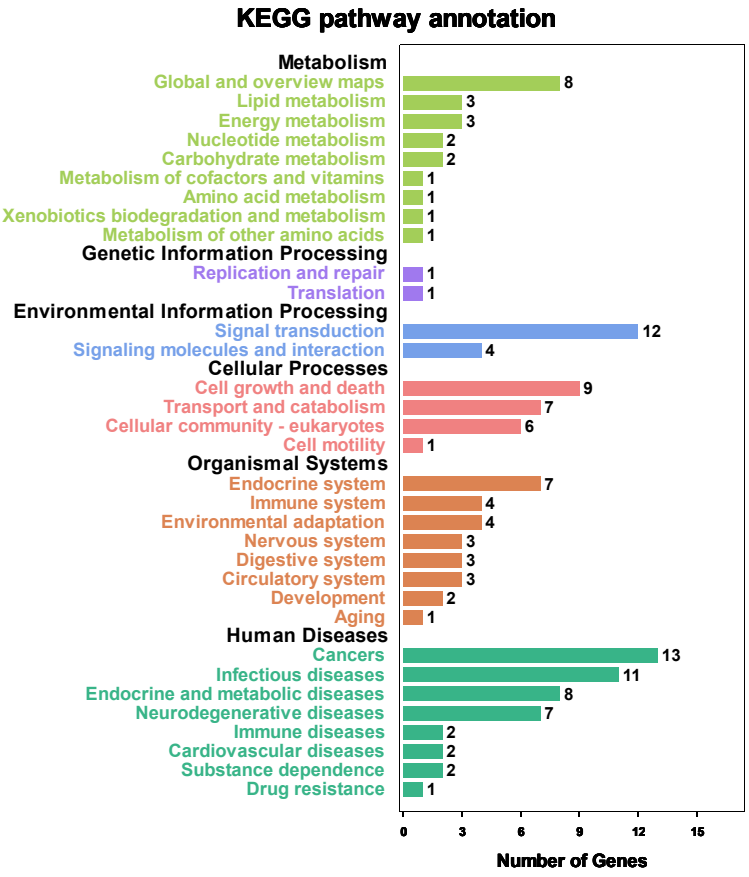

Figure 32. KEGG pathway enrichment analysis of DEGs (2j 6 hours)

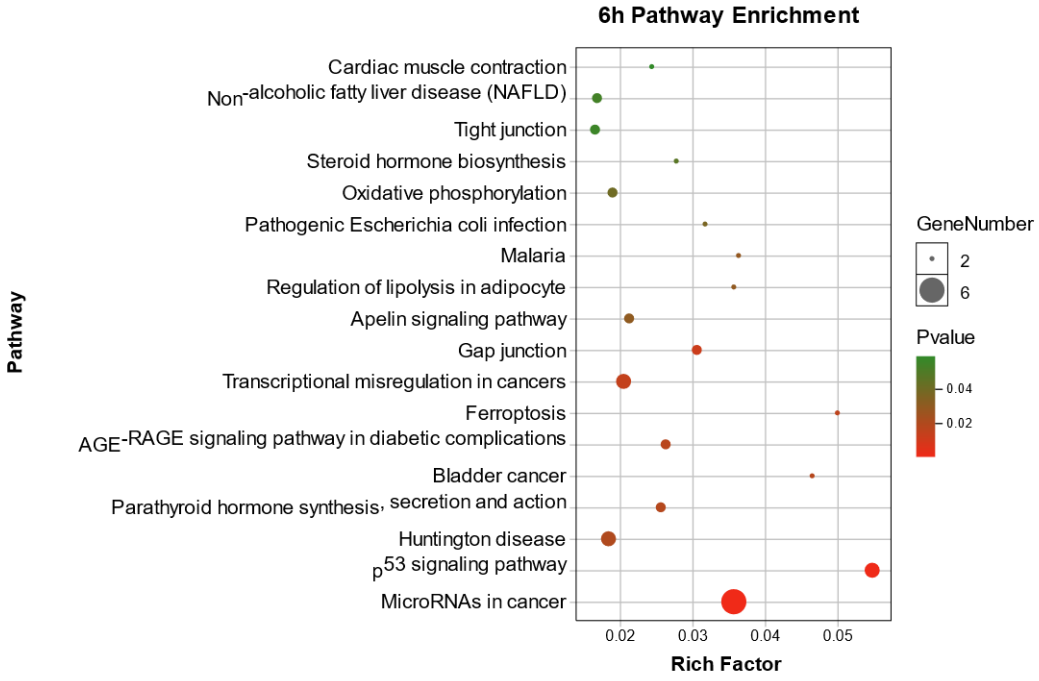

Figure 33. Top KEGG pathway enrichment analysis of DEGs (2j 6 hours)

4.5.2 2j 12 hours

After treatment with 1 μM 2j for 12 hours, compared to DMSO control, DEGs were mainly enriched in cancers, global and overview maps, signal transduction, endocrine system, energy metabolism, translation, transport and catabolism, cell growth and death and cellular community (Figure 34). The top KEGG pathways were mainly enriched in TCA cycle, oxidative phosphorylation, RNA transport, ribosome, tight junction, nucleotide excision repair, propanoate metabolism, and mitophagy (Figure 35).

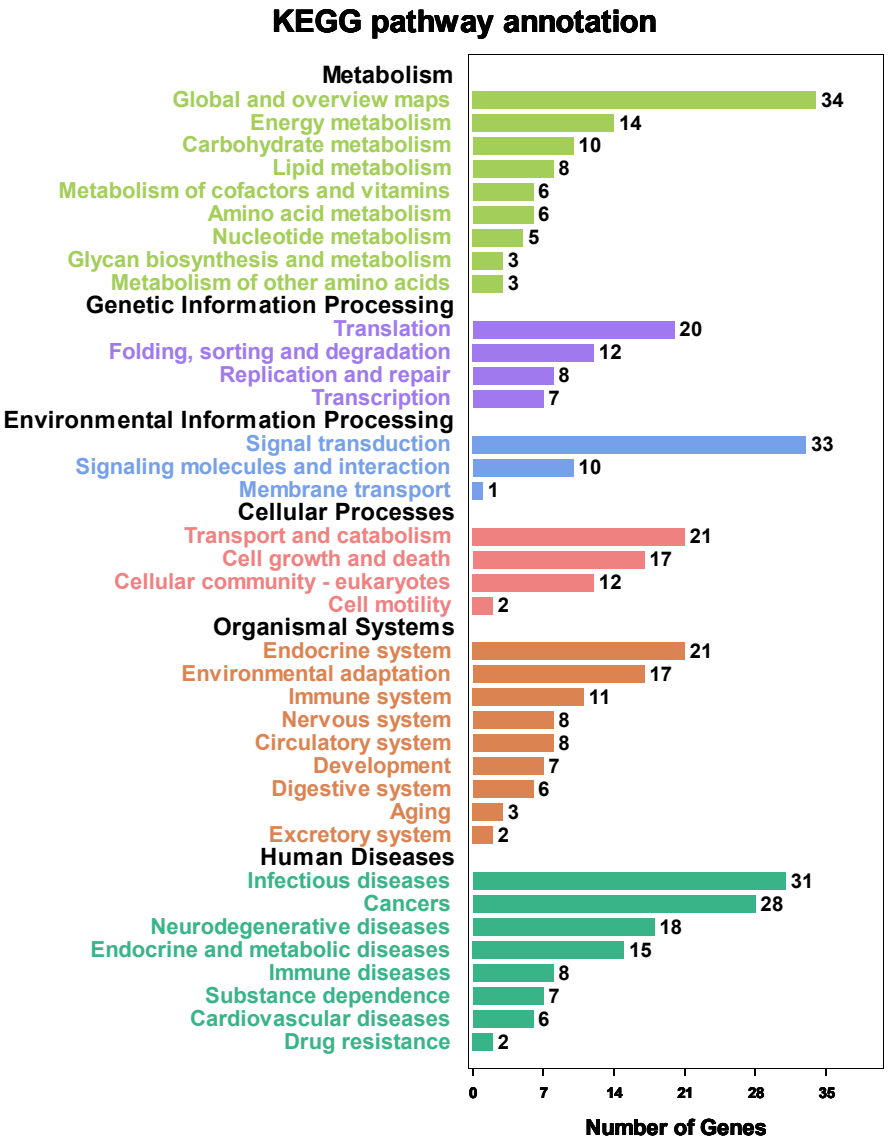

Figure 34. KEGG pathway enrichment analysis of DEGs (2j 12 hours)

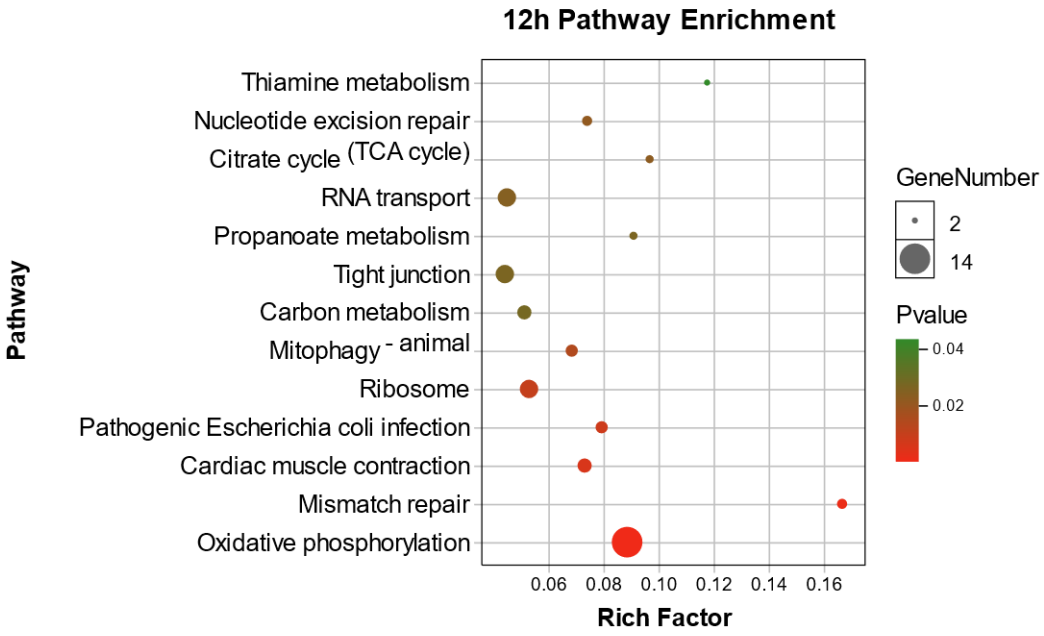

Figure 35. Top KEGG pathway enrichment analysis of DEGs (2j 12 hours)

4.5.3 2j 18 hours

After treatment with 1 μM 2j for 18 hours, compared to DMSO control, DEGs were mainly enriched in cancers, signal transduction, endocrine system, replication and repair, cell growth and death (Figure 36). Top KEGG pathways were mainly enriched in cell cycle, MicroRNAs in cancer, p53 signaling pathway, and nucleotide excision repair, transcription misregulation, base excision repair, and necroptosis (Figure 37).

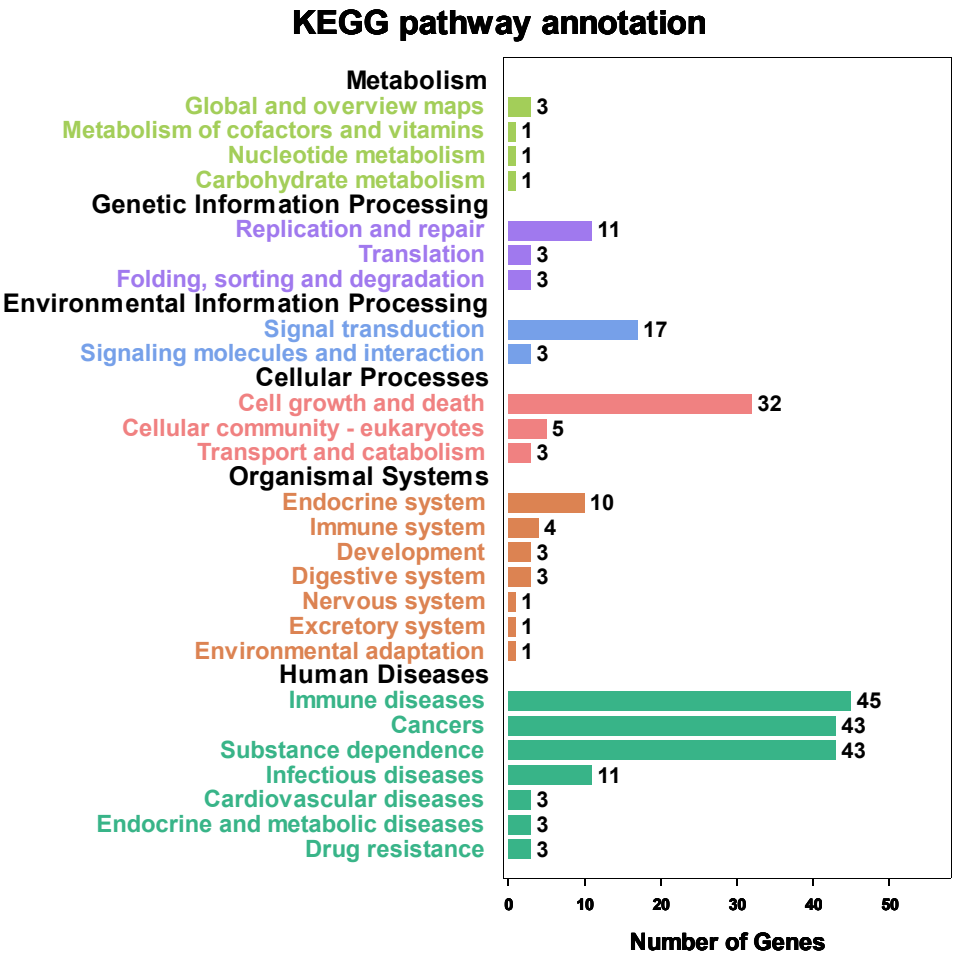

Figure 36. KEGG pathway enrichment analysis of DEGs(2j 18 hours)

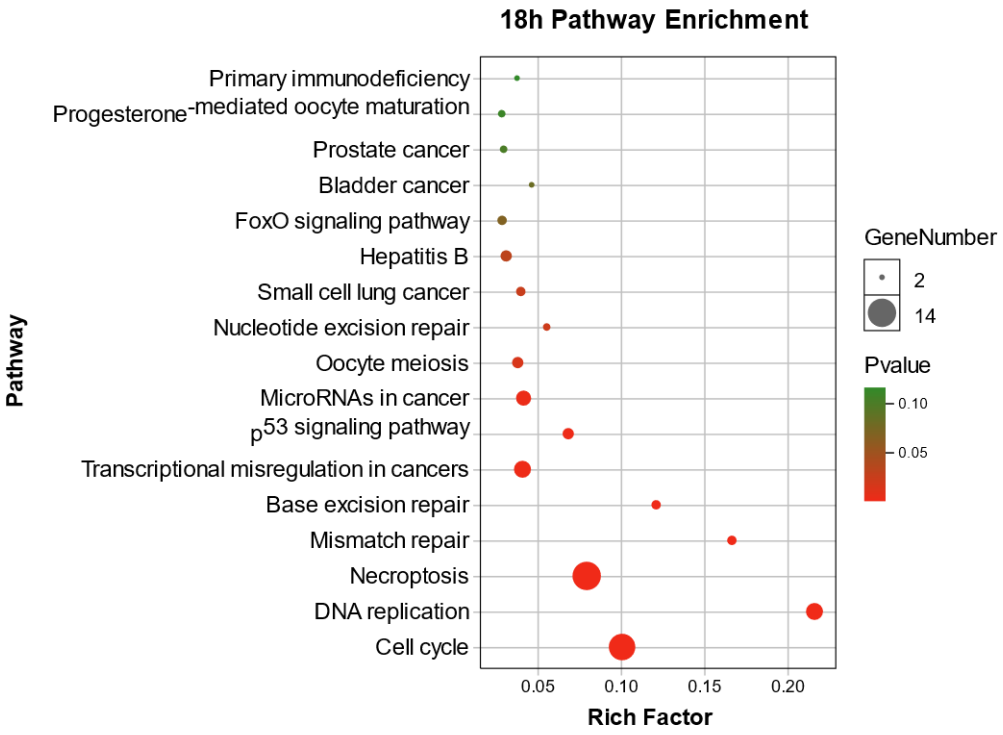

Figure 37. Top KEGG pathway enrichment analysis of DEGs (2j 18 hours)

Summary: after treatment with 2j, compared to control, DEGs were mainly enriched in cancers, signal transduction, endocrine system, replication and repair, cell growth and death. Top KEGG pathways were mainly enriched in cell cycle, MicroRNAs in cancer, p53 signaling pathway, and nucleotide excision repair, transcription misregulation, base excision repair, and necroptosis.

4.5.4 16FB 6 hours

After treatment with 1 μM 16FB for 6 hours, compared to DMSO control, DEGs were mainly enriched in cancers, global and overview maps, signal transduction, and endocrine system (Figure 38). Top KEGG pathways were mainly enriched in MicroRNAs in cancer, p53 signaling pathway, transcriptional misregulation in cancers, gap junction, cell cycle, and pathways in cancer(Figure 39).

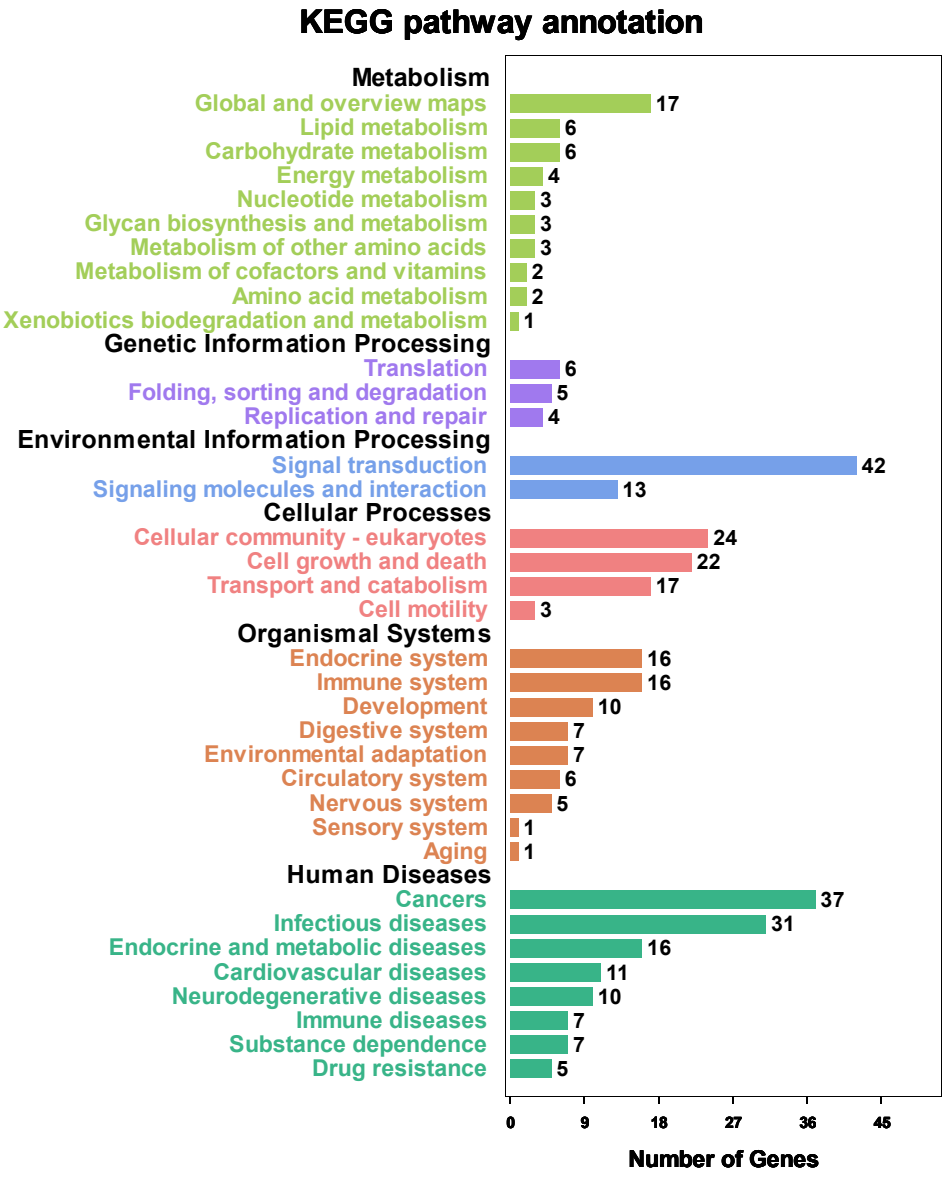

Figure 38. KEGG pathway enrichment analysis of DEGs (16FB 6 hours)

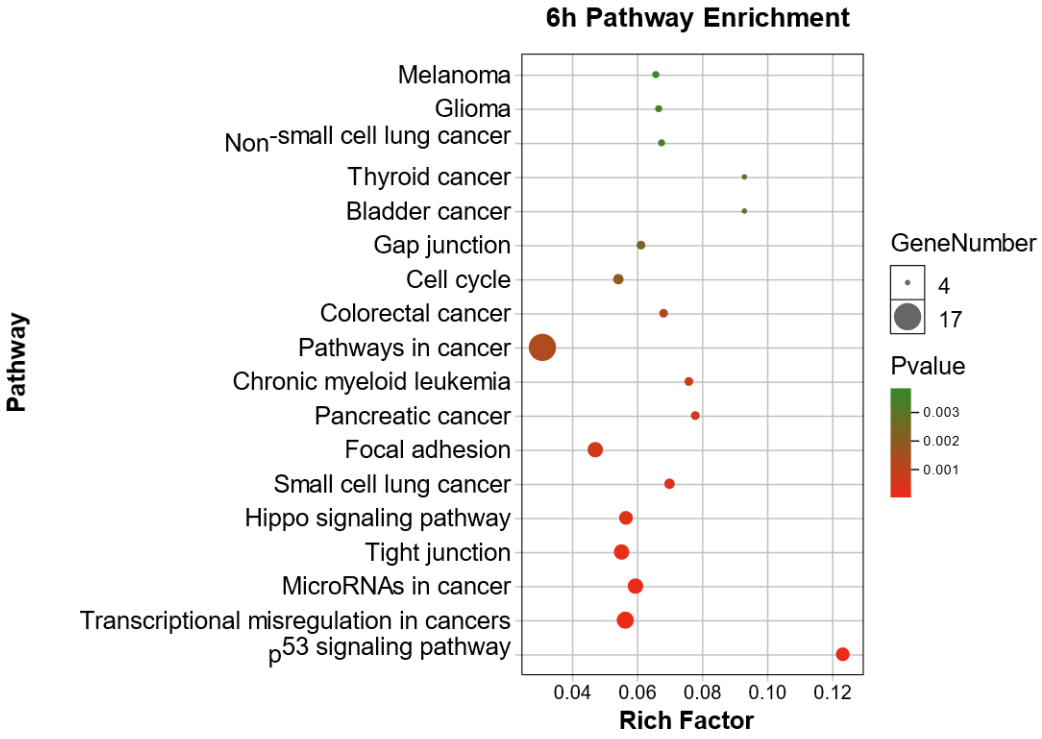

Figure 39. Top KEGG pathway enrichment analysis of DEGs (16FB 6 hours)

4.5.5 16FB 18 hours

After treatment with 1 μM 16FB for 18 hours, compared to DMSO control, DEGs were mainly enriched in cancers, global and overview maps, signal transduction, transport and catabolism, cell growth and death, cellular community and endocrine system (Figure 40). Top KEGG pathways were mainly enriched in MicroRNAs in cancer, p53 signaling pathway, transcriptional misregulation in cancers, gap junction, tight junction, hippo signaling pathway, cell cycle, proteoglycans in cancer, nucleotide excision repair, and mismatch repair (Figure 41).

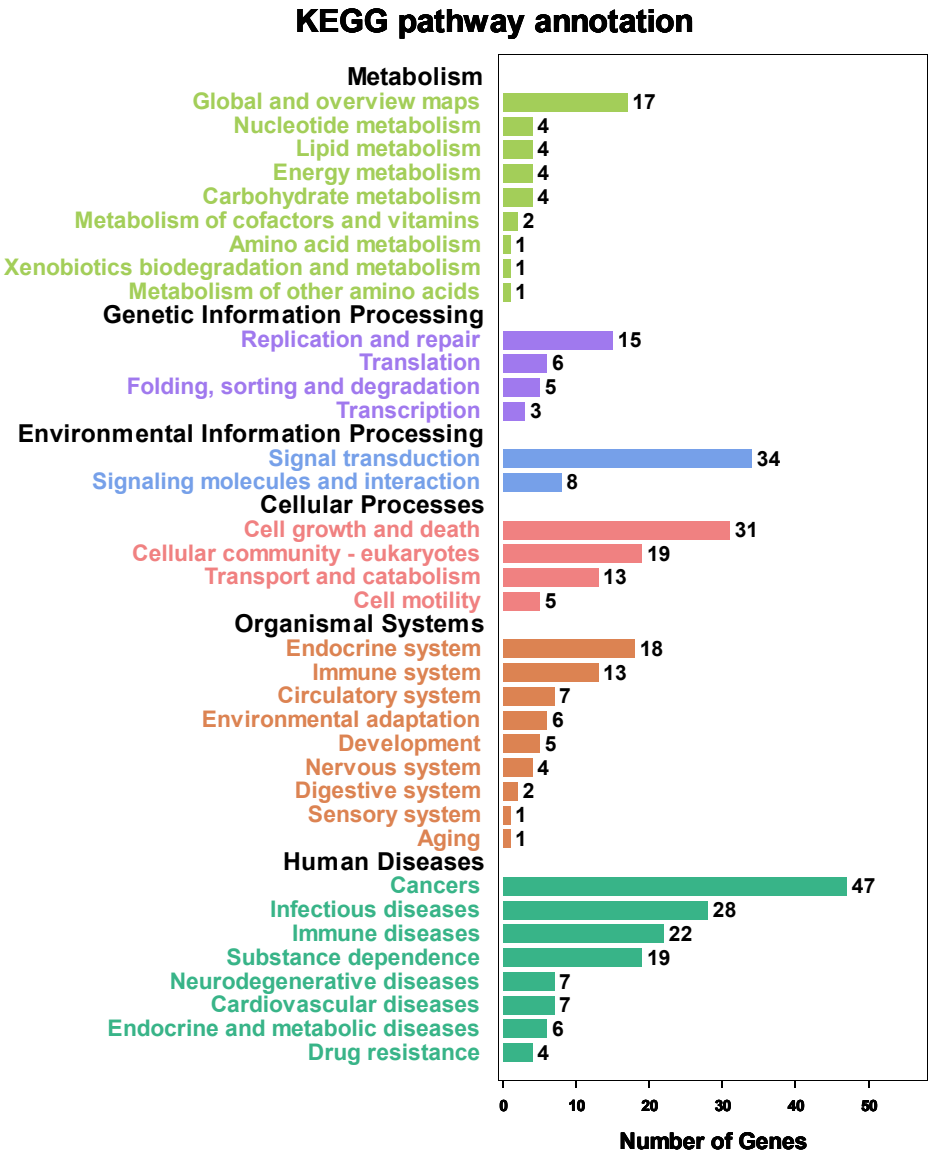

Figure 40. KEGG pathway enrichment analysis of DEGs (16FB 18 hours)

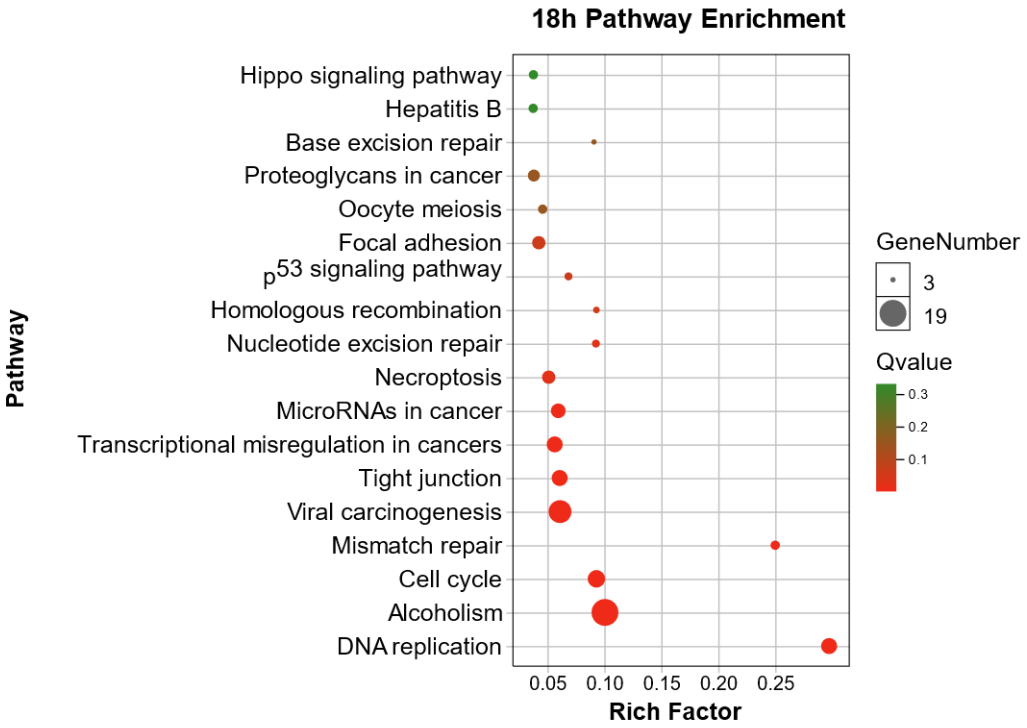

Figure 41. Top KEGG pathway enrichment analysis of DEGs (16FB 18 hours)

Summary: after treatment with 16FB, compared to control, DEGs were mainly enriched in cancers, global and overview maps, signal transduction, transport and catabolism, cell growth and death, cellular community and endocrine system. Top KEGG pathways were mainly enriched in MicroRNAs in cancer, p53 signaling pathway, transcriptional misregulation in cancers, gap junction, tight junction, hippo signaling pathway, cell cycle, proteoglycans in cancer, nucleotide excision repair, and mismatch repair.

4.5.6 8VDB 6 hours

After treatment with 1 μM 8VDB for 6 hours, compared to DMSO control, DEGs were mainly enriched in cancers, global and overview maps, signal transduction, endocrine system, cell growth and death, cell community, transport and catabolism

(Figure 42). Top KEGG pathways were mainly enriched in p53 signaling pathway, transcriptional misregulation in cancers, tight junction, cell cycle, pathways in cancer, hippo signaling pathway, and FoxO signaling pathway (Figure 43).

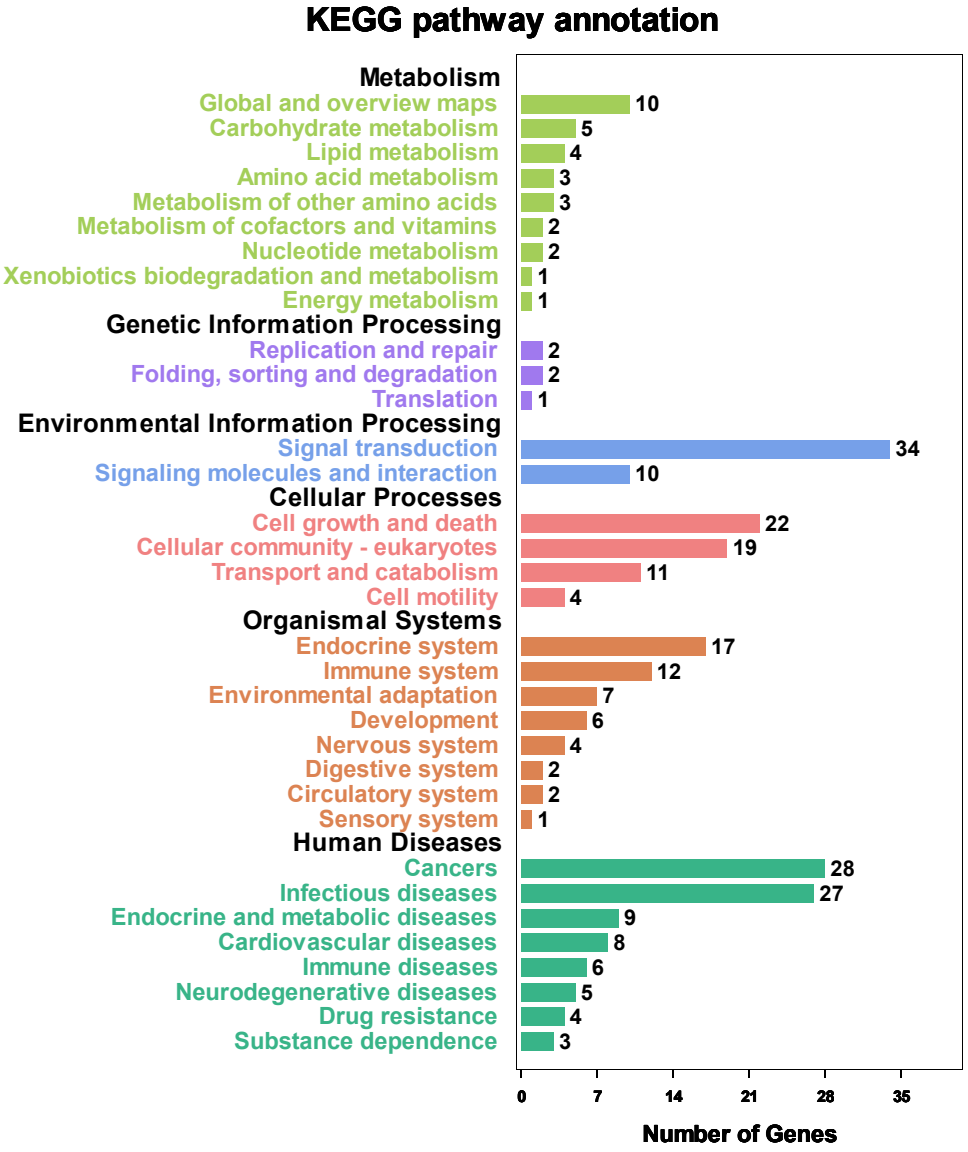

Figure 42. KEGG pathway enrichment analysis of DEGs (8VDB 6 hours)

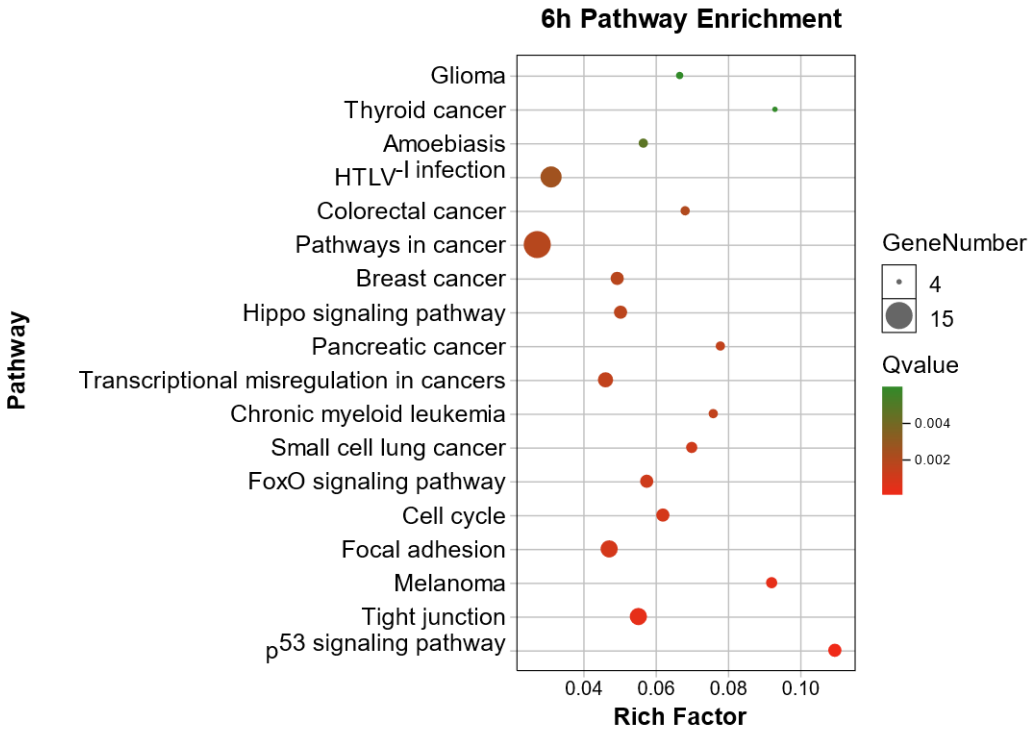

Figure 43.Top KEGG pathway enrichment analysis of DEGs (8VDB 6 hours)

4.5.7 8VDB 18 hours

After treatment with 1 μM 8VDB for 18 hours, compared to DMSO control, DEGs were mainly enriched in cancers, global and overview maps, signal transduction, endocrine system, cell growth and death, cell community, transport and catabolism, and immune system (Figure 44). Top KEGG pathway were mainly enriched in p53 signaling pathway, transcriptional misregulation in cancers, tight junction, cell cycle, pathways in cancer, hippo signaling pathway, apelin signaling pathway, and MicroRNAs in cancer (Figure 45).

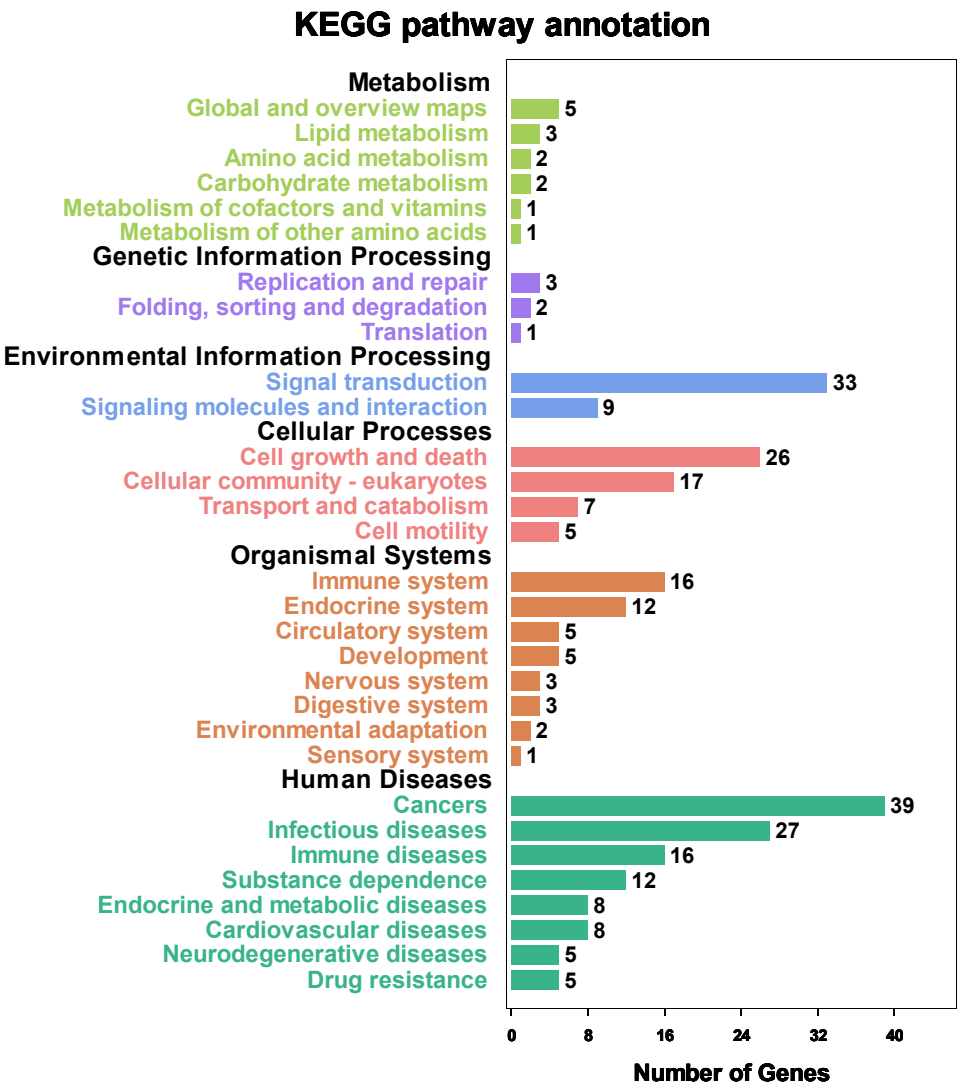

Figure 44. KEGG pathway enrichment analysis of DEGs (8VDB 18 hours)

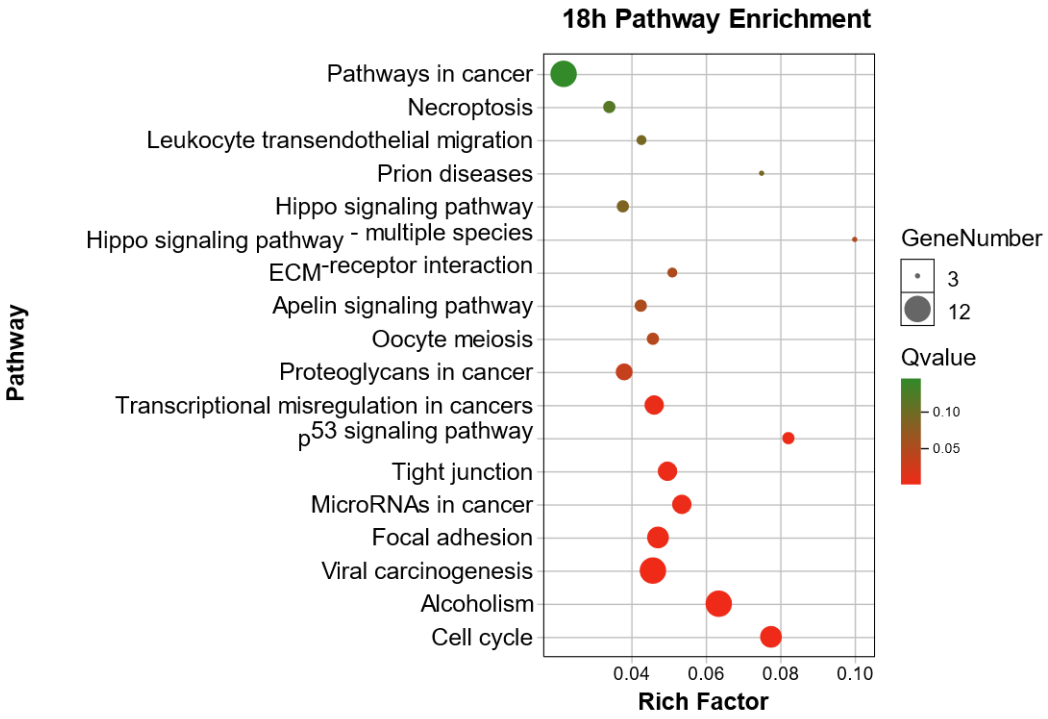

Figure 45. Top KEGG pathway enrichment analysis of DEGs (8VDB 18 hours)

Summary: after treatment with 8VDB, compared to control, DEGs were mainly enriched in cancers, global and overview maps, signal transduction, endocrine system, cell growth and death, cell community, transport and catabolism, and immune system. Top KEGG pathways were mainly enriched in p53 signaling pathway, transcriptional misregulation in cancers, tight junction, cell cycle, pathways in cancer, hippo signaling pathway, apelin signaling pathway, and MicroRNAs in cancer.

4.6 PPI Network Analysis and hub Genes Screening

In order to explore the regulatory relationship between DEGs, the protein-protein interaction network between DEGs was further analyzed, and the interaction network between DEGs (NetworkAnalyst3.0) was constructed by STRING.

4.6.1 PPI network construction and Hub Genes Screening for 2j

Compared to DMSO control, there were 125 DEGs after treatment with 1 μM 2j for 6 hours, 382 DEGs after treatment with 1 μM 2j for 12 hours, and 227 DEGs after treatment with 1 μM 2j for 18 hours, The online mapping tool (NetworkAnalyst3.0) was used to construct the differential protein-protein interaction networks (Figure 46, 47, 48) at different time points. From the PPI network analysis, the top 15 genes were ranked as hub genes by degree, the final hub gene was obtained as follows: CDKN1A, TUBA1A, TUBA4A, RRP12, EGR1, RPL11, EEK2, MRPL24, PSMD4, UBC, PLK1, CCNB1, CDC6, MCM2, CCND1, AURKB (Figure 49). The results of functional and pathway enrichment analysis showed that these 15 hub genes were mainly involved in the biological processes: mitotic cell cycle phase transition, cell cycle checkpoint, microtubule-based process, protein ubiquitination, and positive regulation of cell death. The main signal pathways involved were cell cycle, FoxO signaling pathway, p53 signaling pathway, and cellular senescence (Table 4).

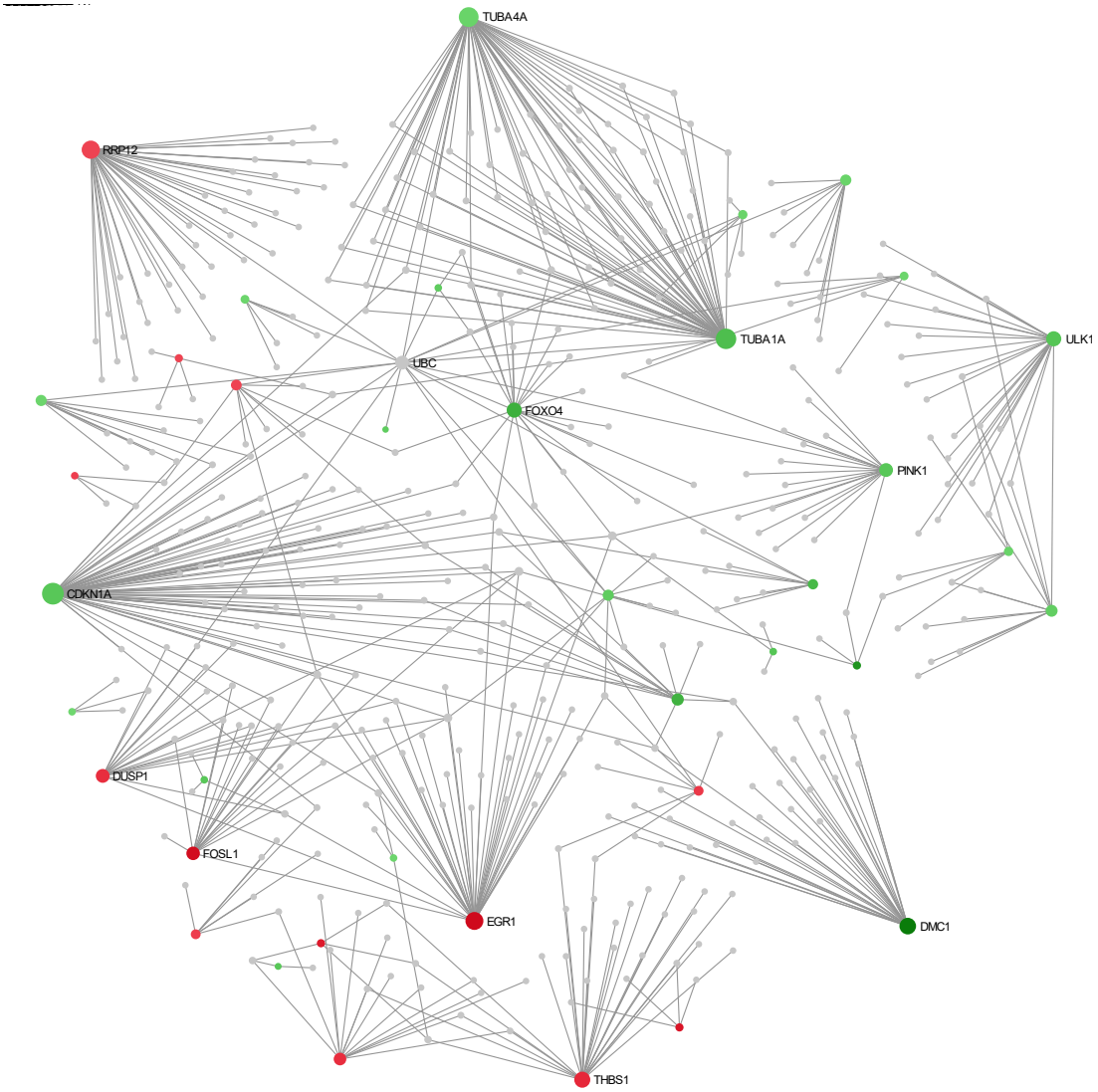

Figure 46. The PPI interaction network of DEGs (2j, 6 hours), the nodes represent the differential genes, the connections between the nodes represent the interactions between the genes, the size of the nodes represents the degree of the genes; red represents the up-regulation, green represents the down-regulation

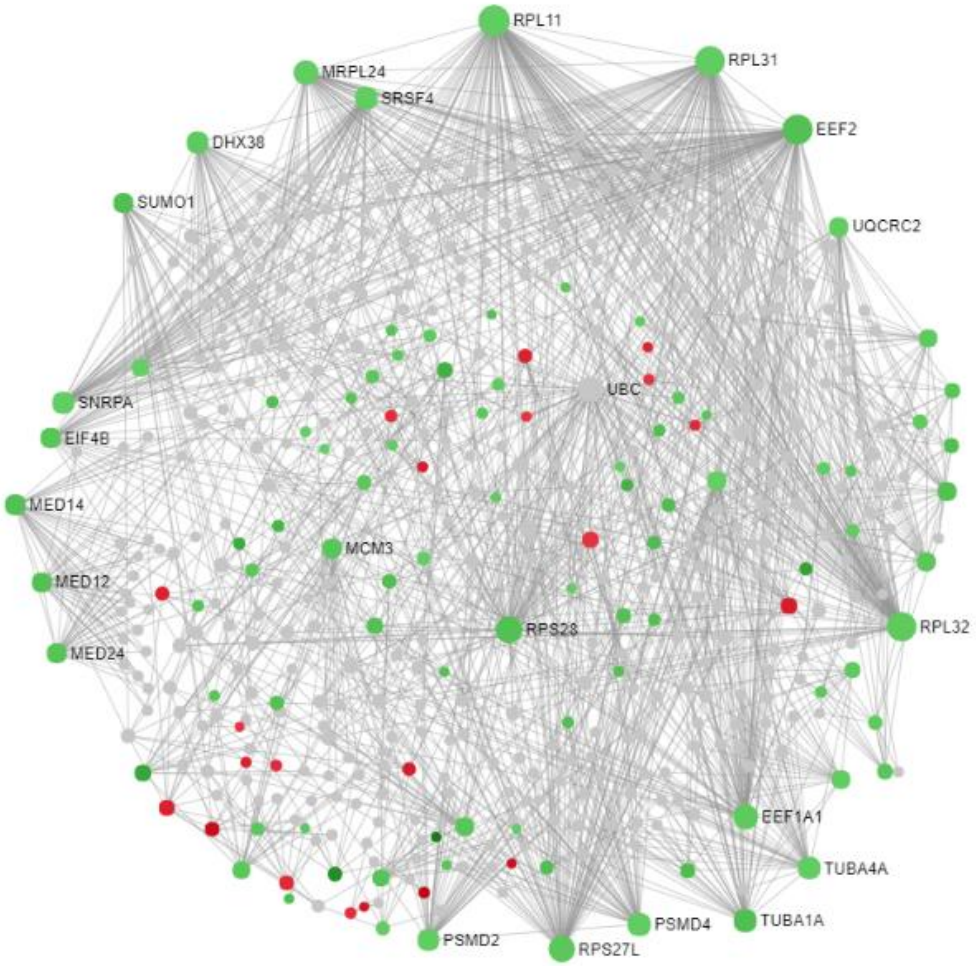

Figure 47. The PPI interaction network of DEGs (2j, 12 hours), the nodes represent the differential genes, the connections between the nodes represent the interactions between the genes, the size of the nodes represents the degree of the genes; red represents the up-regulation, green represents the down-regulation

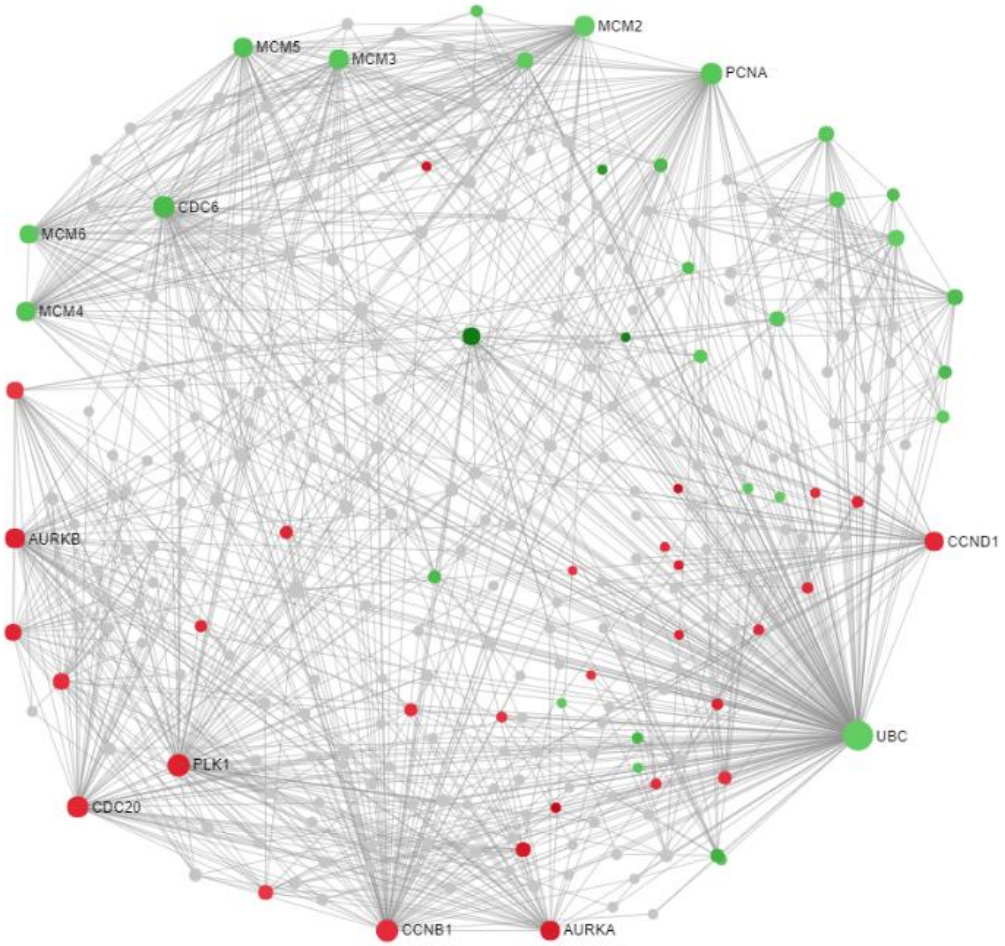

Figure 48. The PPI interaction network of DEGs (2j, 18 hours), nodes represent the differential genes, the connections between the nodes represent the interactions between the genes, the size of the nodes represents the degree of the genes; red represents the up-regulation, green represents the down-regulation

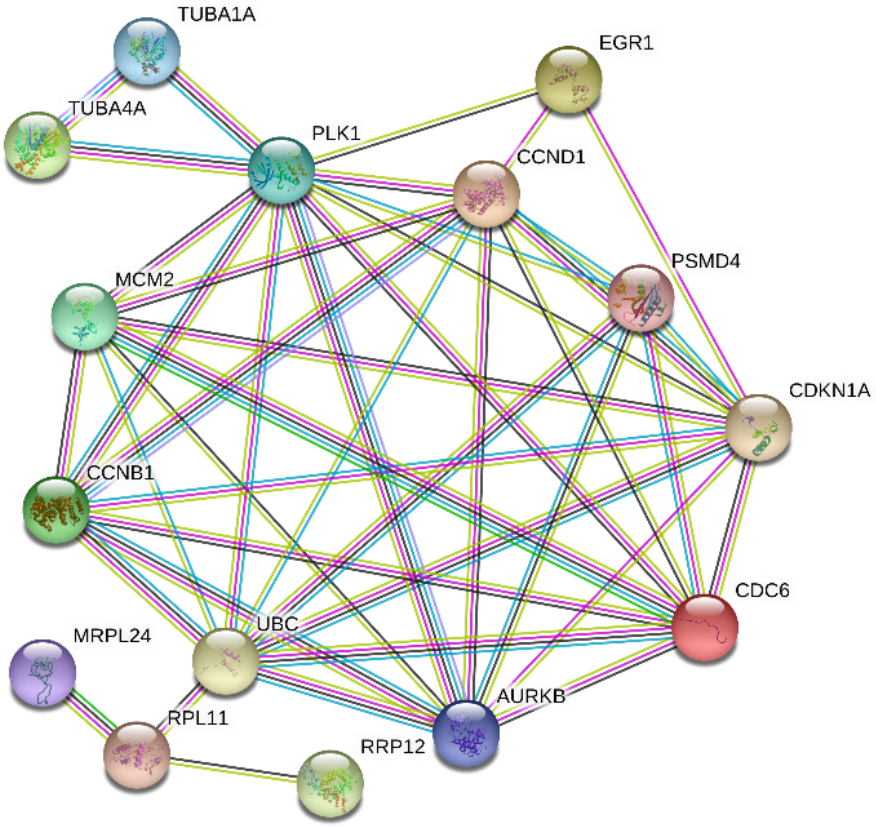

Figure 49. PPI network of the top 15 hub genes in 2j-treated Hela cells, network nodes represent proteins; edges represent PPI.

Table 4. The top 15 hub genes enrichment with GO and KEGG.

Category	Term	Description	Gene Count	*p* Value
Biological Process (GO)	GO:0044772	mitotic cell cycle phase transition	8	4.3e-91
Biological Process (GO)	GO:0000075	cell cycle checkpoint	6	7.49e-82
Biological Process (GO)	GO:1904666	Protein ubiquitination	2	8.55e-61
Biological Process (GO)	GO:0007017	microtubule-based process	5	1.28e-17
Biological Process (GO)	GO:0010942	positive regulation of cell death	3	2.31e-17
KEGG_PATHWAY	hsa04110	Cell cycle	6	5.74e-63
KEGG_PATHWAY	hsa04068	FoxO signaling pathway	4	2.95e-12
KEGG_PATHWAY	hsa04115	p53 signaling pathway	3	1.33e-10
KEGG_PATHWAY	hsa04218	Cellular senescence	3	2.12e-22

4.6.2 PPI network construction and hub Genes Screening for 16FB

Compared to DMSO control, there were 282 DEGs after treatment with 1 μM 16FB for 6 hours, and 331 DEGs after treatment with 1 μM 16FB for 18 hours, The online mapping tool (NetworkAnalyst3.0) was used to construct the differential protein-protein interaction network (Figure 50, 51) at

different time points. From the PPI network analysis, the top 15 genes were ranked as hub genes by degree, the final hub gene was obtained as follows: JUN, RPS27L, TUBB4B, CCND1, CDKN1A, TUBA1A, TUBA4A, AURKA, MCM3, CDC20, BRCA1, PLK1, UBC, PCNA, SUMO1 (Figure 52). The results of functional and pathway enrichment analysis showed that these 15 hub genes were mainly involved in the biological process: mitotic cell cycle phase transition, regulation of cell cycle, DNA damage checkpoint, microtubule-based process, regulation of apoptotic process. The main signal pathways involved were cell cycle, FoxO signaling pathway, apoptosis, and p53 signaling pathway (Table 5).

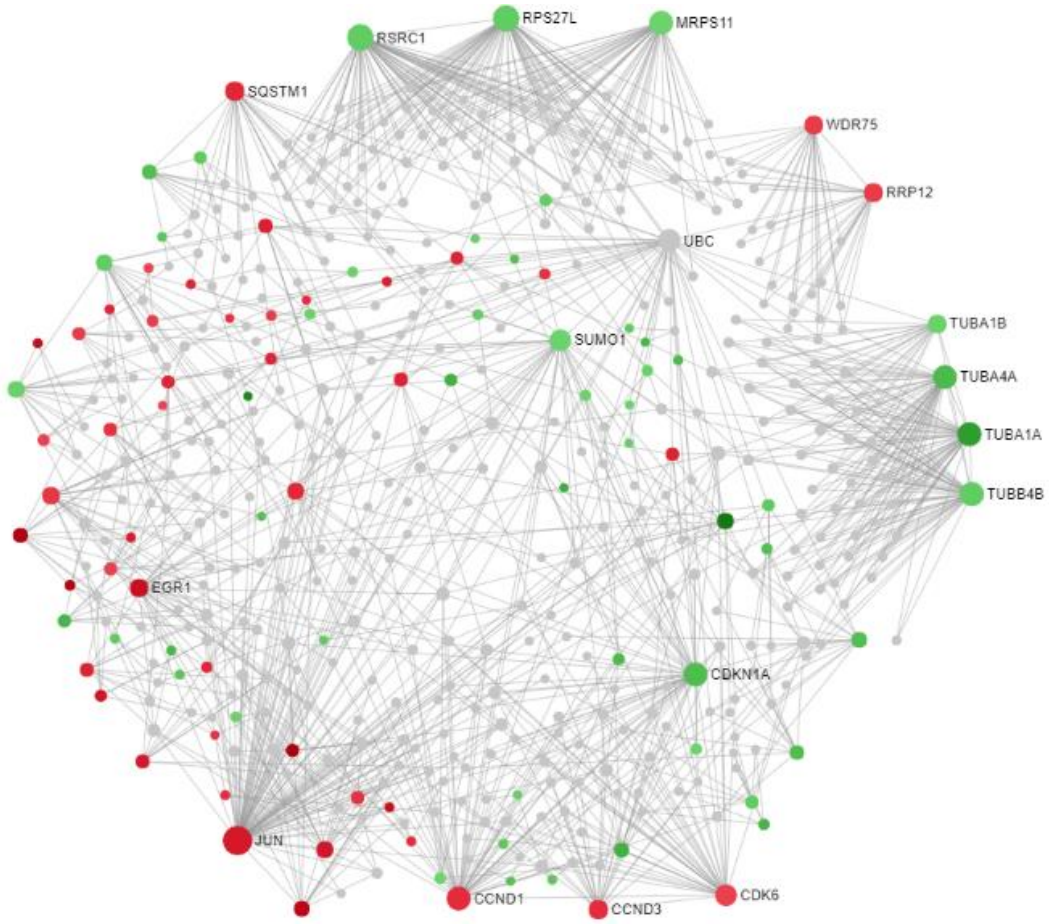

Figure 50. The PPI interaction network of DEGs (16FB, 6 hours), nodes represent the differential genes, the connections between the nodes represent the interactions

between the genes, the size of the nodes represents the degree of the genes; red represents the up-regulation, green represents the down-regulation

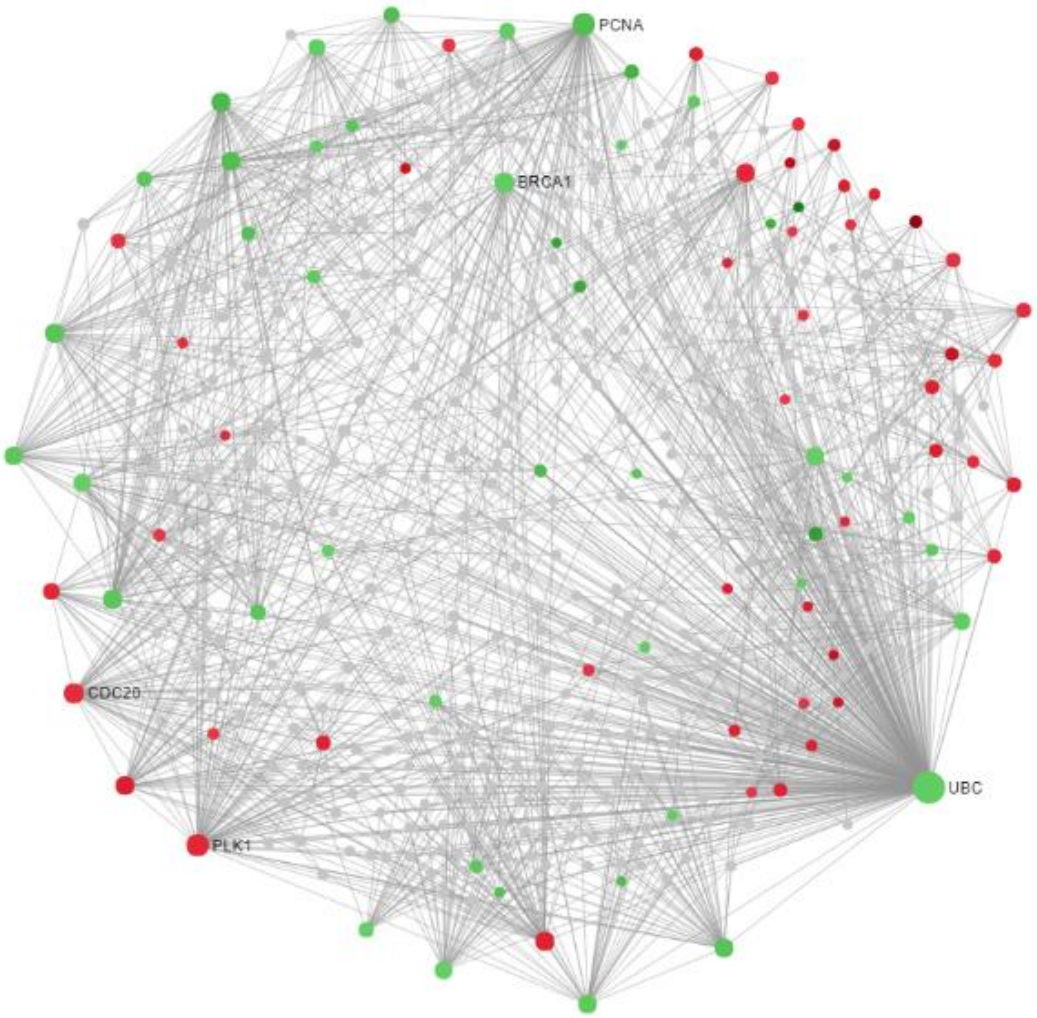

Figure 51. The PPI interaction network of DEGs (16FB, 18 hours), nodes represent the differential genes, the connections between the nodes represent the interactions between the genes, the size of the nodes represents the degree of the genes; red represents the up-regulation, green represents the down-regulation

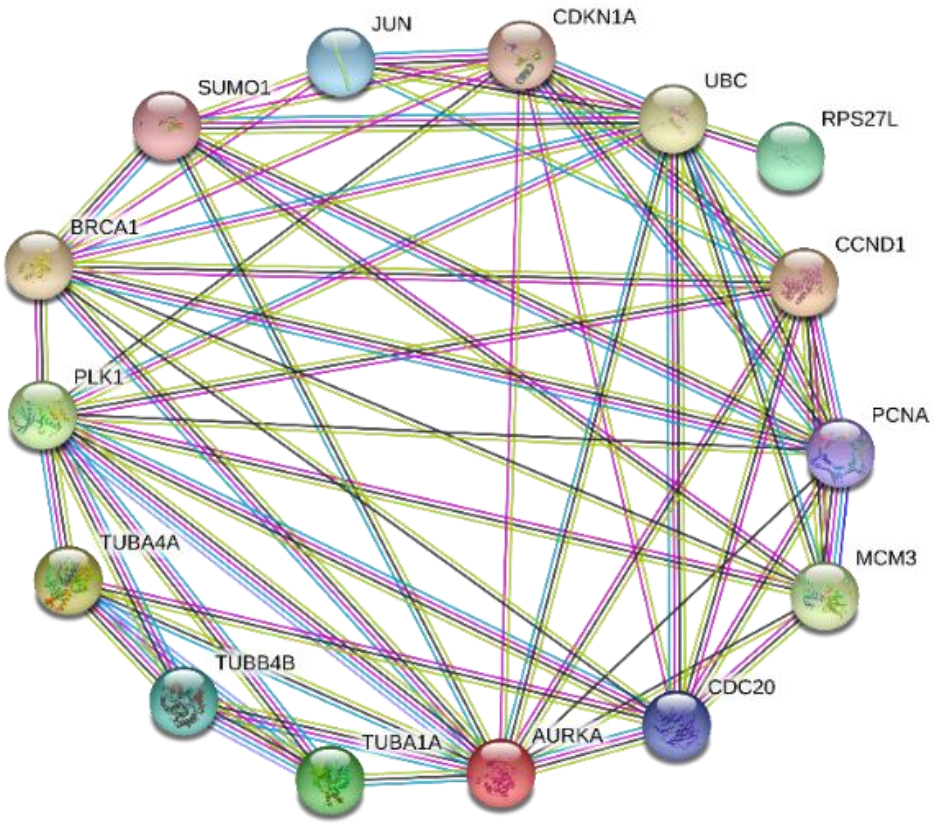

Figure 52. PPI analysis of the top 15 hub genes, network nodes represent proteins; edges represent PPI.

Table 5. The top 15 hub genes enrichment with GO and KEGG.

Category	Term	Description	Gene Count	*p* Value
Biological Process (GO)	GO:0044772	mitotic cell cycle phase transition	12	4.25e-91
Biological Process (GO)	GO:0051726	regulation of cell cycle	12	1.93e-86
Biological Process (GO)	GO:0000077	DNA damage checkpoint	7	1.42e-45

Biological Process (GO)	GO:0007017	microtubule-based process	7	2.8e-19
Biological Process (GO)	GO:0042981	regulation of apoptotic process	7	3.49e-27
KEGG_PATHWAY	hsa04110	Cell cycle	6	5.22e-65
KEGG_PATHWAY	hsa04068	FoxO signaling pathway	4	2.07e-15
KEGG_PATHWAY	hsa04210	Apoptosis	3	3.27e-15
KEGG_PATHWAY	hsa04115	p53 signaling pathway	3	1.01e-11

4.6.3 PPI network construction and hub Genes Screening for 8VDB

Compared to DMSO control, there were 204 DEGs after treatment with 1 μM 8VDB for 6 hours, and 273 DEGs after treatment with 1 μM 8VDB for 18 hours, The online mapping tool (NetworkAnalyst3.0) was used to construct the differential protein-protein interaction network (Figure 53,54) at different time points. From the PPI network analysis, the top 15 genes were ranked as hub genes by degree, the final hub gene was obtained as follows: JUN, AURKB, CCND1, CDKN1A, TUBA1A, TUBA4A, CDK6, UBC, PLK1, CCNB1, PCNA, CDC20, FYN, BUB1B, and KIF18A (Figure 55). The results of functional and pathway enrichment analysis showed that these 15 hub genes were mainly involved in the biological process: regulation of mitotic cell cycle phase transition, DNA damage checkpoint, microtubule-based process and positive regulation of cell death. The main signal pathways involved were cell cycle, FoxO signaling pathway, apoptosis, and p53 signaling pathway (Table 6).

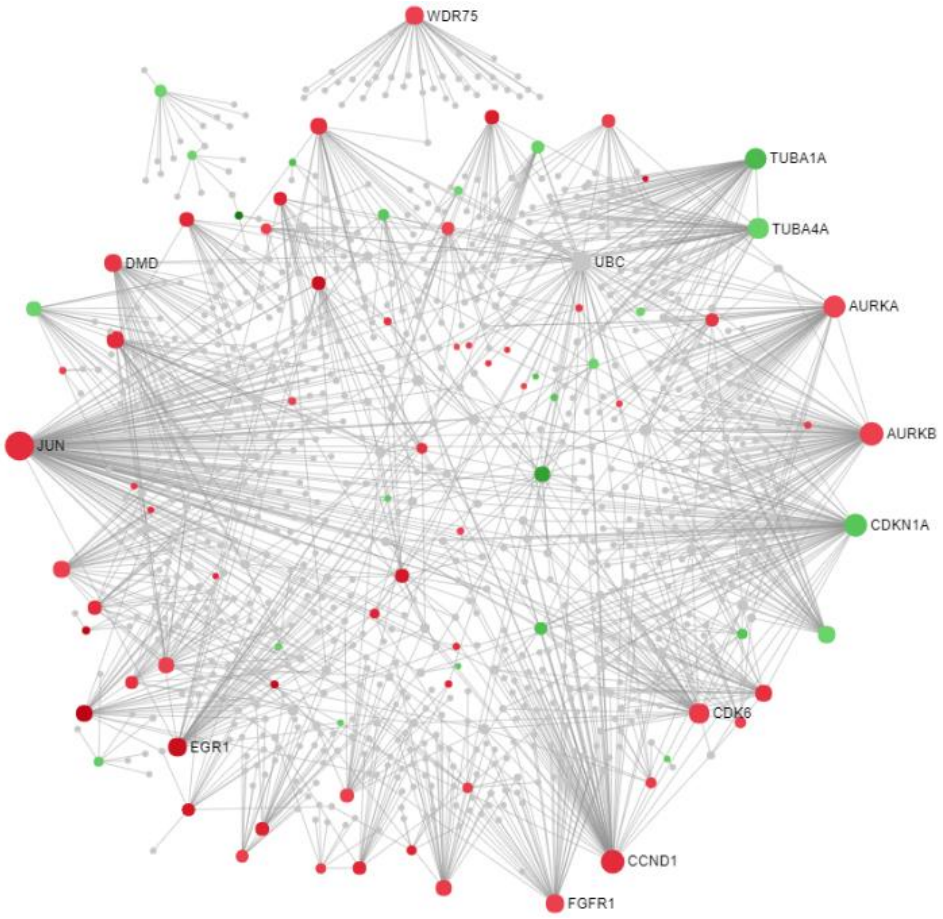

Figure 53. The PPI interaction network of DEGs (8VDB, 6 hours), nodes represent the differential genes, the connections between the nodes represent the interactions between the genes, the size of the nodes represents the degree of the genes; red represents the up-regulation, green represents the down-regulation

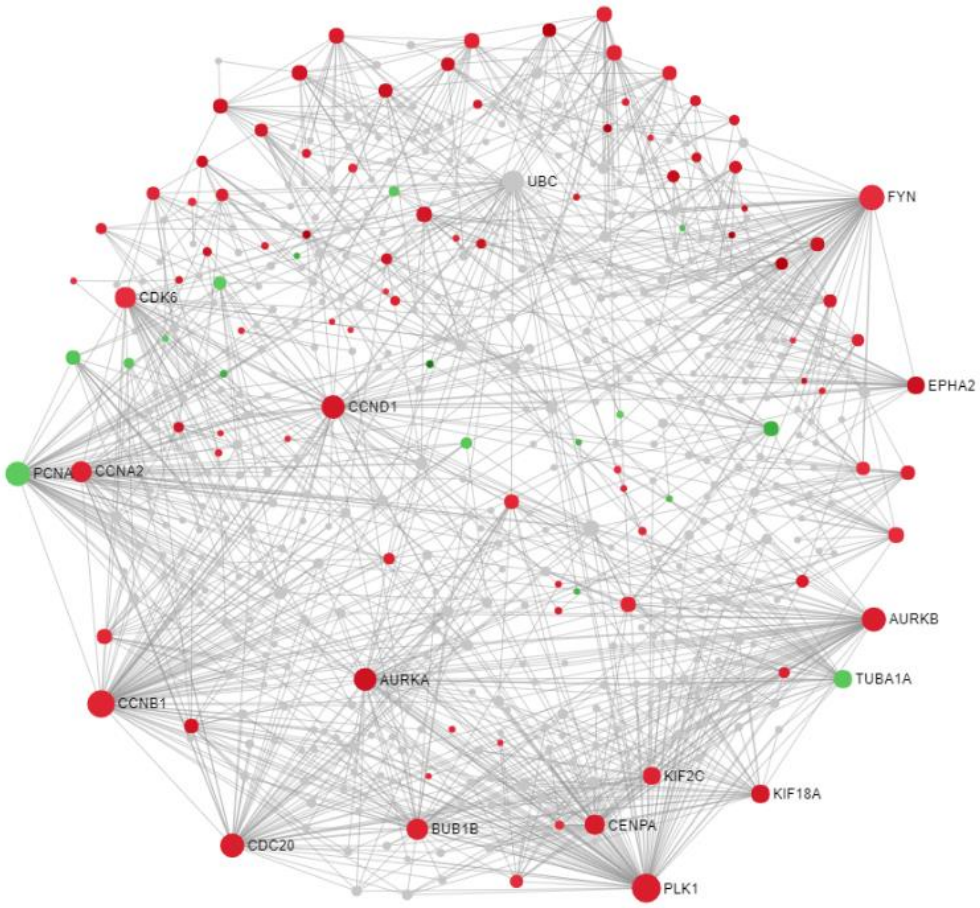

Figure 54. The PPI interaction network of DEGs (8VDB, 18 hours), nodes represent the differential genes, the connections between the nodes represent the interactions between the genes, the size of the nodes represents the degree of the genes; red represents the up-regulation, green represents the down-regulation

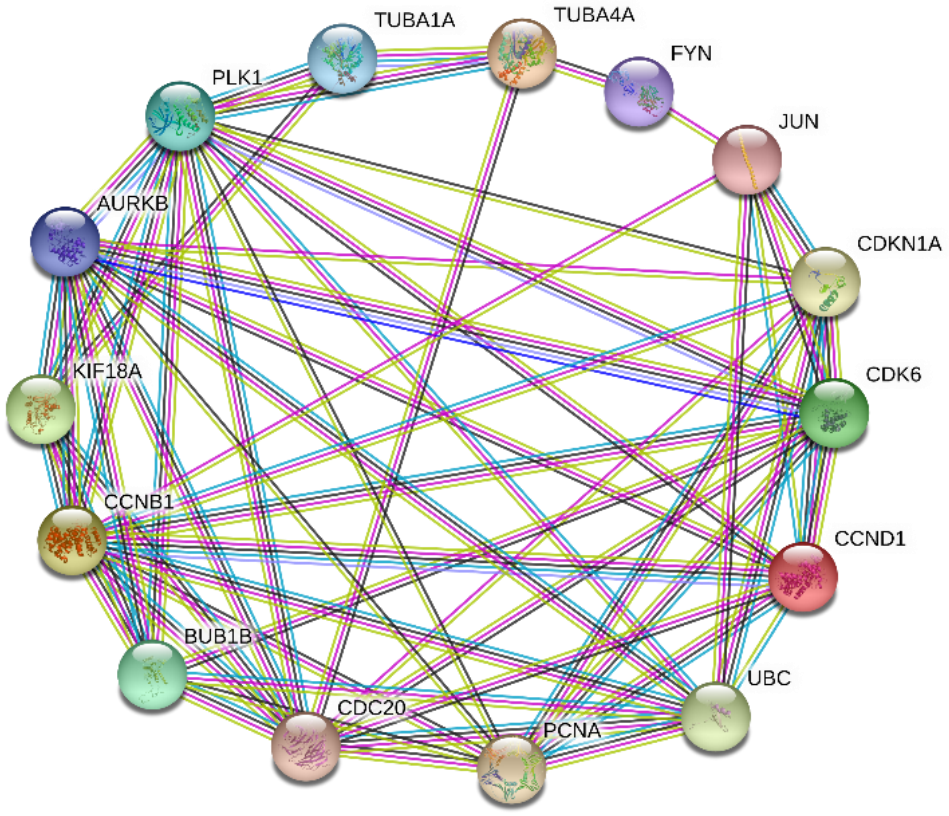

Figure 55. PPI analysis of the top 15 hub genes, network nodes represent proteins; edges represent PPI.

Table 6. The top 15 hub genes enrichment with GO and KEGG.

Category	Term	Description	Gene Count	*p* Value
Biological Process (GO)	GO:0044772	mitotic cell cycle phase transition	12	3.13e-93
Biological Process (GO)	GO:1901990	regulation of mitotic cell cycle phase transition	12	3.43e-88
Biological Process (GO)	GO:0000077	DNA damage checkpoint	5	6.48e-39
Biological Process (GO)	GO:0007017	microtubule-based process	7	7.08e-20

Biological Process (GO)	GO:0010942	positive regulation of cell death	2	4.49e-31
KEGG_PATHWAY	hsa04110	Cell cycle	8	8.75e-67
KEGG_PATHWAY	hsa04068	FoxO signaling pathway	4	1.27e-21
KEGG_PATHWAY	hsa04210	Apoptosis	3	9.32e-18
KEGG_PATHWAY	hsa04115	p53 signaling pathway	4	1.3e-10

4.7 Cmap

The differential gene regions obtained by 1 μM 2j, 16FB, and 8VDB treatment of Hela cells were split into positive and negative regulatory gene groups and compared to the gene expression profiles of drugs or compounds in the CMap database (https://www.Broadinstitute. Org/connectivity-map-cmap). Depending on the correlation degree of drug molecules, the highly related drug molecules were determined and the possible targets and mechanisms of drug molecules were summarized.

4.7.1 2j

Hela cells were treated with 1 μM 2j for 6 hours, 12 hours and 18 hours respectively. The DEGs were queried in the Connectivity Map (CMap) for identification of drugs and their target genes. The results of CMap analysis showed that 2j-induced DEGs were connected with tubulin inhibitors. The small molecular compounds in the top 10 of connectivity score were as follows: albendazole, flubendazole, ABT-751, chelidonine, SA-63133, vincristine, vindesine, nocodazole, fenbendazole, and mebendazole. The main targets of the drug involved

were CYP1A2, CYP2J2, TUBA1A, TUBB, TUBB4B, CSNK1E, CSNK1A1, CSNK1D and CSNK1G2 (Table 7).

Table 7. Pharmacologic perturbagens connected with 2j-induced DEGs

Name	Description	Belongs to	target	score
albendazole	Tubulin inhibitor, acetylcholinesterase inhibitor, microtubule inhibitor	Tubulin inhibitor	CYP1A2,CYP2J2, TUBA1A,TUBB, TUBB4B	98.72
flubendazole	acetylcholinesterase inhibitor, microtubule inhibitor, tubulin inhibitor	Tubulin inhibitor	TUBB	98.68
ABT-751	tubulin inhibitor, dihydropteroate synthase inhibitor, microtubule inhibitor, PABA antagonist, tubulin polymerisation inhibitor	Tubulin inhibitor	TUBB	98.4
chelidonine	tubulin polymerization inhibitor	Tubulin inhibitor		97.15

SA-63133	casein kinase inhibitor, tubulin inhibitor	Tubulin inhibitor	CSNK1E, CSNK1A1, CSNK1D, CSNK1G2	97.08
vincristine	tubulin inhibitor, microtubule inhibitor, microtubule polymerization inhibitor, tubulin polymerisation inhibitor, vinca alkaloid	Tubulin inhibitor	TUBB, TUBA4A	96.42
vindesine	tubulin inhibitor, microtubule inhibitor, vinca alkaloid	Tubulin inhibitor	TUBB, TUBB1	96.39
nocodazole	tubulin inhibitor, Tubulin Polymerization Inhibitors	Tubulin inhibitor	HPGDS	96.37
fenbendazole	cytochrome P450 inhibitor, tubulin inhibitor	Tubulin inhibitor	CYP2C19, CYP2D6, CYP2J2, CYP3A4, TUBB	95.44
mebendazole	acetylcholinesterase inhibitor, microtubule inhibitor, tubulin	Tubulin inhibitor	TUBA1A, TUBB, TUBB4B	95.19

	inhibitor			

4.7.2 16FB

Hela cells were treated with 1 μM 16FB for 6 hours and 18 hours respectively. The DEGs were queried in the Connectivity Map (CMap) for identification of drugs and their target genes. The results of CMap analysis showed that 16FB-induced DEGs were connected with tubulin inhibitors. The small molecular compounds in the top 10 connectivity score were as follows: mebendazole, vindesine, ABT-751, KF-38789, vincristine, nocodazole, flubendazole, SA-792574, NPI-2358, and vinorelbine. The main targets of the drug involved were TUBA1A, TUBB, TUBB4B, TUBB1, SELP and HPGDS (Table 8).

Table 8. Pharmacologic perturbagens connected with 16FB-induced DEGs

Name	Description	Belongs to	target	score
mebendazole	acetylcholinesterase inhibitor, microtubule inhibitor, tubulin inhibitor	Tubulin inhibitor	TUBA1A, TUBB, TUBB4B	99.51
vindesine	tubulin inhibitor, microtubule inhibitor, vinca alkaloid	Tubulin inhibitor	TUBB, TUBB1	99.5
ABT-751	tubulin inhibitor, dihydropteroate synthase inhibitor, microtubule inhibitor, PABA antagonist, tubulin polymerisation inhibitor	Tubulin inhibitor	TUBB	99.42
KF-38789	P selectin inhibitor		SELP	99.4

vincristine	tubulin inhibitor, microtubule inhibitor, microtubule polymerization inhibitor, tubulin polymerisation inhibitor, vinca alkaloid		TUBB, TUBA4A	99.32
nocodazole	tubulin inhibitor, Tubulin Polymerization Inhibitors	Tubulin inhibitor	HPGDS	99.21
flubendazole	acetylcholinesterase inhibitor, microtubule inhibitor, tubulin inhibitor	Tubulin inhibitor	TUBB	99.21
SA-792574	microtubule inhibitor, tubulin inhibitor	Tubulin inhibitor	TUBB	98.97
NPI-2358	tubulin inhibitor, angiogenesis inhibitor, tubulin polymerisation inhibitor	Tubulin inhibitor		98.96
vinorelbine	tubulin inhibitor, apoptosis stimulant, microtubule inhibitor, mitosis inhibitor, mitotic inhibitor, tubulin polymerisation inhibitor, vinca alkaloid	Tubulin inhibitor	TUBB	98.92

4.7.3 8VDB

Hela cells were treated with 1 μM 8VDB for 6 hours and 18 hours respectively. The DEGs were queried in the Connectivity Map (CMap) for identification of drugs and their target genes. The results of CMap analysis showed that 8VDB-induced DEGs were connected with tubulin inhibitors. The

small molecular compounds in the top 10 connectivity score were as follows: albendazole, Flubendazole, oxibendazole, fenbendazole, ABT-751, SA-792574, mebendazole, vincristine, KF-38789, and vincristine. The main targets of the drug involved were CYP1A2, TUBA1A, TUBB, TUBB4B, CYP2C19, CYP2D6, CYP2J2, CYP3A4 and SELP (Table 9).

Table 9. Pharmacologic perturbagens connected with 8VDB-induced DEGs

Name	Description	Belongs to	target	score
albendazole	tubulin inhibitor, acetylcholinesterase inhibitor, microtubule inhibitor	Tubulin inhibitor	CYP1A2, CYP2J2, TUBA1A, TUBB, TUBB4B	99.78
flubendazole	acetylcholinesterase inhibitor, microtubule inhibitor, tubulin inhibitor	Tubulin inhibitor	TUBB	99.65
oxibendazole	DNA polymerase inhibitor, tubulin inhibitor	Tubulin inhibitor	TUBB, TUBB4B	99.55
fenbendazole	cytochrome P450 inhibitor, tubulin inhibitor	Tubulin inhibitor	CYP2C19, CYP2D6, CYP2J2, CYP3A4, TUBB	99.54

ABT-751	tubulin inhibitor, dihydropteroate synthase inhibitor, microtubule inhibitor, PABA antagonist, tubulin polymerisation inhibitor	Tubulin inhibitor	TUBB	99.48
SA-792574	microtubule inhibitor, tubulin inhibitor	Tubulin inhibitor	TUBB	99.38
mebendazole	acetylcholinesterase inhibitor, microtubule inhibitor, tubulin inhibitor	Tubulin inhibitor	TUBA1A, TUBB, TUBB4B	99.38
vincristine	tubulin inhibitor, microtubule inhibitor, microtubule polymerization inhibitor, tubulin polymerisation inhibitor, vinca alkaloid		TUBB, TUBA4A	99.17
KF-38789	P selectin inhibitor		SELP	99.1
vincristine	tubulin inhibitor, microtubule inhibitor, microtubule polymerization inhibitor, tubulin polymerisation inhibitor, vinca alkaloid	Tubulin inhibitor	TUBB, TUBA4A	99.02

4.8 qRT-PCRvalidation of the hub genes

Reliability of RNA-seq results is affected by many factors, such as the quality of

sample RNA, library construction and data analysis scheme, therefore, it is very important to verify the results of RNA-seq. To validate the RNA-seq results, the expression levels of the hub genes and possible targets by compounds were verified by quantitative RT-PCR (qRT-PCR). The results of qRT-PCR showed differential gene expression and the results were consistent with the RNA-seq data (Figure 56, 57, 58).

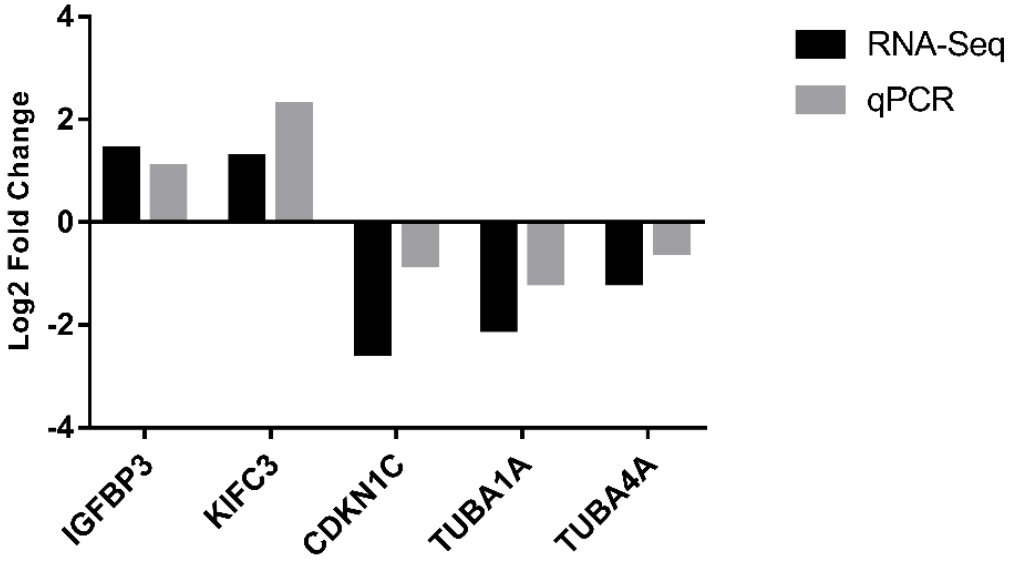

Figure 56. Validation of the 2j RNA-Seq result by qRT-PCR. The x-axis shows the names of selected genes while y-axis represents the log2 fold change of gene expression

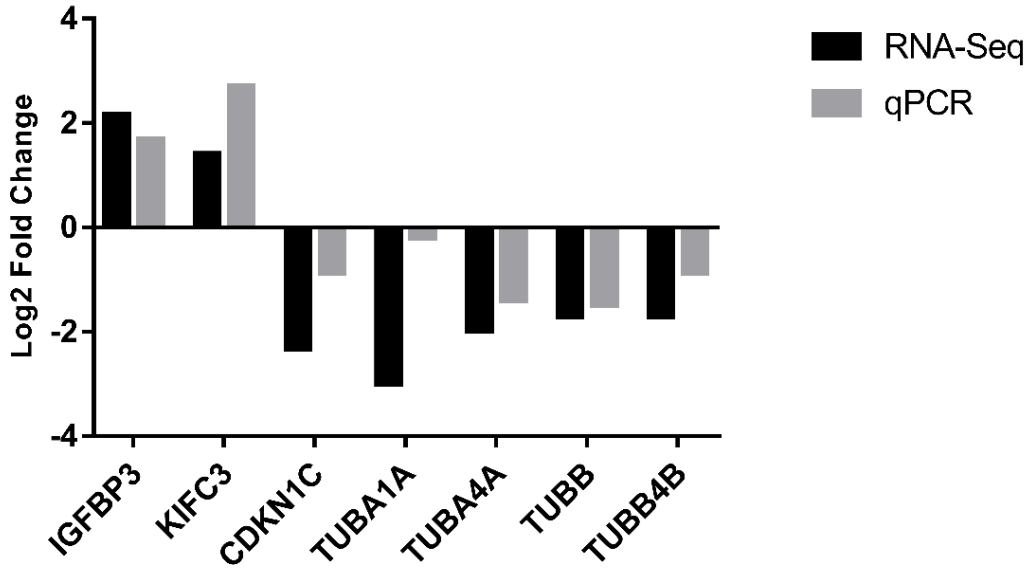

Figure 57. Validation of the 16FB RNA-Seq result by qRT-PCR. The x-axis shows the names of selected genes while y-axis represents the log2 fold change of gene expression

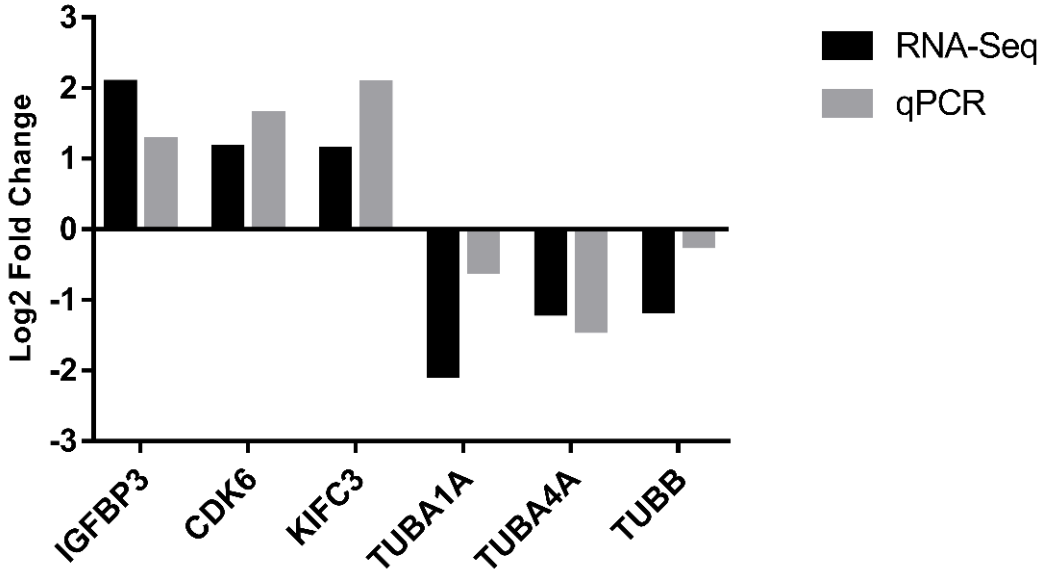

Figure 58. Validation of the 8VDB RNA-Seq result by qRT-PCR. The x-axis shows the names of selected genes while y-axis represents the log2 fold change of gene expression

4.9 Molecular Docking studies

The interactions between small molecule compounds and proteins are mainly caused by non-covalent bond interactions: van der Waals forces, hydrogen bonds, hydrophobic forces, and π-π stacking interactions (Riley and Hobza 2011). Hydrogen bonds are essential for conformations and binding activity in ligand-receptor interactions. According to molecular simulation docking results, N in the oxadiazole ring can form a hydrogen bond with the hydroxyl group on Thr179 residue. The 1,4-dihydroindolo[1,2-b]pyrrole ring can form π stacks with the benzene ring on the Tyr224 residue and form a hydrophobic interaction with Ile171 and Ala12 in the surrounding environment (Figure 59). These factors form the basis for the binding of 2j to tubulin. Molecular docking simulation of colchicine and tubulin was conducted under the same conditions. It can be seen that colchicine binds to tubulin mainly by forming a solid hydrogen bond with Gln11, Ala12, Gln15, Asn101 and Asn206. By comparing the docking results of colchicine, it can be seen that 2j also interacts with tubulin in the same spatial position (Figure 60).

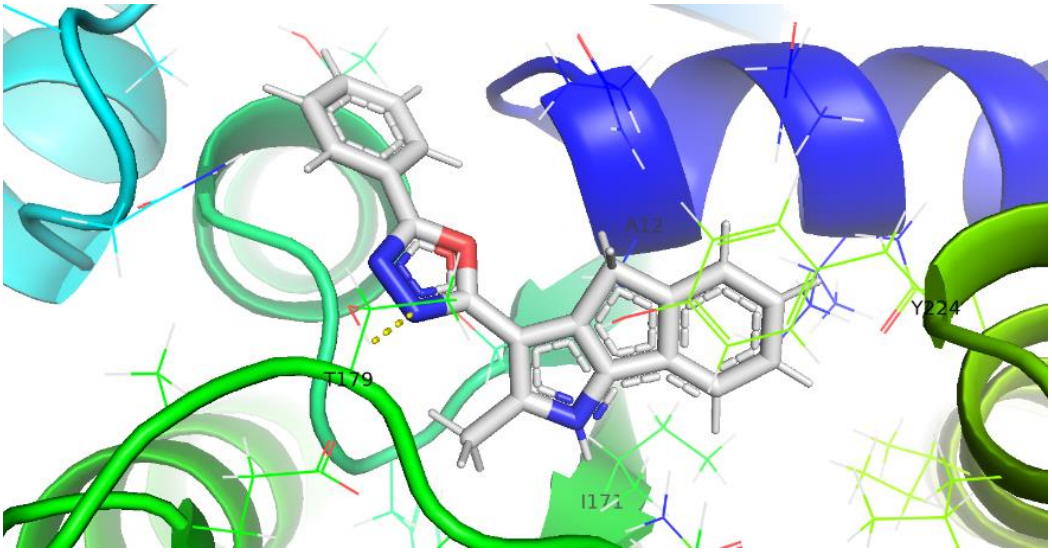

Figure 59. Detailed molecular interactions between the 2j molecule and the tubulin. 2j is shown in white, the yellow dotted line represents the hydrogen bond

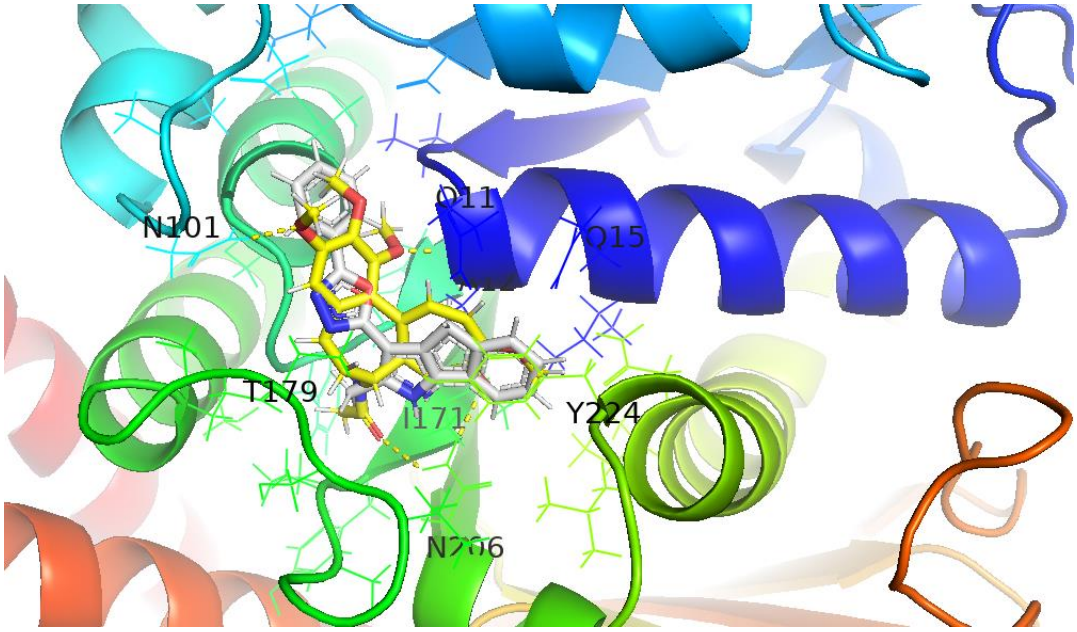

Figure 60. The binding sites analysis for 2j-tubulin complex. 2j is shown in white and colchicine is shown in yellow, the yellow dotted line represents the hydrogen bond

5．Discussion

The treatment of cancer has made remarkable progress in the past decade. However, chemotherapeutic drugs often lead to drug resistance and intolerable toxicity, which unfortunately often lead to the failure of tumor chemotherapy. Therefore, it is urgent to develop new anticancer drugs with superior efficacy, superior tolerability and high safety. Along with the accelerating process of drug discovery, synthetic technology and high-throughput screening technological advances, have generated a large number of active small molecular compounds with good profiles, but their targets and mechanisms of action are difficult to be efficiently identified. The result is that new drugs are slow to progress to clinical studies. Target specific drug molecules are not only beneficial to drug effect mechanism of exploration, but also help clinical

observation of drug metabolism process.

Drug discovery and target selection are intricate, uncertain and expensive processes. Moreover, the mechanism of tumor proliferation and differentiation is very complex, and there are crossover and compensatory mechanisms between signaling pathways. Therefore, the design and synthesis of low-toxic, highly selective and efficient inhibitors are the main directions where the anti-tumor drug research and development are going.1,3,4-oxadiazoles derivatives activity was tested on a variety of cancer cell lines, its antitumor effect is associated with a variety of mechanisms, including growth factor pathways, enzymes, kinase inhibitors and receptors. Specific examples are VEGFR and EGFR, Hdac, NF-κb, and telomerases. 1,3,4-oxadiazoles may become the main new anticancer drugs in the future (Bajaj, Asati et al. 2015, Bajaj, Roy et al. 2018, Glomb, Szymankiewicz et al. 2018).

In the early stage of this research, 1,3,4-oxadiazole compounds with different structure were designed and synthesized and they were found to have strong inhibitory activity on various tumor cell lines. Among them, the most active drug, the 2j showed high anti-tumor activity in different tumor cells (IC50 range is 0.05-1.7 μM).

Cell cycle detection showed that compound 2j is able to induce G2/M cell cycle arrest and had a strong apoptotic response. Based on the previous work, this thesis aimed to utilize 16 recently designed and synthesized 1,3,4-oxadiazole compounds, and determine their antiproliferative activity, action on cell cycle, effect on gene expression, and predict the mechanism of action and potential docking sites. In the present research, CCK8 method was used to screen 16 newly synthesized candidate anti-tumor small molecules, and Hela, McF7 and PC-3 were selected as target cell lines. The results showed that 7FB, 16FB, 8VDB, 22VDB and 23VDB had significant

inhibitory effects on these tumor cell lines. The killing effect on human cervical cancer HeLa cells was the most obvious. The IC50 range of 2j and 2j derivatives was 0.005-0.555 μM.

Microtubules, essential components for the cytoskeleton, are dimers formed by two different types of tubulin subunits, which form a long tubular unit structure (Conde and Caceres 2009). The most important characteristic of tumor cells is that they proliferate uncontrolled and unlimited, and this process depends on the activity of intracellular tubulin, therefore, destroying the dynamic balance of tubulin is an important way to inhibit the growth of tumor cells (Jordan and Wilson 2004).In the process of tumor cell division, tubulin inhibitor drugs can inhibit the aggregation of tubulin into microtubules, or inhibit the depolymerization of tubulin into microtubules, resulting in the failure of mitosis, inducing cell apoptosis, and achieving the purpose of inhibiting the growth of tumor cells (Dumontet and Jordan 2010), in addition to anti-mitosis, tubulin inhibitors inhibit angiogenesis in tumor tissues. Recent studies have demonstrated that microtubule-targeted inhibitors have the potential to inhibit tumor angiogenesis and damage blood vessels (Sun, Li et al. 2013). One of the most classic biological characteristics of tubulin inhibitors as anti-tumor players is the arrest of the G2/M phase of cells (Lu, Chen et al. 2012). In the present research, PI staining and flow cytometry were utilized to detect the influence of 2j and 2j derivatives on Hela and PC-3 cell cycle. The results showed that 2j and 2j derivatives could significantly change the ratio of cell cycle distribution of Hela and PC-3, and considerably block cell growth in G2/M phase, as the proportion of G0/G1 phase and S phase cell number decreased significantly. The dysregulation of the cell cycle is one of the causes of tumor formation. Cell cycle arrest can lead to cell apoptosis, regulation of cell cycle of tumor cells can effectively control the growth of tumor cells. When the DNA of tumor cells is damaged, it selectively arrests in G2 phase. In this study, flow cytometry was used to detect the changes of cell cycle treated with 2j and

its derivatives, the results showed that 2j and the 2j derivatives could induce time-dependent G2/M phase arrest, suggesting that 2j and its derivatives could affect the proliferation of cells by inducing G2/M phase arrest. This research could give important directions for the study of the anti-tumor mechanism of 2j and its derivatives.

The advantage of bioinformatics in the discovery and identification of drug targets is the ability to integrate data from different databases and analyze them from a multidimensional perspective. One of the main objectives of this thesis was to screen and analyze the function of drug targets by differential transcriptome analysis. In order to further investigate the possible targets and molecular mechanisms of 2j and 2j derivatives, this research obtained DEGs based on the analysis of RNA-seq data, and performed functional (GO term) and pathway (KEGG) enrichment analysis of DEGs.

When drugs bind to specific sites of tubulin, they can interfere with the normal structure and function of microtubules by affecting their assembly (Lu, Chen et al. 2012). If the microtubules are destroyed, the internal balance of the cells is disrupted, and this can cause cell cycle arrest and apoptosis. The pathways that cause apoptosis are mediated by the death receptor pathway, the mitochondrial pathway, and the endoplasmic reticulum stress pathway (Bhalla 2003). By comparing the DEGs obtained by 2j and 2j derivatives treatment at different times and the hub gene obtained through the PPI network analysis, it was found that the function (GO term) and KEGG pathway enrichment results were similar. 2j and 2j derivatives mainly affect the regulation of mitotic cell cycle phase transition, DNA checkpoint, microtubule-based process, positive regulation of cell death and other biological processes. They also affect the cell cycle, FoxO signaling pathway, apoptosis, p53 signaling pathway, cellular senescence and other signaling pathways to inhibit cell proliferation may directly lead to tumor cell death. The effects of 2j and 2j derivatives

were studied by CMap, the high-correlation drug molecules are determined according to the correlation degree of drug molecules, and by summarizing the possible target and mechanism of action of drug molecules. The results showed that 2j and 2j derivatives-induced DEGs were mainly correlated with tubulin inhibitors. According to the identified hub genes and the small molecule targets obtained by CMap comparison the possible targets of 2j and 2j derivatives may be TUBA1A, TUBA4A, and TUBB. From the PPI network analysis, the target genes can be found in the hub genes that were finally obtained. The results indicated that the target of 2j and its derivatives was tubulin.

To verify the experimental results, the crystal structure of tubulin was downloaded from RCSB PDB (Arnst, Wang et al. 2018), and the binding mode of 2j and tubulin was verified by molecular docking. The results showed that N in the oxadiazole ring is able to form a hydrogen bond with the hydroxyl group on Thr179 residue. The 1,4-dihydroindolo[1,2-b]pyrrole ring can form π-π stacks with the benzene ring on the Tyr224 residue and form a hydrophobic interaction with Ile171 and Ala12 in the surrounding environment. By comparing the docking results of colchicine, it is visible that 2j also interacts with tubulin in the same spatial position. Molecular docking results showed that 2j interacts at the colchicine-binding site on tubulin. Four tubulin inhibitor binding sites are known: paclitaxel binding site, vinblastine binding site, laulimalide binding site and colchicine binding site. The colchicine binding site is located in the α/β tubulin beta subunit of the dimer interface. Drugs that bound to tubulin mainly through the formation of α/β tubulin-drug complex, changes the conformation of tubulin and promotes microtubule solution, thereby promoting microtubule depolymerization and inhibiting the aggregation (Lu, Chen et al. 2012, Li, Sun et al. 2017). It has been noted that a variety of small molecule compounds can target the colchicine binding site, showing excellent anti-tumor activity and blocking tumor vascular activity *in vitro* and *in vivo* (Hadfield, Ducki et al. 2003, Wilson and

Jordan 2004, Tangutur, Kumar et al. 2017, Kaul, Risinger et al. 2019).

In conclusion, 2j and 2j derivatives are able to target tubulin, inhibit cell division, change the normal physiological functions of tumor cells, cause G2/M phase arrest in the mitotic cycle of tumor cells, affect the regulation of mitotic cell cycle phase transition, DNA damage checkpoint, microtubule-based process, positive regulation of cell death and other biological processes, trigger tumor cell death by effecting cell cycle, FoxO signaling pathway, apoptosis, p53 signaling pathway. However, further experiments are needed to verify the *in vivo* function of the DEGs.

References

Alam-Faruque, Y., E. C. Dimmer, R. P. Huntley, C. O'Donovan, P. Scambler and R. Apweiler (2010). "The Renal Gene Ontology Annotation Initiative." Organogenesis **6**(2): 71-75.

Alsaab, H. O., S. Sau, R. Alzhrani, K. Tatiparti, K. Bhise, S. K. Kashaw and A. K. Iyer (2017). "PD-1 and PD-L1 Checkpoint Signaling Inhibition for Cancer Immunotherapy: Mechanism, Combinations, and Clinical Outcome." Front Pharmacol **8**: 561.

Arnst, K. E., Y. Wang, D. J. Hwang, Y. Xue, T. Costello, D. Hamilton, Q. Chen, J. Yang, F. Park, J. T. Dalton, D. D. Miller and W. Li (2018). "A Potent, Metabolically Stable Tubulin Inhibitor Targets the Colchicine Binding Site and Overcomes Taxane Resistance." Cancer Res **78**(1): 265-277.

Asghar, U., A. K. Witkiewicz, N. C. Turner and E. S. Knudsen (2015). "The history and future of targeting cyclin-dependent kinases in cancer therapy." Nat Rev Drug Discov **14**(2): 130-146.

Bajaj, S., V. Asati, J. Singh and P. P. Roy (2015). "1,3,4-Oxadiazoles: An emerging scaffold to target growth factors, enzymes and kinases as anticancer agents." Eur J Med Chem **97**: 124-141.

Bajaj, S., P. P. Roy and J. Singh (2018). "1,3,4-Oxadiazoles as Telomerase Inhibitor: Potential Anticancer Agents." Anticancer Agents Med Chem **17**(14): 1869-1883.

Baudino, T. A. (2015). "Targeted Cancer Therapy: The Next Generation of Cancer Treatment." Curr Drug Discov Technol **12**(1): 3-20.

Benmansour, F., C. Eydoux, G. Querat, X. de Lamballerie, B. Canard, K. Alvarez, J. C. Guillemot and K. Barral (2016). "Novel 2-phenyl-5-[(E)-2-(thiophen-2-yl)ethenyl]-1,3,4-oxadiazole and 3-phenyl-5-[(E)-2-(thiophen-2-yl)ethenyl]-1,2,4-oxadiazole derivatives as dengue virus inhibitors targeting NS5 polymerase." Eur J Med Chem **109**: 146-156.

Bhalla, K. N. (2003). "Microtubule-targeted anticancer agents and apoptosis." Oncogene **22**(56): 9075-9086.

Boutayeb, S., F. Z. Zakkouri, M. Aitelhaj, M. Mesmoudi, A. Boutayeb, W. Boutayeb, H. Mrabti and H. Errihani (2012). "[Protein tyrosine kinase inhibitors in cancer therapy]." Pathol Biol (Paris) **60**(4): 229-233.

Bray, F., J. Ferlay, I. Soerjomataram, R. L. Siegel, L. A. Torre and A. Jemal (2018). "Global cancer statistics 2018: GLOBOCAN estimates of incidence and mortality worldwide for 36 cancers in 185 countries." CA Cancer J Clin **68**(6): 394-424.

Bray, F., A. Jemal, N. Grey, J. Ferlay and D. Forman (2012). "Global cancer transitions according to the Human Development Index (2008-2030): a population-based study." Lancet Oncol **13**(8): 790-801.

Bray, F. and I. Soerjomataram (2015). The Changing Global Burden of Cancer: Transitions in Human Development and Implications for Cancer Prevention and

Control. Cancer: Disease Control Priorities, Third Edition (Volume 3). H. Gelband, P. Jha, R. Sankaranarayanan and S. Horton. Washington (DC), The International Bank for Reconstruction and Development / The World Bank
(c) 2015 International Bank for Reconstruction and Development / The World Bank.
Buchbinder, E. I. and A. Desai (2016). "CTLA-4 and PD-1 Pathways: Similarities, Differences, and Implications of Their Inhibition." Am J Clin Oncol **39**(1): 98-106.
Calon, A., D. V. Tauriello and E. Batlle (2014). "TGF-beta in CAF-mediated tumor growth and metastasis." Semin Cancer Biol **25**: 15-22.
Chalhoub, N. and S. J. Baker (2009). "PTEN and the PI3-kinase pathway in cancer." Annu Rev Pathol **4**: 127-150.
Chang, J., Y. Kim and H. J. Kwon (2016). "Advances in identification and validation of protein targets of natural products without chemical modification." Nat Prod Rep **33**(5): 719-730.
Chawla, G., B. Naaz and A. A. Siddiqui (2018). "Exploring 1,3,4-Oxadiazole Scaffold for Anti-inflammatory and Analgesic Activities: A Review of Literature From 2005-2016." Mini Rev Med Chem **18**(3): 216-233.
Conde, C. and A. Caceres (2009). "Microtubule assembly, organization and dynamics in axons and dendrites." Nat Rev Neurosci **10**(5): 319-332.
Dagenais, G. R., D. P. Leong, S. Rangarajan, F. Lanas, P. Lopez-Jaramillo, R. Gupta, R. Diaz, A. Avezum, G. B. F. Oliveira, A. Wielgosz, S. R. Parambath, P. Mony, K. F. Alhabib, A. Temizhan, N. Ismail, J. Chifamba, K. Yeates, R. Khatib, O. Rahman, K. Zatonska, K. Kazmi, L. Wei, J. Zhu, A. Rosengren, K. Vijayakumar, M. Kaur, V. Mohan, A. Yusufali, R. Kelishadi, K. K. Teo, P. Joseph and S. Yusuf (2019). "Variations in common diseases, hospital admissions, and deaths in middle-aged adults in 21 countries from five continents (PURE): a prospective cohort study." Lancet.
de Ruijter, A. J., A. H. van Gennip, H. N. Caron, S. Kemp and A. B. van Kuilenburg (2003). "Histone deacetylases (HDACs): characterization of the classical HDAC family." Biochem J **370**(Pt 3): 737-749.
De, S. S., M. P. Khambete and M. S. Degani (2019). "Oxadiazole scaffolds in anti-tuberculosis drug discovery." Bioorg Med Chem Lett **29**(16): 1999-2007.
Dhanak, D., J. P. Edwards, A. Nguyen and P. J. Tummino (2017). "Small-Molecule Targets in Immuno-Oncology." Cell Chem Biol **24**(9): 1148-1160.
Dieterich, L. C. and M. Detmar (2016). "Tumor lymphangiogenesis and new drug development." Adv Drug Deliv Rev **99**(Pt B): 148-160.
Dumontet, C. and M. A. Jordan (2010). "Microtubule-binding agents: a dynamic field of cancer therapeutics." Nat Rev Drug Discov **9**(10): 790-803.
Essebier, A., M. Lamprecht, M. Piper and M. Boden (2017). "Bioinformatics approaches to predict target genes from transcription factor binding data." Methods **131**: 111-119.
Falkenberg, K. J. and R. W. Johnstone (2014). "Histone deacetylases and their inhibitors in cancer, neurological diseases and immune disorders." Nat Rev Drug

Discov **13**(9): 673-691.
Folkman, J. (2006). "Antiangiogenesis in cancer therapy--endostatin and its mechanisms of action." Exp Cell Res **312**(5): 594-607.
Gandalovicova, A., D. Rosel, M. Fernandes, P. Vesely, P. Heneberg, V. Cermak, L. Petruzelka, S. Kumar, V. Sanz-Moreno and J. Brabek (2017). "Migrastatics-Anti-metastatic and Anti-invasion Drugs: Promises and Challenges." Trends Cancer **3**(6): 391-406.
Gentzler, R. D., J. K. Altman and L. C. Platanias (2012). "An overview of the mTOR pathway as a target in cancer therapy." Expert Opin Ther Targets **16**(5): 481-489.
Gerber, D. E. (2008). "Targeted therapies: a new generation of cancer treatments." Am Fam Physician **77**(3): 311-319.
Glomb, T., K. Szymankiewicz and P. Swiatek (2018). "Anti-Cancer Activity of Derivatives of 1,3,4-Oxadiazole." Molecules **23**(12).
Guengerich, F. P. (2011). "Mechanisms of drug toxicity and relevance to pharmaceutical development." Drug Metab Pharmacokinet **26**(1): 3-14.
Haanstra, J. R. and B. M. Bakker (2015). "Drug target identification through systems biology." Drug Discov Today Technol **15**: 17-22.
Hadfield, J. A., S. Ducki, N. Hirst and A. T. McGown (2003). "Tubulin and microtubules as targets for anticancer drugs." Prog Cell Cycle Res **5**: 309-325.
Harley, C. B. (2008). "Telomerase and cancer therapeutics." Nat Rev Cancer **8**(3): 167-179.
Hashimoto, K., S. Goto, S. Kawano, K. F. Aoki-Kinoshita, N. Ueda, M. Hamajima, T. Kawasaki and M. Kanehisa (2006). "KEGG as a glycome informatics resource." Glycobiology **16**(5): 63r-70r.
He, G. and M. Karin (2011). "NF-kappaB and STAT3 - key players in liver inflammation and cancer." Cell Res **21**(1): 159-168.
Hrdlickova, R., M. Toloue and B. Tian (2017). "RNA-Seq methods for transcriptome analysis." Wiley Interdiscip Rev RNA **8**(1).
Hu, J. and W. X. Hu (2018). "Targeting signaling pathways in multiple myeloma: Pathogenesis and implication for treatments." Cancer Lett **414**: 214-221.
Jafri, M. A., S. A. Ansari, M. H. Alqahtani and J. W. Shay (2016). "Roles of telomeres and telomerase in cancer, and advances in telomerase-targeted therapies." Genome Med **8**(1): 69.
Janardhanan, J., M. Chang and S. Mobashery (2016). "The oxadiazole antibacterials." Curr Opin Microbiol **33**: 13-17.
Jha, P. (2009). "Avoidable global cancer deaths and total deaths from smoking." Nat Rev Cancer **9**(9): 655-664.
Jiao, Q., L. Bi, Y. Ren, S. Song, Q. Wang and Y. S. Wang (2018). "Advances in studies of tyrosine kinase inhibitors and their acquired resistance." Mol Cancer **17**(1): 36.
Jordan, M. A. and L. Wilson (2004). "Microtubules as a target for anticancer drugs." Nat Rev Cancer **4**(4): 253-265.
Jung, H. J. and H. J. Kwon (2015). "Target deconvolution of bioactive small

molecules: the heart of chemical biology and drug discovery." Arch Pharm Res **38**(9): 1627-1641.
Kanehisa, M. (2002). "The KEGG database." Novartis Found Symp **247**: 91-101; discussion 101-103, 119-128, 244-152.
Kaul, R., A. L. Risinger and S. L. Mooberry (2019). "Microtubule-Targeting Drugs: More than Antimitotics." J Nat Prod **82**(3): 680-685.
Kavallaris, M. (2010). "Microtubules and resistance to tubulin-binding agents." Nat Rev Cancer **10**(3): 194-204.
Khalilullah, H., M. J. Ahsan, M. Hedaitullah, S. Khan and B. Ahmed (2012). "1,3,4-oxadiazole: a biologically active scaffold." Mini Rev Med Chem **12**(8): 789-801.
Kieran, M. W., R. Kalluri and Y. J. Cho (2012). "The VEGF pathway in cancer and disease: responses, resistance, and the path forward." Cold Spring Harb Perspect Med **2**(12): a006593.
Kiselyov, A. S., M. Semenova, V. V. Semenov and D. Milligan (2006). "Inhibitors of VEGF receptors-1 and -2 based on the 2-((pyridin-4-yl)ethyl)pyridine template." Bioorg Med Chem Lett **16**(7): 1913-1919.
Koeberle, A. (2016). "Target identification and lead discovery by functional lipidomics." Future Med Chem **8**(18): 2169-2171.
Kumar, A., S. S. D'Souza, S. R. Nagaraj, S. L. Gaonkar, B. P. Salimath and K. M. Rai (2009). "Antiangiogenic and antiproliferative effects of substituted-1,3,4-oxadiazole derivatives is mediated by down regulation of VEGF and inhibition of translocation of HIF-1alpha in Ehrlich ascites tumor cells." Cancer Chemother Pharmacol **64**(6): 1221-1233.
Lakshmaiah, K. C., L. A. Jacob, S. Aparna, D. Lokanatha and S. C. Saldanha (2014). "Epigenetic therapy of cancer with histone deacetylase inhibitors." J Cancer Res Ther **10**(3): 469-478.
Lamb, J. (2007). "The Connectivity Map: a new tool for biomedical research." Nat Rev Cancer **7**(1): 54-60.
Lee, C. C., H. Y. Shiao, W. C. Wang and H. P. Hsieh (2014). "Small-molecule EGFR tyrosine kinase inhibitors for the treatment of cancer." Expert Opin Investig Drugs **23**(10): 1333-1348.
Li, W., H. Sun, S. Xu, Z. Zhu and J. Xu (2017). "Tubulin inhibitors targeting the colchicine binding site: a perspective of privileged structures." Future Med Chem **9**(15): 1765-1794.
Li, Y., F. Li, F. Jiang, X. Lv, R. Zhang, A. Lu and G. Zhang (2016). "A Mini-Review for Cancer Immunotherapy: Molecular Understanding of PD-1/PD-L1 Pathway & Translational Blockade of Immune Checkpoints." Int J Mol Sci **17**(7).
Liu, C., J. Su, F. Yang, K. Wei, J. Ma and X. Zhou (2015). "Compound signature detection on LINCS L1000 big data." Mol Biosyst **11**(3): 714-722.
Liu, K., X. Lu, H. J. Zhang, J. Sun and H. L. Zhu (2012). "Synthesis, molecular modeling and biological evaluation of 2-(benzylthio)-5-aryloxadiazole derivatives as

anti-tumor agents." Eur J Med Chem **47**(1): 473-478.
Lu, Y., J. Chen, M. Xiao, W. Li and D. D. Miller (2012). "An overview of tubulin inhibitors that interact with the colchicine binding site." Pharm Res **29**(11): 2943-2971.
Malumbres, M. (2014). "Cyclin-dependent kinases." Genome Biol **15**(6): 122.
Malumbres, M. and M. Barbacid (2009). "Cell cycle, CDKs and cancer: a changing paradigm." Nat Rev Cancer **9**(3): 153-166.
Mano, H. (1999). "Tec family of protein-tyrosine kinases: an overview of their structure and function." Cytokine Growth Factor Rev **10**(3-4): 267-280.
McFedries, A., A. Schwaid and A. Saghatelian (2013). "Methods for the elucidation of protein-small molecule interactions." Chem Biol **20**(5): 667-673.
Miller, J. W. (2016). "VEGF: From Discovery to Therapy: The Champalimaud Award Lecture." Transl Vis Sci Technol **5**(2): 9.
Mocellin, S., K. A. Pooley and D. Nitti (2013). "Telomerase and the search for the end of cancer." Trends Mol Med **19**(2): 125-133.
Mohan, C. D., N. C. Anilkumar, S. Rangappa, M. K. Shanmugam, S. Mishra, A. Chinnathambi, S. A. Alharbi, A. Bhattacharjee, G. Sethi, A. P. Kumar, Basappa and K. S. Rangappa (2018). "Novel 1,3,4-Oxadiazole Induces Anticancer Activity by Targeting NF-kappaB in Hepatocellular Carcinoma Cells." Front Oncol **8**: 42.
Musa, A., L. S. Ghoraie, S. D. Zhang, G. Glazko, O. Yli-Harja, M. Dehmer, B. Haibe-Kains and F. Emmert-Streib (2018). "A review of connectivity map and computational approaches in pharmacogenomics." Brief Bioinform **19**(3): 506-523.
Nieddu, V., G. Pinna, I. Marchesi, L. Sanna, B. Asproni, G. A. Pinna, L. Bagella and G. Murineddu (2016). "Synthesis and Antineoplastic Evaluation of Novel Unsymmetrical 1,3,4-Oxadiazoles." J Med Chem **59**(23): 10451-10469.
Olsen, L. R., B. Campos, M. S. Barnkob, O. Winther, V. Brusic and M. H. Andersen (2014). "Bioinformatics for cancer immunotherapy target discovery." Cancer Immunol Immunother **63**(12): 1235-1249.
Papadopoulos, N. and J. Lennartsson (2018). "The PDGF/PDGFR pathway as a drug target." Mol Aspects Med **62**: 75-88.
Perez-Herrero, E. and A. Fernandez-Medarde (2015). "Advanced targeted therapies in cancer: Drug nanocarriers, the future of chemotherapy." Eur J Pharm Biopharm **93**: 52-79.
Podlevsky, J. D. and J. J. Chen (2012). "It all comes together at the ends: telomerase structure, function, and biogenesis." Mutat Res **730**(1-2): 3-11.
Porta, R., R. Borea, A. Coelho, S. Khan, A. Araujo, P. Reclusa, T. Franchina, N. Van Der Steen, P. Van Dam, J. Ferri, R. Sirera, A. Naing, D. Hong and C. Rolfo (2017). "FGFR a promising druggable target in cancer: Molecular biology and new drugs." Crit Rev Oncol Hematol **113**: 256-267.
Qu, X. A. and D. K. Rajpal (2012). "Applications of Connectivity Map in drug discovery and development." Drug Discov Today **17**(23-24): 1289-1298.
Ren, J., Y. Liu, L. Li, Y. Zhao, Z. Li, C. Wu, L. Chen and K. Hu (2018). "OAMDP, a

novel podophyllotoxin derivative, induces apoptosis, cell cycle arrest and autophagy in hepatoma HepG2 cells." Cell Biol Int **42**(2): 194-204.
Riley, K. E. and P. Hobza (2011). "Noncovalent interactions in biochemistry." Wiley Interdisciplinary Reviews: Computational Molecular Science **1**(1): 3-17.
Rodriguez-Enriquez, S., J. C. Gallardo-Perez, I. Hernandez-Resendiz, A. Marin-Hernandez, S. C. Pacheco-Velazquez, S. Y. Lopez-Ramirez, F. D. Rumjanek and R. Moreno-Sanchez (2014). "Canonical and new generation anticancer drugs also target energy metabolism." Arch Toxicol **88**(7): 1327-1350.
Ropero, S. and M. Esteller (2007). "The role of histone deacetylases (HDACs) in human cancer." Mol Oncol **1**(1): 19-25.
Ruden, M. and N. Puri (2013). "Novel anticancer therapeutics targeting telomerase." Cancer Treat Rev **39**(5): 444-456.
Sanchez-Martinez, C., M. J. Lallena, S. G. Sanfeliciano and A. de Dios (2019). "Cyclin dependent kinase (CDK) inhibitors as anticancer drugs: Recent advances (2015-2019)." Bioorg Med Chem Lett **29**(20): 126637.
Sasikumar, P. G. N. R., M.; Naremaddepalli, S.S.S. (December 25, 2018.). 1,3,4-oxadiazole and 1,3,4-
thiadiazole derivatives as immunomodulators.
Schizas, D., A. Mastoraki, L. Naar, E. Spartalis, D. I. Tsilimigras, G. S. Karachaliou, G. Bagias and D. Moris (2018). "Concept of histone deacetylases in cancer: Reflections on esophageal carcinogenesis and treatment." World J Gastroenterol **24**(41): 4635-4642.
Singh, D., B. K. Attri, R. K. Gill and J. Bariwal (2016). "Review on EGFR Inhibitors: Critical Updates." Mini Rev Med Chem **16**(14): 1134-1166.
Sun, X., F. Li, B. Dong, S. Suo, M. Liu, D. Li and J. Zhou (2013). "Regulation of tumor angiogenesis by the microtubule-binding protein CLIP-170." Protein Cell **4**(4): 266-276.
Tamura, T., M. Ohira, H. Tanaka, K. Muguruma, T. Toyokawa, N. Kubo, K. Sakurai, R. Amano, K. Kimura, M. Shibutani, K. Maeda and K. Hirakawa (2015). "Programmed Death-1 Ligand-1 (PDL1) Expression Is Associated with the Prognosis of Patients with Stage II/III Gastric Cancer." Anticancer Res **35**(10): 5369-5376.
Tangutur, A. D., D. Kumar, K. V. Krishna and S. Kantevari (2017). "Microtubule Targeting Agents as Cancer Chemotherapeutics: An Overview of Molecular Hybrids as Stabilizing and Destabilizing Agents." Curr Top Med Chem **17**(22): 2523-2537.
Tutone, M., B. Pecoraro and A. M. Almerico (2018). "Investigation on Quantitative Structure-Activity Relationships of 1,3,4 Oxadiazole Derivatives as Potential Telomerase Inhibitors." Curr Drug Discov Technol.
Vaidya, A., S. Jain, P. Jain, P. Jain, N. Tiwari, R. Jain, R. Jain, A. K. Jain and R. K. Agrawal (2016). "Synthesis and Biological Activities of Oxadiazole Derivatives: A Review." Mini Rev Med Chem **16**(10): 825-845.
Valente, S., D. Trisciuoglio, T. De Luca, A. Nebbioso, D. Labella, A. Lenoci, C. Bigogno, G. Dondio, M. Miceli, G. Brosch, D. Del Bufalo, L. Altucci and A. Mai

(2014). "1,3,4-Oxadiazole-containing histone deacetylase inhibitors: anticancer activities in cancer cells." J Med Chem **57**(14): 6259-6265.
Vera-Badillo, F. E., M. Al-Mubarak, A. J. Templeton and E. Amir (2013). "Benefit and harms of new anti-cancer drugs." Curr Oncol Rep **15**(3): 270-275.
Vermeulen, K., D. R. Van Bockstaele and Z. N. Berneman (2003). "The cell cycle: a review of regulation, deregulation and therapeutic targets in cancer." Cell Prolif **36**(3): 131-149.
Vijayaraghavan, S., S. Moulder, K. Keyomarsi and R. M. Layman (2018). "Inhibiting CDK in Cancer Therapy: Current Evidence and Future Directions." Target Oncol **13**(1): 21-38.
Weidner, N. and J. Folkman (1996). "Tumoral vascularity as a prognostic factor in cancer." Important Adv Oncol: 167-190.
Wilson, L. and M. A. Jordan (2004). "New microtubule/tubulin-targeted anticancer drugs and novel chemotherapeutic strategies." J Chemother **16 Suppl 4**: 83-85.
Young, R. J. and M. W. Reed (2012). "Anti-angiogenic therapy: concept to clinic." Microcirculation **19**(2): 115-125.
Yusuf, S., P. Joseph, S. Rangarajan, S. Islam, A. Mente, P. Hystad, M. Brauer, V. R. Kutty, R. Gupta, A. Wielgosz, K. F. AlHabib, A. Dans, P. Lopez-Jaramillo, A. Avezum, F. Lanas, A. Oguz, I. M. Kruger, R. Diaz, K. Yusoff, P. Mony, J. Chifamba, K. Yeates, R. Kelishadi, A. Yusufali, R. Khatib, O. Rahman, K. Zatonska, R. Iqbal, L. Wei, H. Bo, A. Rosengren, M. Kaur, V. Mohan, S. A. Lear, K. K. Teo, D. Leong, M. O'Donnell, M. McKee and G. Dagenais (2019). "Modifiable risk factors, cardiovascular disease, and mortality in 155 722 individuals from 21 high-income, middle-income, and low-income countries (PURE): a prospective cohort study." Lancet.
Zhao, Y., X. Mu and G. Du (2016). "Microtubule-stabilizing agents: New drug discovery and cancer therapy." Pharmacol Ther **162**: 134-143.
Zvereva, M. I., D. M. Shcherbakova and O. A. Dontsova (2010). "Telomerase: structure, functions, and activity regulation." Biochemistry (Mosc) **75**(13): 1563-1583.

ACKNOWLEDGMENTS

I would like to thank my supervisor, Professor Luigi Marco Bagella, for his careful guidance during my Ph.D.

I would like to thank my Shantou University Medical College supervisor Professor David J. Kelvin for providing me with experimental conditions, financial support and careful guidance for my research subject.

I would like to thank all the members of the laboratories located in Sassari and Shantou for their help and support!

Finally, I would like to thank my family for the support!